Modelling the impact of antenna installation error on network performance

BL Prinsloo

Orcid.org/0000-0003-1912-1534

Dissertation accepted in fulfilment of the requirements for the degree *Master of Engineering in Computer and Electronic Engineering* at the North-West University

Supervisor: Prof ASJ Helberg

Co-supervisor: Dr M Ferreira

Graduation: May 2020

Student number: 24128546

Acknowledgements

I would firstly like to thank my heavenly Father and Saviour for giving me the opportunity to do this research. I thank Him for blessing me and standing by my side every step of the way.

I thank my study leaders and mentors Prof. Albert Helberg and Dr. Melvin Ferreira for believing in me and supporting me to grow as a researcher. Thank you for the long hours and input not only so that could gain academic knowledge, but also teaching me some important principles that I will take with me on my journey toward future achievements in my life.

I am grateful to Mr. Koenie Schutte and LS of SA Radio Communication Services Ltd. who supported me financially and gave me the necessary advice. They also provided me with the CHIRPLus BC software for validation of my simulations.

My thanks go to Vodacom for the data provided as a platform on which to base the research.

I am grateful to Prof. Suria Ellis at the North-West University statistical consultation services for the advice and input in analysing my results.

I am indebted to the Telenet study group for their support and friendship in the challenging times.

Words are not enough to thank all my family members and friends for supporting me during all those late nights and trialling times.

To my family in particular, Hermanus Prinsloo, Jeanne Prinsloo and Stefan Prinsloo, thank you for always believing in me and giving me the opportunity to study, and for helping me to be where I am today. A special thank you to Hermanus Prinsloo, my earthly father, my advisor and my hero, who supported me and helped me to strive to be significant. I especially thank him for his contributions in the final stages of my research.

Abstract

This dissertation models the impact of antenna installation errors on network performance of a Long Term Evolution (LTE) site. To test the impact of antenna installation parameters (antenna height and mechanical tilt), simulations were done on different LTE sites situated in specifically chosen environments with a variety of terrain heights. This enables the correlation of the site coverage with terrain height variation in order to see how the installation parameters influence coverage of sites in different locations.

Coverage results derived from the developed Matlab simulation were verified and validated by commercialised software (CHIRPlus BC) to ensure that the methods used are correctly implemented to obtain valid results. Using statistical analysis, the verified results enabled us to calculate tolerances for the installation parameters, taking terrain height variation into account. The statistical analysis was an important step towards understanding the extent of the impact of practice on the adjustments.

Given the results obtained from the statistical analysis, it was found that a minimum tilt adjustment error of 0.5° can have an impact of 7% on coverage. A minimum height adjustment error of 2 m has an impact of 6% on coverage.

A parameter called effect size was used to describe the practical significance of the impact of the antenna installation errors. It was found that a minimum tilt adjustment error of 3° has a high effect size and can therefore have a significant practical effect on coverage. Height adjustment errors do not have the same amount of practical impact as tilt adjustment errors where a practical effect on coverage is only observed when height adjustment errors exceed 2 m.

It was also found that the Terrain Roughness Factor (TRF) cannot be used as a good predictor for coverage, but effective height can.

Keywords: *Modelling network performance, Coverage, LTE, Mechanical tilt, Antenna height, Terrain height variation*

Contents

List of Figures

List of Tables

List of Acronyms

AM Amplitude Modulation

AMSL above mean sea level

BW Bandwidth

CDMA Code Division Multiple Access

CID Cell Identification

DEM digital elevation model

DL Downlink

DTT Digital Terrestrial Television

E-UTRA Evolved Universal Mobile Telecommunications System Terrestrial Radio Access

E-UTRAN Evolved Universal Mobile Telecommunications System Terrestrial Radio Access Network

EARFCN E-Utra Absolute Radio Frequency Channel Number

ECC Electronic Communications Committee

EDGE Enhanced Data for GSM Evolution

EIRP effective isotropic radiated power

ERP effective radiated power

FDD Frequency Division Duplexing

FDMA Frequency Division Multiple Access

FFT Fast Fourier Transform

FM Frequency Modulation

FSPL Free Space Path Loss

GCD Great Circle Distance

GPRS General Packet Radio Service

GSM Global System for Mobile communication

HAGL Height Above Ground Level

HASL Height Above Mean Sea Level

HSPA High Speed Packet Access

IMSI International Mobile Subscriber Identity

IMT International Mobile Communications

IMT-Advanced International Mobile Communications Advanced

ITM Irregular Terrain Model

ITU International Telecommunications Union

LAC Location Area Code

LTE-Advanced Long Term Evolution Advanced

LTE Long Term Evolution

MAE mean absolute error

mcc Mobile Country Code

ME mean error

MIMO Multiple Input-Multiple Output

mnc Mobile Network Code

MSE mean square error

NID Network Identification

OFDM Orthogonal Frequency Division Modulation

OFDMA Orthogonal Frequency Division Multiple Access

PIP Process Improvement Plan

QAM Quadrature Amplitude Modulation

QoS quality of service

QPSK Quadrature Phase Shift-Keying

RMSE Root Mean Square Error

RPA Remotely Piloted Aircraft

PLF Polarisation Loss Factor

RSRP Radiated Signal Received Power

RSSI Received Signal Strength Indicator

RX Receiver

SC-FDMA Single Carrier-Frequency Division Multiplexing

SINR signal to interference and noise ratio

SRTM Shuttle Radar Topography Mission

TAC Tracking Area Code

TDD Time Division Duplexing

TDMA Time Division Multiple Access

TRF Terrain Roughness Factor

TV television

UL Uplink

UMTS Universal Mobile Telecommunications System

VHF Very High Frequency

Chapter 1

Introduction

Chapter 1 is an introduction to the research reported in this dissertation. The research problem is defined and divided into three sub-questions. The methodology used to conduct the research is also discussed.

1.1 Contextualisation

Measured wireless network performance that does not meet the design criteria is of great concern to cellular network operators [10].

In general, network performance can be defined by different parameters such as coverage, capacity and data throughput. For this research, mobile network performance is defined as the amount of coverage that a single Long Term Evolution (LTE) tower can provide to the area around the tower.

One of the main reasons for a difference in measured performance versus planned performance is faulty antenna installations. When the antenna on an LTE site is installed, there is the possibility for an installation error to occur, which influences the network's

performance. Installation errors such as antenna orientation or physical antenna height are not always accounted for and can have a negative effect on the overall single cell performance [4].

A network performance parameter such as coverage can be verified by measuring the area which has a minimum specified received signal power. The area that does not comply with the coverage specification is called a gap [11]. Methods such as ground measurements, measurements via crewed helicopter or even Remotely Piloted Aircraft (RPA) measurements are very costly and are constrained by a difficult terrain where towers are situated [12].

When there is a decrease in network performance due to faulty installation, operational costs increase [10]. Operational costs include the labour expenses involved in repairing the faulty installations when it has been found to affect the network to such an extent that users are not satisfied with the network's performance.

The next section will give some background on wireless networks.

1.2 Introduction to wireless networks

Broadcasting and cellular networks are two common types of wireless networks. Broadcasting consists of two main services, namely television (TV) and audio broadcasting. Audio broadcasting normally operates in the Very High Frequency (VHF) band, which is between 30 and 300 MHz [13]. The International Telecommunications Union (ITU) Region 1 frequency allocation for VHF is between 68 and 74 MHz for analogue TV and sound broadcasting (Amplitude Modulation (AM)), between 87.5 and 108 MHz is for sound broadcasting (Frequency Modulation (FM)) and between 216 and 230 MHz is for digital broadcasting [14]. The TV broadcasting service normally operates in the UHF band, which is between 300 and 3000 MHz [13]. The ITU region 1 frequency allocation is 470 to 694 MHz for Digital Terrestrial Television (DTT), between 694 and 960 MHz is for normal analogue television broadcasting [14]. A broadcasting network does not

link with devices individually, but broadcasts a specific service (such as radio) to any device that can receive from the broadcasting network.

A wireless cellular network consists of a combination of macro-cells or base stations. Each base station consists of one or more antennas in order to communicate with the other base stations or to provide a service to mobile users. Cellular base stations are divided into sectors that operate at different frequencies in order to increase cell capacity [15]. Each wireless LTE network consists of an Evolved Universal Mobile Telecommunications System Terrestrial Radio Access Network (E-UTRAN) methodology, which comprises of a set of e-NodeB controllers, one for each tower [16].

1.2.1 Base station multiple access techniques

Different access methods such as Frequency Division Multiple Access (FDMA), Code Division Multiple Access (CDMA) and Time Division Multiple Access (TDMA) can be used to initiate a connection with a base station. The abovementioned multiple access methods are the most basic types of access methods.

Wireless technologies such as LTE use Orthogonal Frequency Division Multiple Access (OFDMA). OFDMA improves capacity and increases the number of users that can use the network service without interruption and the number of frequency bands used effectively in the spectrum. To enable the use of OFDMA technique, LTE comprises a frequency duplexing technique called FDMA. FDMA is explained in more detail in Chapter 2.

1.2.2 Base station antennas

Every base station has one or more installed antennas. Antennas differ in shape and size and each antenna is used for a different frequency band. There are various installation parameters that are used to set up an antenna at a base station. These parameters also determine whether the base station network performance is within designed spec-

ifications. These important parameters are electrical tilt, mechanical tilt, polarisation, azimuth, Height Above Ground Level (HAGL) and effective height [17].

1.2.3 Capacity and coverage

The capacity of a wireless network is defined as the maximum number of users that can be connected to the network with the available resources while sustaining designed throughput. A high-traffic area is normally measured by capacity, which means that the focus is on the number of users and not the area of network coverage. Coverage is the measure of the geographical area that can provide continuous network service with available resources. A low-traffic area is normally measured by coverage [16].

In this dissertation, the coverage was used as the network performance metric in order to directly determine the impact of antenna installation parameter deviation on the performance of an LTE cell. The capacity of a network can be determined by considering population density and other statistics as part of the coverage of the network, but these are not used as a network performance metric in this study.

1.3 Antenna installation and network performance

Network performance degrades because of inaccurate antenna installations. An antenna is installed using specified installation parameters, such as azimuth, tilt (mechanical and electrical), transmitting frequency and antenna height. Each of the aforementioned parameters are important for the following reasons [18]:

- Azimuth: The azimuth of an antenna is the direction in which the antenna is pointed. This can influence the area that will be covered by the network. If the antenna is not installed with the correct azimuth it can influence the amount of users able to access the network.

- Tilt: Tilt can be adjusted to define the coverage area in order to reduce interference or coverage in unwanted areas.
- Transmitting frequency: Each antenna is designed to perform optimally at certain transmitting frequencies, in which case it is important to install the correct antenna in order for the network to perform as designed.
- Antenna height: If the antenna height is too low it will not be able to cover long distances due to obstructions, but if the antenna height is too high, the coverage can decrease due to the increase in Free Space Path Loss (FSPL).

Not all installation techniques are accurate enough for antennas to be installed within the designed installation tolerance, which has a negative impact on network performance. According to [12], a network normally has poor coverage because of faulty antenna manufacturing and antenna installation errors.

Some antenna installation techniques include:

- Directing the antenna to specified landmarks (azimuth adjustment).
- Using a compass to obtain the correct azimuth angle (azimuth adjustment).
- Mechanical alignment brackets (tilt adjustment).

When measuring the network performance, it is possible to detect a difference between the designed and actual installation. The difference between measured and designed network performance can give a good indication of the possible antenna installation errors [12]. In 2015 an RPA site measurement was done in Europe to characterise different network performance parameters. The results of these network parameters were then used to identify any errors in the antenna installation.

If any modifications had to be made to the site because of a discrepancy in performance, a re-iteration of the measurement has to be done. It is very time consuming

and costly to repeat RPA measurements more than once in order to correct the antenna until the designed network performance specification is met.

Measured network performance information is also beneficial for accurately defing the changes that have to be made to the antenna to ensure it is within designed specifications. The measured data can also be imported into planning tools to improve network planning models [19]. If the correct antenna installations are accurately implemented initially, fewer or no iterations of on-site optimisation may be necessary.

1.3.1 Near- and far-field measurements

Radio waves consist of an electric and magnetic field. Close to the antenna, these two fields are still distinct. While these fields cannot be seen as the radio waves seperately, they do contain the information being propagated. Therefore, measurements are normally done in the far-field or Fraunhofer zone of the radio wave, which begins at approximately 10 wavelengths from the antenna being measured. Within the Fraunhofer zone, a radio wave being propagated consists of the combined electric and magnetic radio waves. The region around the antenna before the Fraunhofer zone is called the near-field or the Fresnel zone. In [20], measurements are done within the Fresnel zone because of physical limitations such as difficult terrain or long wavelengths. A technique using a Fast Fourier Transform (FFT) can be implemented to transform the near-field measurement to a far-field pattern.

1.3.2 Existing antenna installation measurement techniques

One of the main limitations mentioned in [20] is the amount of time in which the measurements take place. Measuring all of the antenna rotating points on a base station with a static ground measurement system can take a whole day compared to other methods [20], which take only a few hours.

As an alternative to the static ground measurement, RPA measurements can be used.

In 2015 LS Telcom AG was contracted to perform 25 RPA measurements in Namibia using an RPA. Unlike other measurement options, the RPA enabled successful measurement without disturbing any operational services [21] and it was done in a short time, thus saving on operational costs. Operators appreciated the value added with RPA measurements, as the results when compared to other measurement techniques showed significant improvements [22].

It is important to realise that certain measurement techniques can require significant time and resources. Standard industry planning tools must therefor be used to determine optimal site installations and to ensure that wireless sites are installed to their design specifications.

In summary, antennas must be installed accurately because installation errors can have a negative impact on network performance. Correct installation can reduce the scope of post-installation fault finding, thus reducing operating costs of the service provider.

1.4 Research problem

Antenna installations made without due consideration to accurate tolerances or parameters will affect the coverage of a mobile site. The goal of the research is to determine the effect of certain antenna installation parameters on coverage.

LTE is recognised as a very popular mobile network technology in South Africa, yet very few published research articles on the impact of antenna installations errors on LTE network performance could be found during the literature search. Mobile network base stations are installed on different terrains. It is therefore critical to take terrain data into account when studying the impact of antenna faults on network performance, especially in relation to coverage.

During this research, the impact of two antenna installation parameters (mechanical tilt and antenna height above ground) on the coverage of an LTE site will be modelled,

simulated and analysed.

The research problem is addressed by answering the following three research questions:

- What is the impact of a tilt adjustment error on coverage?
- What is the impact of a height adjustment error on coverage?
- What influence does the terrain have on coverage, having taken the tilt and height into account?

1.5 Research methodology

To successfully answer the research questions, the following method is used:

- Modelling and simulating a reference LTE site;
- Adjusting antenna mechanical tilt and antenna height, as well as obtaining the coverage for each sector of the cell;
- Repeating the above mentioned steps for multiple sites to analyse the coverage results statistically;
- Defining parameters to model the terrain surrounding the LTE site; and
- Calculating the parameters for multiple sites and analysing the parameters statistically.

1.6 Dissertation overview

The layout of the dissertation is as follows:

- Chapter 1: Introduction (The introduction to the research problem, followed by an initial literature review and a definition of the research questions and methodology).
- Chapter 2: Literature Study (A comprehensive study of the literature related to the research problem).
- Chapter 3: System Model (The design and methodology of the simulation system model).
- Chapter 4: Verification and Validation (The software used to obtain the results to answer the research questions is verified and validated).
- Chapter 5: Results and Analysis (An overview, discussion and statistical analysis of the results obtained in Chapter 4).
- Chapter 6: Conclusion and Recommendations (This chapter includes concluding remarks as well as proposed future work).

1.7 Summary

In Chapter 1, the study and relevant background were introduced. After a clear introduction to the study, the problem was described followed by the research questions and the structure of the research. It concluded by stating how the research was conducted to answer the research questions.

The next chapter will provide more in-depth information on the relevant literature for this study.

Chapter 2

Literature study

Chapter 2 provides an overview of the relevant literature that supports the context and outcomes of the research. The first section explains LTE technology, which is the technology implemented in this research. It includes literature discussing antennas, multipath models, propagation models and parameters. The last section includes information on previous studies that relates to the research and simulations done in this dissertation.

2.1 LTE

There are two types of LTE technologies, LTE and Long Term Evolution Advanced (LTE-Advanced). LTE-Advanced is an improvement from LTE on the following :

- The data rates are increased to a maximum of 3 Gbps on the Downlink (DL) and to 1.5 Gbps on the Uplink (UL).
- Improved cell edge performance of a minimum of 2.4 bps/Hz/cell.

To increase capacity, the bandwidth must be increased through the aggregation of the

bandwidth component carriers. The component carriers can have a bandwidth of 1.4, 3, 5, 10, 15, 20 MHz. For LTE-Advanced, the maximum bandwidth will be 100 MHz. Increased capacity was one of the main focus points with LTE-Advanced. [23].

LTE or 4G is one of the most recently implemented technologies in mobile networks. It is an improvement on 3G technology in terms of data rates. 3G technology has theoretical data rates of up to 10 Mbps. 5G will soon be introduced as an improvement on 4G, which entails increased data rates, improved spectrum efficiency and more efficient placements on masts. 5G will use higher operating frequencies, between a 30 and 300 GHz range. The next section provides more detail on the physical layer of LTE and how it works.

2.1.1 General information

LTE offers a peak download speed of up to 100 Mbps per 20 MHz of bandwidth for mobile users and an upload speed of 50 Mbps per 20 MHz bandwidth [24], [25]. LTE is also backwards-compatible with High Speed Packet Access (HSPA), Enhanced Data for GSM Evolution (EDGE) and General Packet Radio Service (GPRS). LTE uses 64-Quadrature Amplitude Modulation (QAM), 16-QAM or Quadrature Phase Shift-Keying (QPSK) modulation techniques on the sub-carriers, and depending on the data speed needed, Orthogonal Frequency Division Modulation (OFDM) is used as the modulation scheme to divide the channel into sub-carriers, which increases the spectrum efficiency and helps to achieve high data rates [26], [4].

LTE bandwidth is standardised at 1.4, 3, 5, 10, 15 and 20 MHz, where 5 and 10 MHz are the most commonly used. The use of certain bandwidths is dependent on the carrier frequency [4].

The carrier frequency is also an important consideration for installation of the antenna. An antenna is designed to operate in certain frequency bands. If the transmitter carrier frequency is not set-up to operate in the designed frequency of the antenna, it will not function properly, which can have a negative effect on network performance.

2.1.2 LTE frequency band layout

LTE uses separate bands for both the UL and the DL. Certain frequency bands are set up for Time Division Duplexing (TDD) and some of the frequency bands are set up for Frequency Division Duplexing (FDD). A detailed description of FDD and TDD follows. The UL and DL are divided into pairs in a specific frequency band.

Table 2.1 gives an example of how the ITU distributed the frequency ranges between 1710-2200 MHz for LTE. The Evolved Universal Mobile Telecommunications System Terrestrial Radio Access (E-UTRA) bands are bands setup to be used for International Mobile Communications (IMT). LTE fulfils the requirements set by ITU for IMT and LTE-Advanced fulfils the requirements set by ITU for International Mobile Communications Advanced (IMT-Advanced). The IMT E-UTRA operating band 3 is implemented so that the DL band ranges between 1805 and 1880 MHz and the UL band ranges between 1710 and 1785 MHz, with a centre frequency band gap of 20 MHz between the paired UL and DL channel.

Table 2.1: IMT paired bands in the range 1710-2200 MHz ([8], [9])

E-Utra Operating Band	UL Range (MHz)	DL Range (MHz)	Duplexing Type
1	1920-1980	2110-2170	FDD
2	1850-1910	1930-1990	FDD
3	1710-1785	1805-1880	FDD
33	1900-1920	1900-1920	TDD
34	2010-2025	2010-2025	TDD

Figure 2.1 is an example of a single frequency UL and DL pair layout that also shows the frequency gap between the two bands.

Frequency ranges are normally referred to with frequency codes called E-Utra Absolute Radio Frequency Channel Number (EARFCN), which are defined in the range 0-262143. Equations (2.1) and (2.2) are the equations used to find the UL and DL centre frequency of the specific EARFCN.

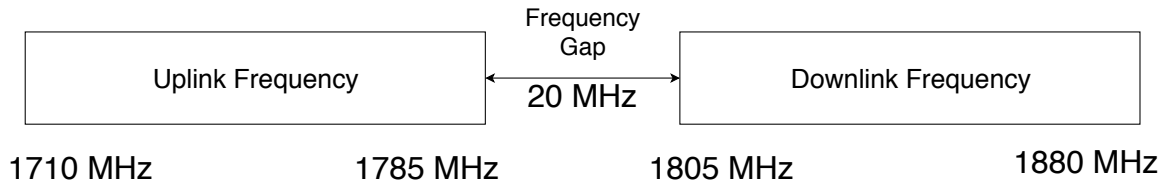

Figure 2.1: Layout of a frequency UL and frequency DL pair as defined in the 3GPP TS 36.101 specification [3]

$$F_{DL} = F_{DL-low} + 0.1(N_{DL} - N_{Offs-DL}) \tag{2.1}$$

$$F_{UL} = F_{UL-low} + 0.1(N_{UL} - N_{Offs-UL}) \tag{2.2}$$

F_{DL-low} and $N_{Offs-DL}$ are given in table 5.7.3-1 in the 3GPP TS 36.101 specification and N_{DL} is the EARFCN. F_{DL-low} is the lower edge of the DL frequency band and $N_{Offs-DL}$ is the lower edge of the EARFCN for the DL frequency band, this also counts for the UL equation [27].

The EARFCN frequency codes are used by operators to define LTE frequency bands.

2.1.3 LTE channel bandwidth

Table 2.2 shows the different channel bandwidths that can be found in an E-UTRA carrier. The transmission bandwidth ($BW_{Transmission}$) configuration is the bandwidth of the actual resource block, excluding the channel edges (see Figure 2.2). The channel edges for a specific channel bandwidth ($BW_{Channel}$) at a specific centre frequency (F_C) can be calculated as:

$$BW_{Transmission} = F_C \pm BW_{Channel}/2. \tag{2.3}$$

Figure 2.2 shows the layout of the channel bandwidth, transmission bandwidth configuration and the bandwidth of the active resource blocks.

LTE bandwidth can evidently be configured in different manners depending on the type of service it is used for.

Table 2.2: Channel sub-carrier bandwidth configuration

Channel bandwidth (MHz)	Transmission bandwidth configuration (MHz)
1.4	6
3	15
5	20
10	25
15	50
20	100

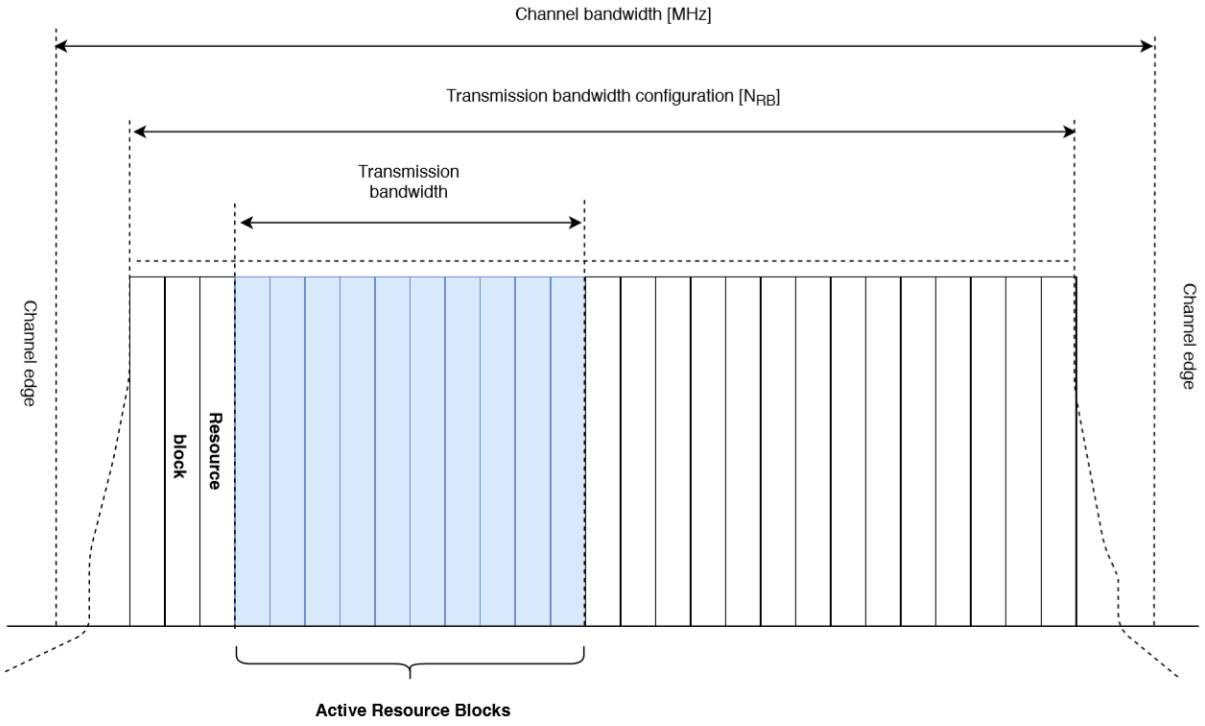

Figure 2.2: Bandwidth of an E-UTRA channel [3]

2.1.4 LTE modulation

OFDM is used in the DL, which provides better spectral efficiency and decreases the risk of multiple users using the same channel. It divides the channel into smaller sub-carriers orthogonally, so they will not interfere with each other. The sub-carrier spacing for LTE is 15 kHz.

Figure 2.3 shows how OFDM was implemented on a single LTE resource block. The

modulation uses time and frequency to spread the data over the resource block, which increases the data rate. A single resource block is 180 kHz wide, which consists of multiple 15 kHz sub-carriers. When using QPSK, the data rate is 15 kbps, but can be higher if a higher-level modulation is used, such as 64 QAM. There are seven OFDM symbols per resource block, which are 0.5 ms time slots.

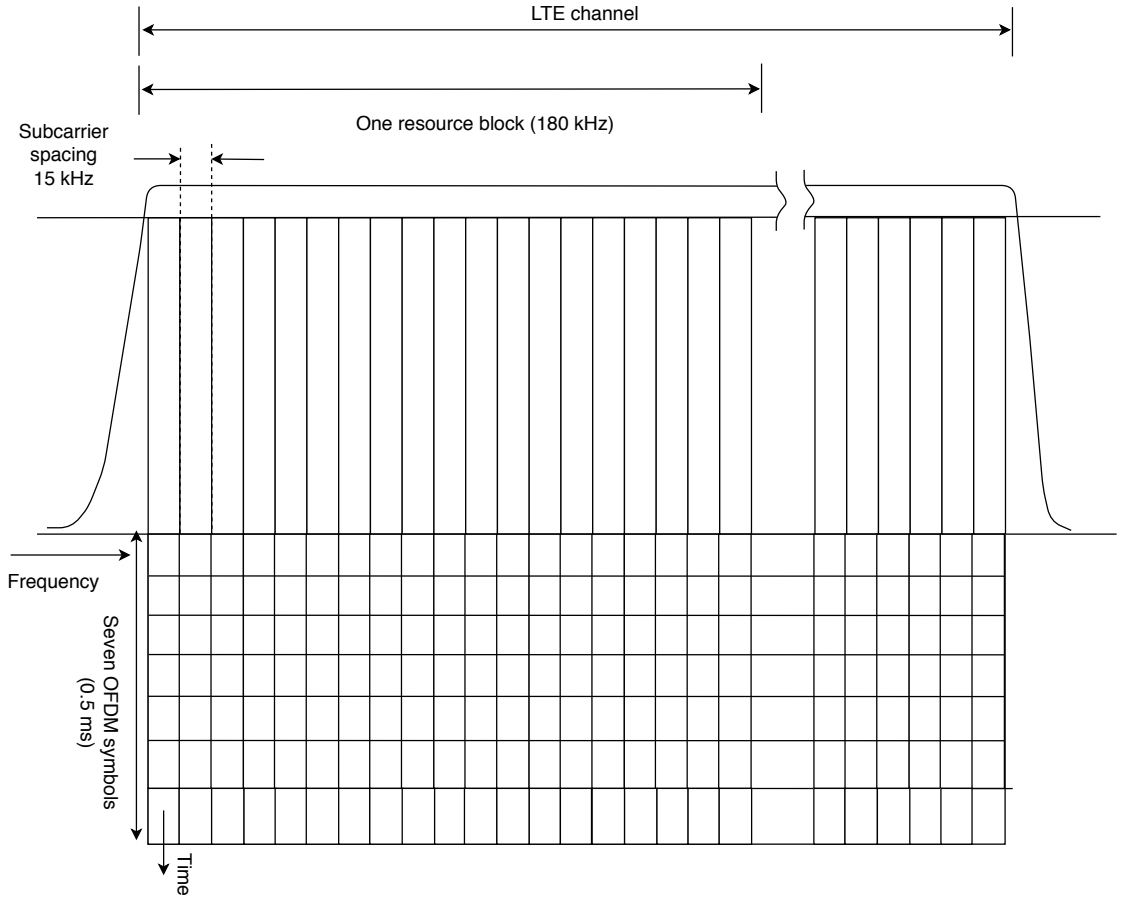

Figure 2.3: OFDM in an LTE resource block [4]

In the UL of an LTE signal, Single Carrier-Frequency Division Multiplexing (SC-FDMA) was used. SC-FDMA has a lower peak-to-average-power ratio than OFDM, which is more suitable to implement on mobile devices. The use of OFDM needed a linear power amplifier to operate with low efficiency, and this is not ideal for a mobile implementation.

2.1.5 Duplexing techniques

TDD and FDD are the duplexing methods of how the two allocated frequency bands are used while data is being transferred. TDD takes the pair frequency as a whole, which means that TDD can use the whole allocated frequency for UL and DL at various time frames. FDD uses two frequencies separately- one for UL and the other for DL.

Figure 2.4 shows the difference between a TDD- and an FDD-implemented frequency range pair [9].

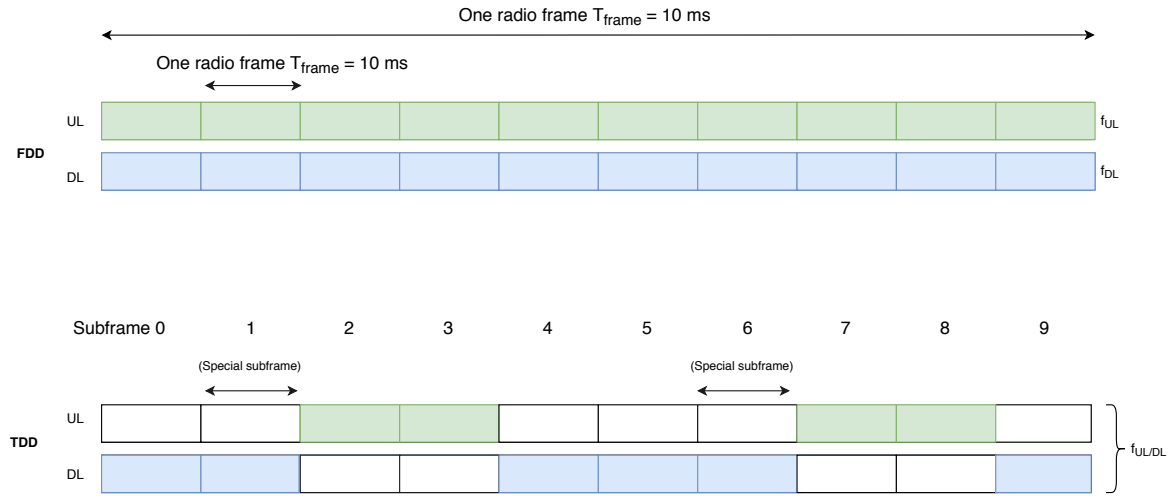

Figure 2.4: Difference between FDD and TDD on spectrum allocation

In order to obtain information for coverage, the focus must be on the DL because the power is measured from the transmitter at the receiver and not the power from the receiver at the transmitter. It is not of importance which of the two techniques are used in this specific link.

2.2 Antenna types

Various antennas are available for different implementations. Specific antennas were implemented on LTE base stations and mobile devices. The next section provides an overview of common antenna configurations and types.

2.2.1 Wire antennas

Wire antennas consist of loop, single wire and helical antennas. These antennas are normally used in applications such as mobile radios, automobiles, mobile handsets or wireless modems and routers. These systems normally have low gains between 2 and 15 dBi. Wire antennas are normally narrowband antennas. Linear polarisation and omni-directional patterns are acceptable for their implementation [16].

Wire antennas are commonly implemented as dipole or monopole antennas, which are mainly used in mobile communication systems and devices.

2.2.2 Aperture antennas

Aperture antennas, such as reflector, parabolic dishes, lens, spiral, panel and horn antennas, radiate electromagnetic energy from a physical aperture. They are used in moderate to high gain applications, which can be larger than 20 dBi. Aperture antennas can be easily covered by a dielectric material to prevent possible damage [16].

2.2.3 Microstrip antennas

The microstrip antenna is a small antenna that consists of a metallic patch on a grounded substrate. The metallic patches can be manufactured in different shapes and sizes, but circular and rectangular patches are the most popular because of ease of analysis and fabrication. The antenna is designed to be mounted on planar and non-planar surfaces and is inexpensive to manufacture. They are manufactured to be mounted on mobile and high-performance systems, such as aircraft, missiles, cars or hand-held devices.

The microstrip antenna has some disadvantages, such as low efficiency, low power handling, poor polarisation purity, poor scan performance, spurious feed radiation and a narrow bandwidth [5]. Methods such as increasing the substrate height can increase the antenna's efficiency. To increase the bandwidth of the antenna, methods

such as the stacking of multiple microstrips can be implemented.

Smartphone multiband antennas

Mobile units such as smart phones need a small antenna designed to operate with multiple frequencies. The rectangular microstrip antenna, which has multiple U-slots, is commonly implemented in mobile devices. Each U-shape on the antenna is designed to resonate at a certain frequency by making the overall length half of the length of each U-slot. [5]

Figure 2.5 illustrates a three-band U-shot microstrip antenna. The first frequency is defined through the rectangular patch and the two U-slots represent the other two bands. [5]

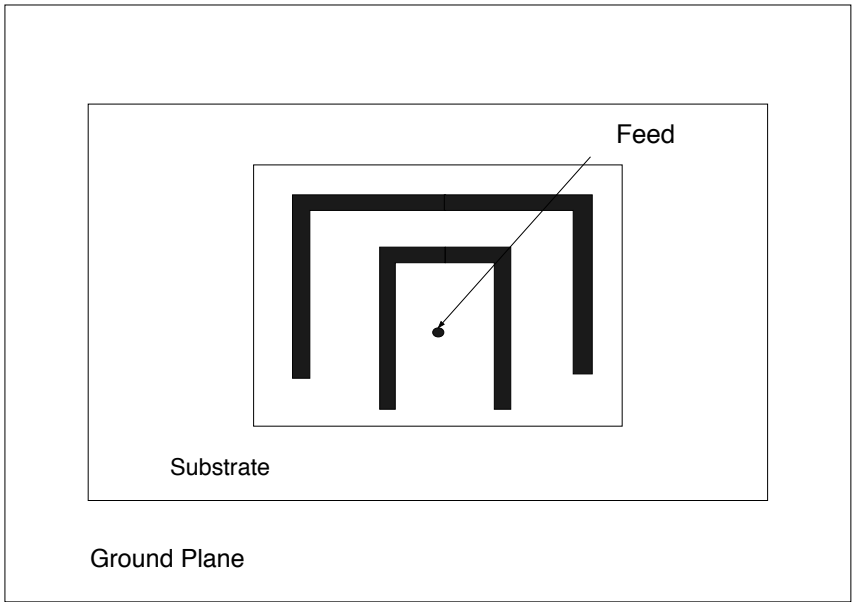

Figure 2.5: Three-band U-slot microstrip antenna design [5]

2.2.4 Monopole and dipole antennas

Monopole and dipole antennas are classified as single wire antennas as discussed in subsection 2.2.1 and are mainly used as wireless transmitters on base stations.

Monopole antennas

Monopoles are normally used in mobile handsets such as cellphones, cordless telephones, automobiles and trains. Monopoles have good broadband characteristics and have a simple construction. The position of the monopole in a mobile device influences its radiation pattern, but not the impedance or the resonant frequency [5].

Electric dipole

A commonly used antenna configurations on base stations for mobile communication is a triangular array configurations which consists of twelve dipole antennas with four dipoles on each side of the triangle. This is normally used as a sectoral array for a sectored base station. [5]

Dipoles can be mounted horizontally or mounted vertically on a base station which determines the polarisation of the beam.

2.2.5 Antenna arrays

An antenna array is an antenna comprised of a number of radiating elements of which the inputs or outputs are combined [28]. In an array of identical antenna elements it is important to know the following different control elements used to configure an antenna array [5]:

- A geometrical configuration such as linear, circular, rectangular or spherical.
- The relative distance between the antenna elements.
- The excitation amplitude of the antenna elements.
- The excitation phase of the antenna elements.
- Each antenna element's relative gain pattern.

Multi-element linear antenna arrays are normally used to increase the directivity of the pattern. This is done by increasing the gain of a specific part of the antenna pattern using the different controlling elements mentioned above [5].

The number of control elements of an array can be increased by placing the antenna elements on a plane instead of a straight line. Planar arrays can provide more symmetrical patterns and lower the pattern side lobes. These arrays are normally used in radar, remote sensing and communication [5].

A phased array antenna can be used to control the antenna gain pattern. Changing the amplitude and the inter-element spacing, the side lobes can be controlled, and by changing the relative phase of each antenna element, the main beam position can be controlled [16].

2.2.6 Lens antennas

According to the IEEE standard for definitions of terms for antennas, a lens antenna is an antenna that consists of an electromagnetic lens and a feed that illuminates [28]. The electromagnetic lens is a three-dimensional structure through which electromagnetic waves can pass, possessing an index of refraction that may be a function of position, and a shape that is chosen so as to control the exiting aperture illumination [28]. It can therefore be concluded that lens antennas can be applied to increase the accuracy of radiation direction [5].

2.2.7 Multiple Input-Multiple Output (MIMO)

LTE uses multi-antenna mechanisms to increase coverage and physical layer capacity. MIMO antenna systems must therefore be required on LTE systems [29]. Common MIMO arrangements are 2x2 and 4x4. The MIMO process divides the information being sent into different segments, which are then transmitted simultaneously through the same channel. This brings a solution to multipath (section 2.1) phenomena and

increases the diversity of received signals.

One of the problems with MIMO is that the mobile receivers have limited space, making it more difficult to install numerous antennas on a mobile device. It is, therefore, easier to implement more antennas on a base station. One of the most common arrangement for MIMO is 4x2 for improved coverage. This is an arrangement of four transmitter antennas and two receiver antennas [4].

2.3 Antenna installation

When installing an antenna, certain installation techniques are used. Some are more effective, and this has an impact on the accuracy of the installation. The accuracy of the installation can have a noticeable impact on the performance of an LTE site. The parameters described in subsection 2.3.2 give some more details on the installation parameters.

2.3.1 Installation techniques

Different antenna installation techniques for various antenna adjustments are used. Adjusting the azimuth of an antenna can be done by pointing the antenna in the direction of a verified landmark. Another method is to use a compass, but the compass can be affected by a number of factors such as magnetic interference, which can result in possible installation faults. A Global Positioning System (GPS) can also be used to adjust an antenna. In [11], a Six Sigma Process Improvement Plan (PIP) methodology was used to drive a procedure to measure the accuracies of antenna installations. It was implemented by climbing Universal Mobile Telecommunications System (UMTS) towers, measuring the actual antenna azimuth and comparing them to the designed azimuths. The PIP indicated that current methods of azimuth installation had a minimum of 6° and a maximum of 10° of error.

A cell normally has sub-optimal coverage because of design and installation errors and these installation errors can occur because of the complex design of these antenna systems [12].

2.3.2 Installation parameters

An antenna is installed using certain prescribed design parameters such as azimuth, tilt (mechanical and electrical), transmitting frequency, polarisation and antenna height. Different measurement tools and techniques are used to assess the accuracy of the installation. Not all tools and techniques are accurate enough to install within the designed installation tolerance, which has an impact on the cell performance. [17]

The combined impact of the mentioned installation parameters makes it difficult to simulate coverage because of the various degrees of freedom.

The following describes the antenna installation parameters [17]:

- Electrical tilt is achieved by using a phase change at the feeder of the antenna. Therefore the shape of the antenna beam can be directed upwards or downwards without mechanical adjustment.
- Mechanical tilt is achieved changing the direction of the main lobe by physically adjusting the vertical axis of the antenna (refer to Figure 2.6(a)).
- Transmitting frequency: Each antenna is designed to perform optimally at certain transmitting frequencies, in which case it is important to install the correct antenna in order for the network to perform as designed.
- Polarisation means the antenna can be vertically or horizontally positioned on the mast. The polarisation of the antenna determines the rotational directivity of the radiation pattern. The rotational directivity can be vertical, horizontal or even at an offset from vertical or horizontal orientation.
- Azimuth is the horizontal direction of the main antenna lobe.

- HAGL is the vertical distance above the ground, refer to figure 2.6(b), where h_{TX} is the HAGL of the antenna.

(a) Mechanical tilt

(b) Antenna height h_{TX} above ground

Figure 2.6: Visual representation of mechanical tilt and antenna height h_{TX} above ground

The conditions of choosing the analysis parameters are firstly a parameter that can be adjusted. For the course of this study electrical tilt, transmitting frequency and polarisation needs to be fixed, leaving the mechanical tilt, azimuth and antenna HAGL as adjustable parameters. Due to the complexity of the analysis, only two of these parameters are chosen for analysis.

In [11], it is concluded that network performance is 10 times more sensitive to antenna tilt errors, than azimuth errors. Therefore tilt is the first analysis parameters.

The second parameter chosen is height adjustment. In the course of the study, each sector is analysed individually and thus co-cell interference is not taken into account. It will be more suitable to use height adjustment as an analysis parameter.

2.3.3 Polarisation impact on field strength

In a practical point-point or point-multipoint link, the polarisation of the receiving antenna will not always be the same as the incoming wave. This phenomenon is normally called polarisation mismatch. The total amount of power extracted from the incident wave will not be maximum if the polarisation angle differs and therefore a Polarisation Loss Factor (PLF) is introduced. Equation (2.4) gives the PLF (in power) with an angle difference of ψ_p (in degrees) between the incident wave and the receiving antenna. [5]

$$PLF = \left|cos\psi_p\right|^2 \tag{2.4}$$

In [30] the impact of polarisation diversity was tested. A vertical or horizontally polarised antenna was set up at a base station antenna, and the receiver antenna was $\pm 45^\circ$ dual polarised. The measurements were done at 920 MHz in an urban area. The PLF of the dual polarisation was about 6 dB and independent of the distance between the antennas. If there is a polarisation mismatch, it is important to take the polarisation mismatch into account in the link budget.

2.4 Fading

Fading is the effect that the environment through which the signal propagates has on the received signal. Fading is a change in the amplitude of the signal strength. In some cases, it is possible that some environmental conditions can cause an increase in signal strength, but the signal amplitude is mostly decreased in cases of fading. The following subsections discuss different factors that cause fading at a receiver [15], [4].

2.4.1 Multipath fading

Multipath fading is a phenomenon that appears when the transmitted signal reflects against different objects in the environment, and this causes the problem that the re-

ceiver receives different phases of the same signal. Rician fading takes the line of sight component into account, where Riley fading does not take the line of sight component into account [15], [4].

2.4.2 Other fading

Fading is common when the transmitter or the receiver starts to move away from each other, for instance in a car or a plane. When the car or plane rapidly moves away from or towards the transmitter, it is possible that the signal can undergo a Doppler Shift, which means the signal frequency and phases change. The Doppler effect normally causes data errors in phase-shift modulators [15], [4].

2.5 Diffraction

Diffraction can be explained by the Huygen's principle, which assumes that all electromagnetic waves that pass an obstacle form a new wave front off the edge of the obstacle. This phenomenon can also be called knife-edge diffraction. Diffraction attenuates the propagation waves and can be strong enough to have a significant impact. The attenuated signal area that is created by diffraction is called a shadow zone. Figure 2.7 shows how the propagation wave diffracts around a building [15], [4].

Path loss models used in a system to obtain coverage, should take the effect of diffraction and multipath into account. Empirical and statistical path loss models are studied in section 2.4 to understand and summarise the impact of the abovementioned effects.

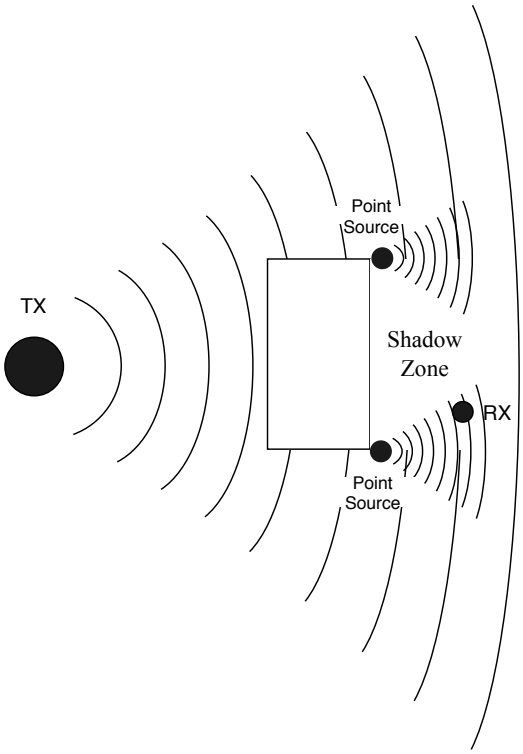

Figure 2.7: Diagram of the Huygens principle of diffraction points around an object

2.6 Location - and time probability

In [31], it is shown that the coverage area of the site depends on the covered area location probability. The field strength level normally follows a Gaussian distribution. This means that 50% of the area is above the coverage cut-off and the other 50% below the cut-off. If a covered area probability of 90% of the location is chosen, the location probability indicates a fair outdoor coverage. Ninety-five percent [95%] is considered to be a good quality coverage and 99% is considered to be an excellent quality coverage. The same logic can be used for time probability, where 50% time probability means an area is covered for 50% of the time and for the other 50% it is not. To simulate a practical environment, a Gaussian distribution was used and therefore a coverage area location - and time probability of 50% was used to simulate coverage predictions.

2.7 RF propagation models

Different propagation models exist, which can be divided into site-specific models, empirical models and a combination of empirical and site-specific models. Site-specific models are models that characterise the received signal strength using statistics. Empirical models require recorded data that consists of geometry, terrain profiles, locations and buildings [32]. Different types of models were investigated in order to select a suitable model to be implemented in this study.

In subsequent sections, several of these models will be presented. The Okumura-Hata model, which is an empirical model mostly used in urban areas for cellular planning [32]. The Longley-Rice model is a model that combines empirical data and site-specific data. The site-specific data are data such as terrain profile data. The Longley-Rice model makes a small adjustment for climate. Different time and location variability can be introduced to the model, but no correction factors are incorporated for clutter data [33]. The ITU-R P.1546 model can be implemented in two different ways, described in subsection 2.7.5. Table 2.3 shows the valid input parameter ranges of each propagation model.

Table 2.3: Valid input parameter ranges for propagation models

		Propagation Model		
Parameter	**Unit**	**Okumura Hata**	**Longley Rice**	**ITU-R P.1546-5**
Frequency	MHz	150-2000	20-20000	30-3000
Transmitter Height	m	30-200	0.5-3000	10-3000
Receiver Height	m	1-10	1-13	1-3
Receiver Distance	km	1-20	1-2000	1-1000

2.7.1 FSPL model

The FSPL model is used when there are no blocking objects between the transmitter and receiver. The Friis transmission equation gives the relationship between wavelength (frequency) and propagation velocity and is written as [33]:

$$\frac{P_R}{P_T} = G_T G_R \left(\frac{c}{4\pi f d}\right)^2 \tag{2.5}$$

From equation (2.5) the FSPL can be written as:

$$L_F\,(dB) = 10log\left(\frac{P_T}{P_R}\right) = -10log_{10}(G_T) - 10log_{10}(G_R) + 20log_{10}(f) + 20log_{10}(d) + k \tag{2.6}$$

In equations (2.5) and (2.6), G_T is the transmitter gain in dB; G_R is the receiver gain in dB; c is the speed of light; d is the distance between the transmitter and the receiver in m and f is the frequency in Hz. The constant k can then be defined in equation (2.7) as:

$$k = 20log_{10}\left(\frac{4\pi}{3\times 10^8}\right) = -147.56dB \tag{2.7}$$

for the frequency in Hz and the distance in m.

2.7.2 Two-ray ground reflection model

The two-ray ground reflection model considers both the direct path as well as the ground reflected propagation path between transmitter and receiver. This is a more accurate way of predicting the large-scale signal strength over longer distances (several kilometres).

The received power at a distance d (m) from the transmitter can be determined as P_R using the following equation:

$$P_R = P_T G_T G_R \left(\frac{h_t^2 h_r^2}{d^4}\right) \tag{2.8}$$

G_T is the transmitter gain in dBm, G_R is the receiver gain in dBm, ht is the transmitter antenna HAGL, h_r is the receiver antenna HAGL and P_T is the transmitter power.

Equation (2.9) contains the same parameters.

The path loss using the 2-ray model can be expressed using equation

$$PL(dB) = 40log(d) - [10log(G_T) + 10log(G_r) + 20log(h_t) + 20log(h_r)] \tag{2.9}$$

2.7.3 Longley-Rice ITM model

The Irregular Terrain Model (ITM) is one of the models that are further investigated as part of this study. This path loss model is applicable to any frequency above 20 MHz. The model can be implemented on an actual terrain path of which the terrain profile is present or pre-defined terrain profiles which represent median terrain characteristics of a specified terrain. The ITM uses the two-ray reflection theory and the attenuation caused by diffraction to calculate PL in line-of-sight paths [34].

The Longley-Rice ITM model was used within the following parameter ranges in Table 2.4:

Table 2.4: Parameter ranges for the Longley-Rice ITM model

Parameter	**unit**	**Range**
Frequency	MHz	20-20000
Receiver Height	m	1-13
Transmitter Height	m	0.5-3000
Receiver Distance	km	1-2000
Surface refractivity	N-units	250-400

The limitations include that the total mechanical tilt cannot be more than 12° and the distance between the transmitter and receiver antennas cannot be less than a tenth or more than three times the smooth-earth distance (a distance on the earth's surface without any obstructions) [34].

2.7.4 Okumura Hata model

The Okumura Hata model is based on the Okumura model, which is a well-established empirical model for high-frequency bands. The original Okumura model was designed to be implemented for frequencies only up to 3 GHz, but the Okumura Hata model can calculate path loss for frequencies higher than 3 GHz.

The path loss in dBm of the Okumura Hata model can be calculated using [35]:

$$PL = A_{fs} + A_{bm} - G_b - Gr, \tag{2.10}$$

where A_{fs} is the free space attenuation, A_{bm} is the median path loss of a specific path, G_b is the transmitter antenna height gain factor and G_r is the receiver antenna height gain factor, all in dBm. Each of the above-mentioned factors can be extended and are defined in [36].

If the model is implemented in urban areas, it is also divided into large city and medium city. G_r is differently defined for medium cities and large cities and incorporates propagation factors such as the distance between transmitter and receiver (d), the frequency (f), the transmitter antenna height (h_b) and the receiver antenna height (h_r).

2.7.5 ITU-R P.1546-5 model

The ITU-R P.1546-5 method uses empirically derived field-strength curves which are functions of percentage time, frequency, antenna height and distance between transmitter and receiver. The field-strength values can be obtained by interpolation or extrapolation using the curves from the ITU specification. To account for terrain clearance and terminal clutter obstructions, corrections are made to the field-strength values as part of the calculation.

Using the equations from ITU-R P.1546-5 (annexure 5, paragraph 9), the correction factor for a receiver height (that differs from the reference receiving antenna height of 10m above ground level) can be calculated [37].

Corrections to the field strength curves are made if the location probability is not 50%. This correction is valid for terrestrial propagation only. The field strength curves in the recommendation account for field strength time probability values of 50%, 10% and 1%, therefore an interpolation algorithm (ITU-R P.1546 paragraph 7) can be used to obtain field strength time probabilities. [37]

If the coverage area is over or adjacent to land where there is clutter, a correction factor is used, except if the terminal is higher than a frequency-dependent clearance height above the clutter [37].

There are two implementations of the ITU-R P.1546 model. The following paragraphs explain the database - and terrain model implementations in more detail.

The database model is a point-to-area propagation model and does not take any terrain data into account. The field strength values can be read from the recommendation in [37] for certain frequencies.

The terrain model is a point-to-point propagation model. For every calculation from the transmitter to the receiver, a new terrain profile is created from which correction terms and effective transmitter height can be calculated. There are different techniques for determining the effective height of the transmitter. The effective height on radii was calculated every 10° for distances 3-15 km from the transmitter. Interpolation was done to obtain the other effective height calculations [37]. The effective height per radial is given by the equation below and illustrated in Figure 2.8.

$$h_{eff_{Base}} = \begin{cases} h_{Base_{terr}} + h_{Base_{ant}} - h_{Mobile_{terr}} & \text{if } h_{Base_{terr}} > h_{Mobile_{terr}} \\ h_{Base_{terr}} & \text{otherwise} \end{cases} \tag{2.11}$$

where $h_{eff,Base}$ is the calculated effective height; $h_{Base,ant}$ is the transmitter HAGL; $h_{Mobile,terr}$ is the mobile terminal HAGL and $h_{Base,terr}$ is the height of the LTE transmitter and receiver of the base station above mean sea level (AMSL). The receiver AMSL is the height of the receiver above mean sea level. The mean efficient height of the site is the average of all the radials.

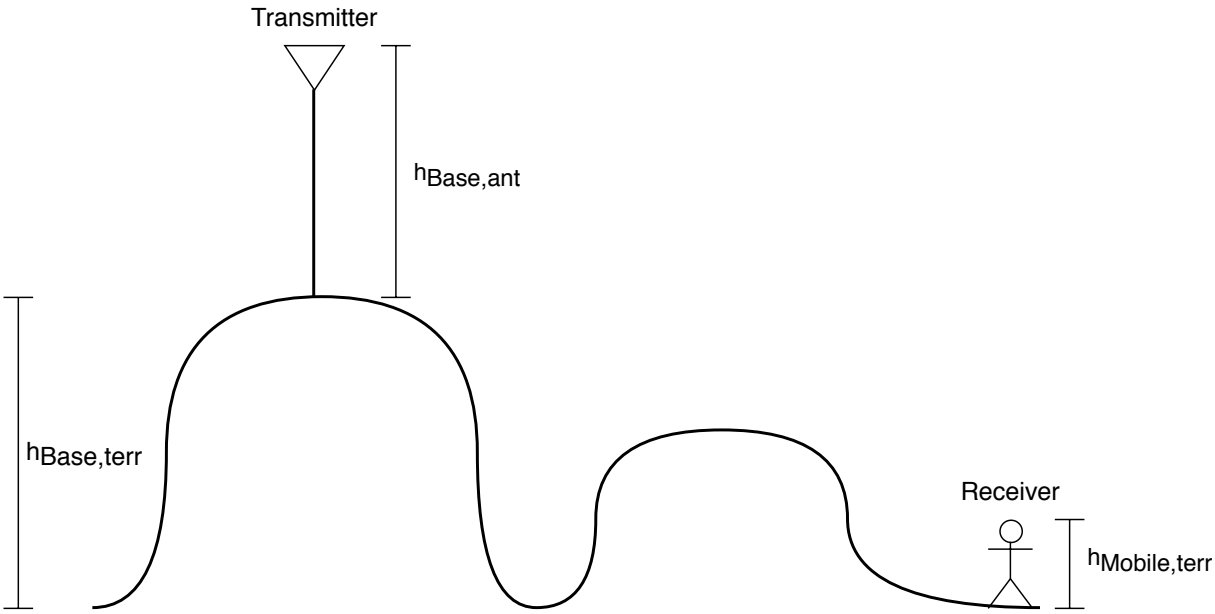

Figure 2.8: Calculating the effective antenna height

The terrain model takes the effective height into account when a field-strength analysis is done. The database model takes no correction factors into account and implements a time - and location probability of 50%.

It is possible for the effective height calculation to have a negative value. The effect of diffraction should then be taken into account, and a correction factor is added. This clearance factor is dependent on digital elevation model data [37].

2.7.6 ITU-R P.1546-4/5 differences

The following are changes made in version 4 to version 5 ([38], [37]):

- The height of the transmitter antenna above the clutter at the antenna is taken into account when the land path is shorter than 15 km.

- If the transmitter antenna on which there is clutter is over land, a new correction should be applied. The height of the transmitter antenna above ground is not taken into account. Equation (2.12) defines the correction factor:

$$C_f = -J(v) \tag{2.12}$$

where,

$$J(v) = \begin{cases} \left[6.9 + 20log\left(\sqrt{(v-0.1)^2+1} + v - 0.1\right)\right] & \text{for } v > -0.7806 \\ 0 & \text{otherwise} \end{cases} \tag{2.13}$$

$$v = K_v\theta_{eff}(-h_1/9000)^\circ \tag{2.14}$$

where, K_v = 1.35 for 100 MHz, K_v = 3.31 for 600 MHz, K_v = 6.00 for 2000 MHz, h_1 is the transmitting antenna height and θ_{eff} is the positive terrain clearance angle.

- A correction is added for the difference between the two antenna heights above the ground. The correction factor can be defined as:

$$C_f = 20log\left(\frac{d}{d_{slope}}\right) \tag{2.15}$$

Where d is the horizontal distance and d_{slope} is the slope distance on the curvature of the earth.

- A new method is added to define the field strength for distances smaller than 1 km.

- Annexure 8 was added to the newer version to give the Okumura Hata equations for field strength prediction for mobile services in an urban area. It also describes that version 5 of the ITU-R P.1546 will give the same results as the Okumura Hata model for distances up to 10 km.

The information on the difference between ITU-R P.1546 version 4 and 5 is described in order to know if it would be feasible to use version 4, which is the version available to be used in the simulations described in Chapter 3.

2.8 Network performance metrics

There are various types of network performance metrics, such as network capacity, coverage and data throughput. The cell performance in this study was measured by coverage, which is the total of all the Radiated Signal Received Power (RSRP) measurements above the outdoor threshold as shown in equation (2.16).

2.8.1 LTE reference signal

LTE network field strength can be measured by RSRP. RSRP is the average received power of a single Reference Signal resource element of an LTE signal. The resource element carries cell-specific signals within the measured bandwidth [39]. RSRP is measured in Watt, but should be translated to field strength (dBμV/m) for the implementation of the coverage cut-off values in the simulation data. The RSRP value is measured at the position where the receiver device operates. The height of the measurement depends on the height where the device operates.

According to the ECC report [40] on LTE coverage measurements as well as in the 3GPP TS 36.304 specification [41], the threshold for RSRP measurements should not be lower than -110 dBm when LTE coverage measurements are made.

According to the ITU recommendation ITU-T E.811, the minimum level of RSRP needed for LTE coverage is -105 dBm for outdoor coverage and -88 dBm for indoor coverage [42]. Equations (2.16) and (2.17) show the logic of how the coverage is determined using the RSRP values (0 = no coverage and 1 = coverage).

$$C_{outdoor} = \begin{cases} 0 & \text{RSRP} < -105dBm \\ 1 & \text{RSRP} \geq -105dBm \end{cases} \tag{2.16}$$

$$C_{indoor} = \begin{cases} 0 & \text{RSRP} < -88dBm \\ 1 & \text{RSRP} \geq -88dBm \end{cases} \tag{2.17}$$

For the importance of the study, the concern lies only with the cut-off values themselves. The cut-off value is used to be able to abstract the wanted LTE receiver signal strength, and obtain coverage data.

Received Signal Strength Indicator (RSSI) can be calculated using (2.18). RSSI is the quality predictor for RSRP, which provide information about total wide-band power and it includes all thermal noise and interference. Without noise or interference RSSI can be calculated as [39]:

$$RSSI = 12 * N * RSRP \tag{2.18}$$

RSRP is given by (2.19). N is the number of reference signal blocks across the RSSI and it depends on the bandwidth.

$$RSRP = RSSI - 10 * log(12 * N) \tag{2.19}$$

The RSRP value is measured in dBm, but can be converted to a dBμV/m value by using equation (2.20) [5]. The RSRP values range from -140 dBμV/m to -44 dBμV/m.

$$P(dBm) = -75.07 + G(dB) - 20log_{10}(f) + E(dB\mu V/m) \tag{2.20}$$

2.8.2 Terrain roughness

Terrain roughness is a measure of how much the terrain height of a specific terrain changes. It was found in the literature that there are different ways to describe terrain roughness.

ITU-R P.452-12 implementation

In ITU-R P.452-12 the terrain roughness parameter is defined by h_m (m), which is the maximum height of the terrain above the smooth surface of the earth on a path between the transmitter and the receiver as calculated in equation (2.21) [43].

$$h_m = \max_{i=i_{lt}}^{i_{lr}} \left[h_i - (h_{st} + m \cdot d_i) \right], \tag{2.21}$$

where i_{lt} is the index of the coordinate at a distance d_{lt} from the transmitter, i_{lr} the index of the coordinate at a distance d_{lr} from the receiver, h_i is the height of the terrain point *(i)* AMSL in meters, h_{st} is the height of the smooth-earth surface (AMSL) at the transmitter, m is the slope (m/km) of the least-squares surface relative to mean sea level and d_i is the great-circle distance of the terrain point *(i)* from the transmitter.

Figure 2.9 shows an example of the smooth-earth surface and terrain roughness parameter.

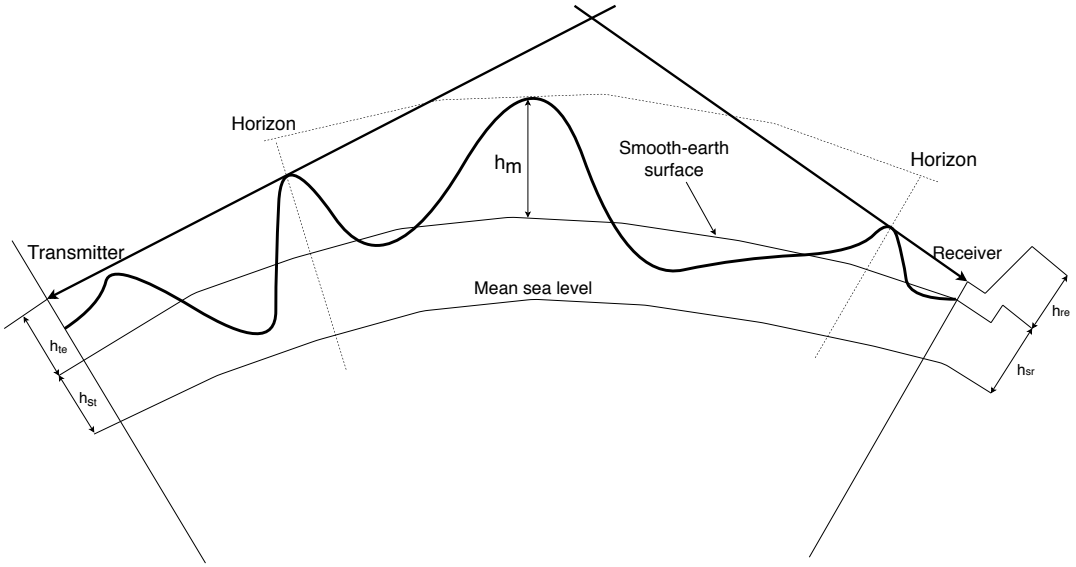

Figure 2.9: An example of the smooth-earth surface and terrain roughness parameter

The parameters h_{te}, h_{re} and h_{sr} are used to calculate the slope m. The calculations can be seen in [43].

Longley Rice ITM model [44]

In this implementation, the deviation in height was calculated as the difference between the 10% and 90% interquartile range between the transmitter and the receiver on a specific path; this means it was calculated for the middle 80 % of the path. The next step is removing the 10% of the highest and 10% of the lowest height values. The first calculation to obtain the terrain roughness parameter or σ_h is the least mean square regression line ($h(x)$) of the heights found in this area (equation (2.22)).

$$h(x) = \overline{h} + m(x - \overline{x}) \tag{2.22}$$

$\overline{h}$ can be obtained using equation (2.23):

$$\overline{h} = \frac{\sum_{i=1}^{i_{total}} h_i}{i_{total}} \tag{2.23}$$

The standard deviation from this mean value was calculated at each point (N), which becomes δ_h (equation (2.24)) [44].

$$\delta_h = \sigma^2 = \sum \frac{(x-\mu)^2}{N} \tag{2.24}$$

To obtain σ_h or the terrain roughness factor, the square root of δ_h is determined using equation (2.25).

$$\sigma_h = \sigma = \left[\sum \frac{(x-\mu)^2}{N}\right]^{\frac{1}{2}} \tag{2.25}$$

The Longley Rice ITM model is well explained in [44], and there is enough information available for it to be implemented in the simulation. However, the ITM model requires several assumptions that makes implementation difficult.

2.9 Antenna radiation pattern interpolation methods from 2D to 3D

An antenna radiation pattern contains both an azimuth and elevation power radiation pattern. If it is possible to obtain the gain values of these two-dimensional patterns, a mathematical technique is used to obtain the three-dimensional radiation pattern. Two techniques were researched and are discussed [45].

2.9.1 Conventional method

The conventional method or, as referred to in [46] as the product algorithm is a product of the normalised two-dimensional azimuth and elevation patterns. As mentioned in [46], this is a very good approximation for the main lobe of the radiation pattern,

but the main lobe is normally reduced slightly. This means the method underestimates the radiation pattern main lobe. The method is reflected in the following equation:

$$G(\phi,\theta) = G_H(\phi) + G_V(\theta) \tag{2.26}$$

where $G(\phi,\theta)$ is the power gain value (dB) of the three-dimensional power radiation pattern. $G_H(\phi)$ and $G_V(\theta)$ are the azimuth and elevation power gain values (dB) respectively.

2.9.2 Weighted technique

The weighted technique, also known as the Novel technique (named by authors in [45]) [47], uses weighted gain values to extrapolate the three-dimensional gain. Equation (2.27) shows the equation used to calculate the radiation gain of the three-dimensional power radiation pattern with the Novel technique [47].

$$G(\phi,\theta) = \underbrace{\frac{\omega_1}{\sqrt[k]{\omega_1^k + \omega_2^k}}}_{A_1} G_H(\phi) + \underbrace{\frac{\omega_2}{\sqrt[k]{\omega_1^k + \omega_2^k}}}_{A_2} G_V(\theta) \tag{2.27}$$

$$\omega_1(\phi,\theta) = vert(\theta)\cdot[1 - hor(\phi)], \omega_2(\phi,\theta) = hor(\phi)\cdot[1 - vert(\theta)]$$

ω_1 and ω_2 are the weighted functions. k is a normalization parameter which has the best results if defined as $k = 2$. A_1 and A_2 (the divisors) vary between 0 and 1. $vert(\theta)$ (degrees) is the vertical power radiation pattern angle and $hor(\phi)$ (degrees) is the horizontal power radiation pattern angle respectively.

In [45], the conventional method suppresses the side lobes in the vertical dimension, whereas the Novel technique causes the main lobe to deform. Due to the fact that the main lobe has a more significant impact on the coverage results, the conventional method is preferred in the research, because the three-dimensional pattern gain is closer to realistic values.

2.10 Related work

2.10.1 The effect of antenna orientation errors on UMTS network performance

A study was done in [11] on the effects of antenna orientation errors on UMTS network performance. The performance metrics used were coverage area, coverage quality of service (QoS) and soft hand-off. The impact of antenna tilt and azimuth were tested, and it was found that the tolerance for tilt can be estimated to $\pm 0.5^{\circ}$ and the azimuth tolerances should be estimated to approximately between 6° and 8°.

From the results in [11], it was found that a 3° antenna tilt error can decrease the coverage by 100% and an azimuth error of 30° can have an impact on a coverage of up to 30%.

2.10.2 Impact of base station antenna height and antenna tilt on performance of LTE systems

The impact of the base station antenna height and antenna tilt was investigated on LTE system performance, using a simulation method in [48]. The 3GPP TR 36.942 Urban model was used in this paper, which uses no topographical height information or clutter data [49]. A seven-cell reuse system with three sectors per cell was simulated in an urban area where the sites were 500 m apart. It was shown that as antenna height increases, signal to interference and noise ratio (SINR) decreases because of increased coverage; therefore, cell-edge interference increases [50]. Antenna tilt has been found to improve SINR and help with interference management.

2.10.3 Effect of vertical tilt on the horizontal gain

Antenna vertical tilt directs the RF pattern null points to the horizontal plane, which ensures less propagation in the neighbouring cells resulting in less interference. Electrical tilting is sufficient for use in smaller cells, but mechanical tilting results in decreased coverage in the central direction of the beam and in increased coverage at the side lobes of the beam [48].

The effect of antenna tilt on the sensitivity of height adjustment has been evaluated using Monte-Carlo simulations with a static radio network planning tool in [51]. A Macro Cell propagation loss model applicable to urban or suburban areas was used. The propagation loss was calculated using the base station antenna height, frequency and the distance between the receiver and transmitter. It was found that when choosing an effective antenna tilt, it can overcome performance loss due to sub-optimal height adjustment. No digital elevation model (DEM) or terrain models have been integrated into the study.

2.10.4 Notch effect of vertical tilt

The impact of mechanical antenna downtilt on the design of a wireless system was studied in [52]. It was found that when a directional antenna is down tilted enough, it forms a notch (an intentional indent in the coverage area) which can have a reduced co-interference impact between neighbouring cells. The impact of the notch effect can be seen in Figure 2.10. The notch appears when vertical downtilt increases; the vertical radiation pattern gain increases. The notch forms when the vertical radiation pattern gain increase is more than the horizontal gain increase. Figure 2.10 shows how the radiation pattern from the transmitter does not coincide with the interfering transmitter (IT 1).

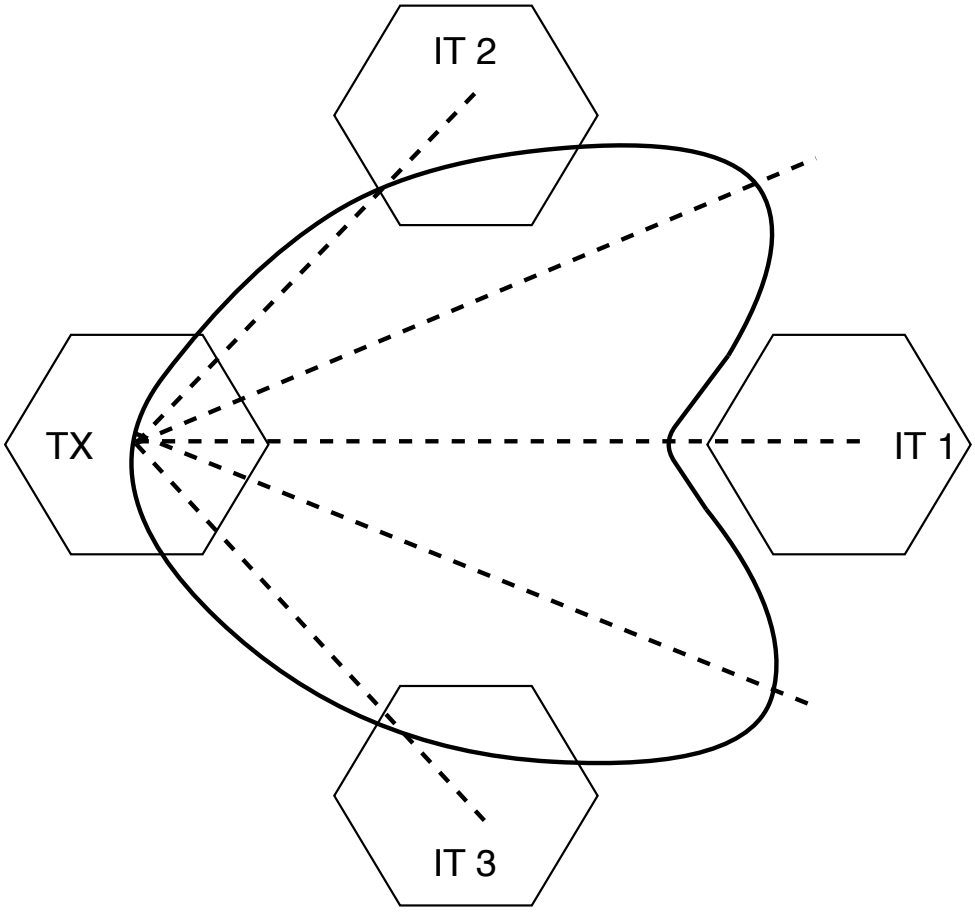

Figure 2.10: Impact of notch effect on co-frequency interference

2.10.5 Related work summary

In [11], the impact of antenna tilt and antenna azimuth was tested on an UMTS network performance. The impact of tilt was significant, which supports the reason for further study. In [48], the impact of antenna tilt and height was tested on network interference. It was found that the tilt can be used to manage network interference.

In [48], a study was done that confirmed the impact of choosing effective antenna tilt to overcome performance loss due to sub-optimal height adjustment. It was found that tilt can be used to "compensate" any performance discrepancies due to height error. The study did not take any terrain models into account, which supports the need for a study on tilt and height impact that take terrain into account.

In [52], a study was done to test the impact of mechanical downtilt on the notch effect.

It was found that with optimal tilt settings, the notch effect can decrease interference. This supports studying the sensitivity of tilt, due to the impact it can have on optimal coverage.

It can be seen that no study was done taking terrain data into account. There was also no study done using the ITU-R P.1546 propagation model.

2.11 Conclusion

This chapter introduced the different concepts related to this research, followed by a literature review discussing all the fundamentals necessary to support the research. The necessary mathematical equations and definitions to be used in the simulations were defined in this chapter.

In-depth information was given about LTE, including frequencies, channel information, modulation and duplexing techniques. The study is based on an LTE site and it is therefore especially important to understand the impact that frequency deviation can have on the performance of an LTE system and to understand duplexing techniques and how they are implemented in the UL and DL of an LTE network.

Research was done on different types of antennas for better understanding. Antenna installation techniques and parameters were also discussed. It must be understood that there are various parameters that can influence coverage and what the combined effect of these parameters will be. Because of the complexity of the combined effect of these parameters, only the impact of tilt and height are evaluated for a single antenna source on coverage.

Multipath, diffraction, location probability and time probability were discussed due to their importance in RF propagation models. Various propagation models were discussed in order to choose which model would be suitable for simulation.

It was also important to know which metrics will be used to obtain coverage by analysing LTE performance parameters. LTE field strength are measured by RSRP (dBμV/m). A technique to find the coverage cut-off threshold was also discussed.

Two methods were studied (conventional method and weighted technique) to be able to obtain the values of a three-dimensional radiation pattern. Given the deformity of the main lobe of the antenna power radiation pattern from using the weighted method, the conventional method is preferred.

Four different related studies were presented. These studies included various impacts of height and tilt adjustment errors using different technologies. None of these studies considered or implemented the ITU-R P.1546 propagation model.

The literature presented in this chapter offers an understanding of the research problem. It is now possible to design and implement the simulation software with appropriate simulation parameters that address the research problem.

Chapter 3

System model

This chapter offers a description of the system model that was implemented in order to test the impact of tilt and height adjustment on an LTE base station coverage. The simulation software methodology and the parameters that were used in the simulation software are discussed. The simulation software model is described using flow diagrams and tables. An explanation of why certain assumptions were made, is provided. All the equations and calculations used in the simulations are explained, together with the methods on how the input data and parameters for the simulation were chosen.

3.1 Introduction

A simulation model was used to test the effect of tilt and height adjustment on coverage. To obtain the coverage of each sector of a transmitter site, each sector was modeled separately and was analysed to determine the impact of the tilt and height adjustments on coverage. The terrain around each site was also analysed to correlate the impact of these adjustments with changes in the terrain. To obtain the coverage of an LTE base station, the following must be done:

The first step is to calculate the field strength for one receiver. All the receivers around the transmitter site that met the coverage threshold were counted to obtain the coverage for one sector for each of the adjustment combinations.

There were 10 height adjustments (5 m to 15 m in 1 m increments) and there were 150 tilt adjustments (-5° to 10° in 0.5° increments). The number of receivers was dependent on the resolution of the DEM. Figure 3.1 explains how the simulation model for a single path between transmitter and receiver was implemented.

The reference site used to validate results had an antenna height of 10.9 meters. The height adjustments simulated where therefore chosen 5 m higher and 5 m lower respectively to test the impact of height error above and below the reference site antenna height.

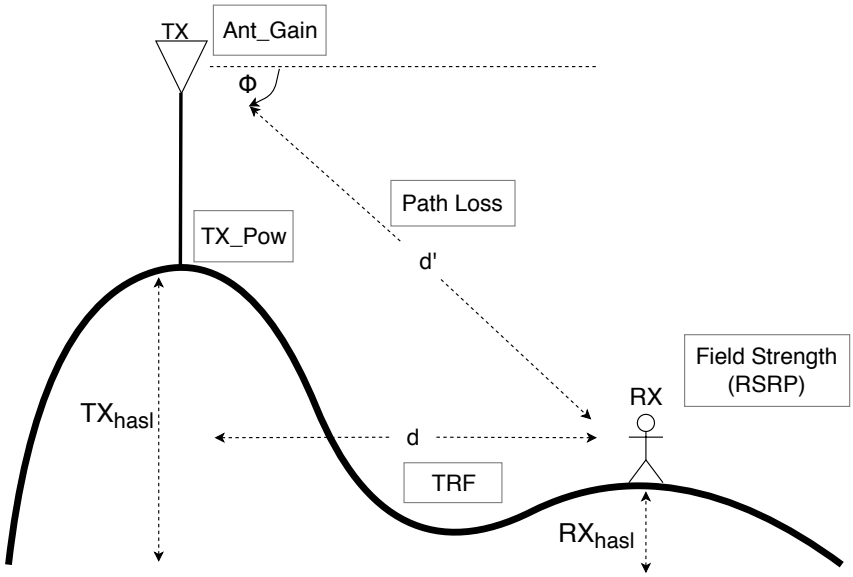

Figure 3.1: Single path model between transmitter and receiver

For every antenna adjustment, calculations were done by using the transmitter power (TX_{Pow}), antenna gain (Ant_{Gain}) and Path Loss in combination with the position of the transmitter and receiver (relative angle (ϕ) in °, distance (d') in m and heights in m) to calculate the field strength at the receiver. Distance (d) is the flat earth distance between the transmitter and receiver. The Terrain Roughness Factor (TRF) and the effective height (Eff height) were calculated for every path by using the information of

the path between the applicable transmitter-receiver pair.

3.2 Simulation model

In Appendix A, Figure A.1, a full layout of the simulation software model can be seen.

The simulation software model is described by flow diagrams which are marked according to a sub-diagram and block convention. For example, the main diagram is named block 1.0, its sub-diagram is block 1.1, and the sub-sub diagram has the convention of block 1.1.1.

The following section defines the design of the simulation software that is used to obtain the experiment results. As explained in Chapter 2, the RF propagation model that was used in the simulation, which is the ITU P.1546 model, for its broad input parameters, variety of correction factors and ability to take terrain data into account. The software is designed to implement the ITU-R P.1546 propagation model, which was used to test the impact of LTE antenna adjustments on cell coverage over different terrains. Flow diagrams describe the flow of the program using different levels of logical flow.

3.2.1 The main program (Level 1)

The program was written to be able to repeat the simulation for more than one LTE site in order to obtain multiple results for a complete statistical analysis. The following describes how the logical flow of the program works:

Figure 3.2 is the highest level (Level 1) flow diagram describing the logical flow of the program. Block 1.0 is the process of filtering the sites found in an open database. The process was defined in more detail in section 3.6. Block 2.0 is the loop enumerating through all the defined LTE sites. Block 3.0 is the obtainment of important informa-

tion of each grid point within the defined area (maximum covered area) around the transmitter. This data was computed and stored. The information was stored as geographical locations. Blocks 4.0 and 5.0 are the two most important output variables, namely site terrain data and site coverage. The logic operator "Sites Enumerated" checks whether all of the sites have been enumerated.

Block 6.0 is the process of putting the obtained data through a statistical analysis, where the data can be analysed and results obtained.

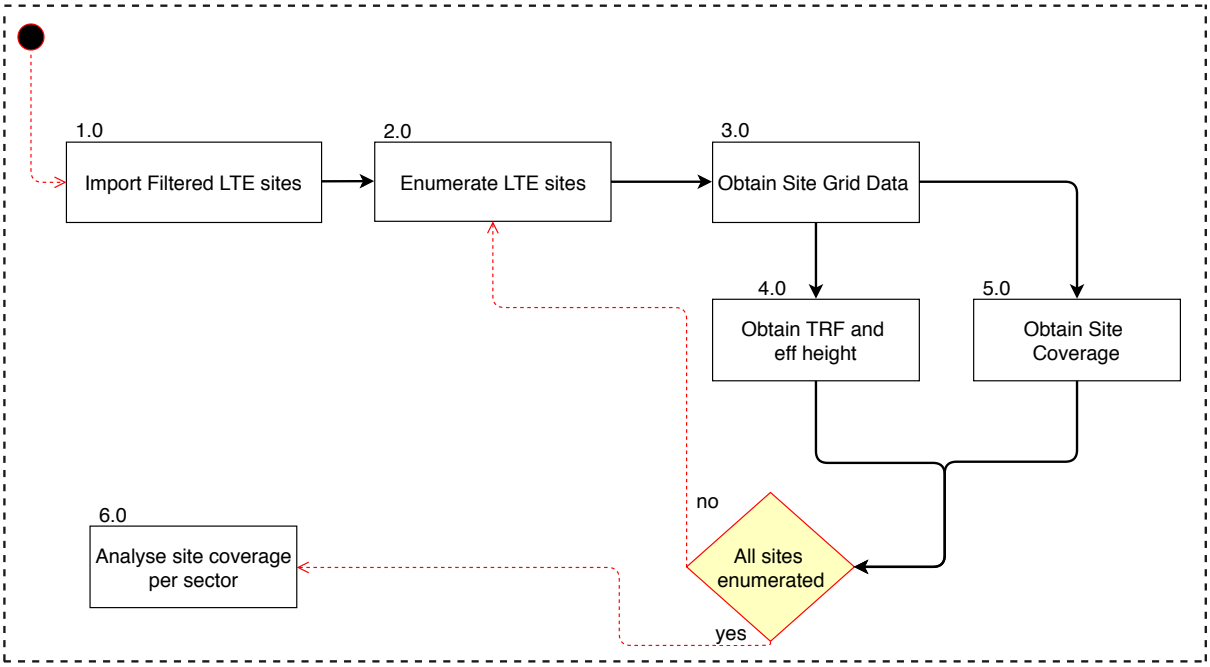

Figure 3.2: Level 1 flow diagram

Table 3.1 gives a description of each of the LTE sites imported into the simulation software. The sites are stored using a structure that defines the important variables of each LTE site.

Table 3.1: LTE sites Matlab structure description

Variable	**Description**	**Unit**	**Type**
Name	LTE site name	n/a	string
Site ID	Site identification number	n/a	integer
AMSL	Site height above mean sea level	m	double
Sector Azimuths	Sector main beam angles	°	1x3 Array (double)
Sector count	Number of sectors	n/a	integer
lat	Site latitude	decimal format	double
lon	Site longitude	decimal format	double
latdms	site latitude	degrees minutes seconds format	1x3 Array (double)
londms	site longitude	degrees minutes seconds format	1x3 Array (double)
latbounds	site area boundary square latitudes	n/a	1x5 Array (double)
lonbounds	site area boundary square longitudes	n/a	1x5 Array (double)
frequency	site center frequency	MHz	double

Table 3.2 gives a description of how the antenna pattern is saved in the simulation software. The horizontal and vertical gain pattern are stored separately in an array, together with inverse (reflected over a 180° line running from 270° to 90°) of the vertical pattern. The inverse pattern is needed when tilt is implemented on the site. The horizontal gain pattern is of size 360x2, because the horizontal pattern has a column for the degrees and a column for each gain value per degree. The vertical pattern has a dimension of 181x2, because the vertical pattern obtains only 181 gain values, where the first column is the number and the second column consists of the value. The vertical pattern is only measured for 180° (from -90° to 90°) and it is the same for every azimuth angle.

Table 3.2: Anenna pattern data storage description

Variable	**Description**	**Type**
Hor_{Gain}	Horizontal gain pattern	Array (double)
Ver_{Gain}	Vertical gain pattern	Array (double)
Ver_{Inv}	Inverse Vertical gain pattern	Array (double)

3.2.2 Grid data (Level 2)

Figure 3.3 is a level 2 flow diagram breaking down block 3.0. This flow diagram enumerates through the site sectors (block 3.1), adjusts the antenna parameters (tilt and height (block 3.2)) and enumerates through the grid points in each sector (block 3.3). The following computations have to be done for every grid block:

- Block 3.4: Calculate the great circle distance for every grid point.
- Block 3.5: Calculate the effective radiated power (ERP) of the specific bearing from the transmitter to the specific receiver grid point.
- Block 3.6: Calculate the Path Loss using the ITU-R P.1546 propagation model and calculate the field strength at the receiver grid point using a link budget (sector 3.9).

The logical operators after block 3.6 are a check to see if all the grids for each sector have been iterated; all the antenna parameters were swept, and the three sectors were enumerated.

Table 3.3 describes the input and output variables of the function that implements the tilt adjustment of the antenna. The output is a shifted vertical pattern array.

Table 3.3: Input/Output variables to adjust the antenna tilt

Variable	**Variable type**	**Description**	**Unit**	**Type**
Direction	Input	0: downtilt, 1: uptilt	n/a	Boolean
Number	Input	Amount of tilt	°	Integer
Ver_{Gain}	Input	Vertical gain pattern	n/a	Array (double)
Ver_{Inv}	Input	Inverse vertical gain pattern	n/a	Array (double)
Shifted_{Ver}	Output	Shifted vertical gain pattern	n/a	Array (double)

Table 3.4 describes the input and output variables of the function that implements the azimuth adjustment of the antenna. The output is a shifted horizontal pattern array. The direction of rotation is not given, because the azimuth is always adjusted clockwise.

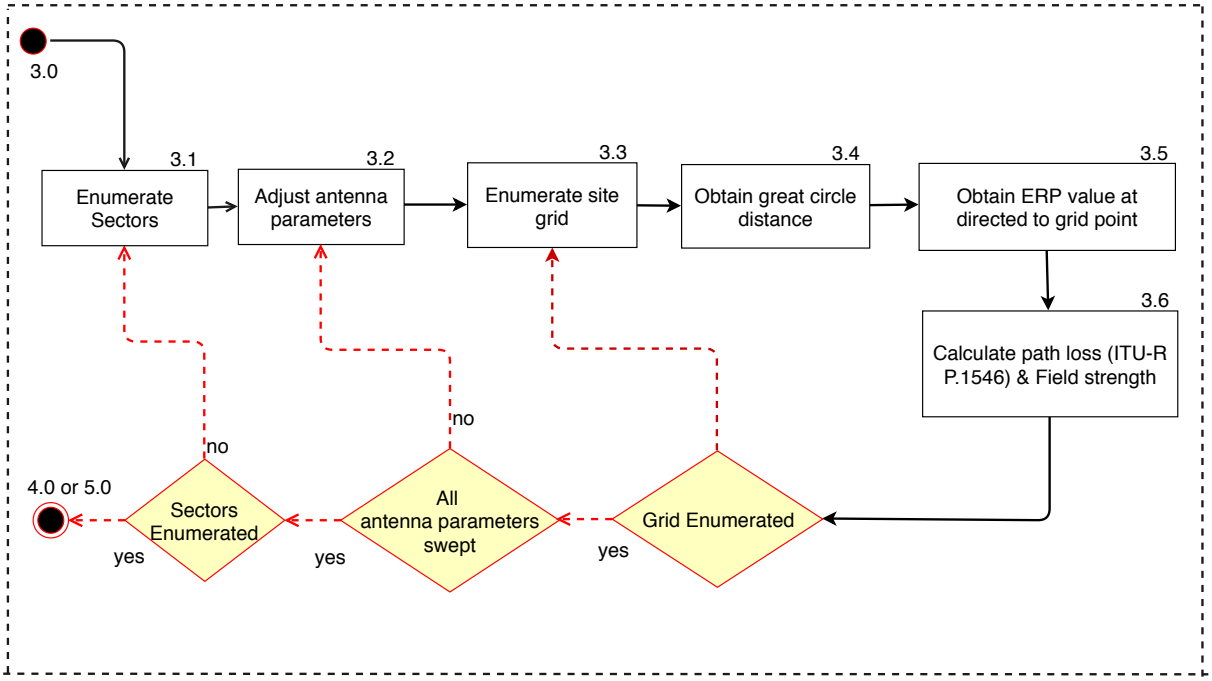

Figure 3.3: Level 2 flow diagram: Obtain grid data

Table 3.4: Input/Output variables to adjust the antenna azimuth

Input Variable	**Variable type**	**Description**	**Unit**	**Type**
Number	Input	Amount of horizontal shift	°	Integer
Hor_{Gain}	Input	Horizontal gain pattern	n/a	181x1 Array (double)
Shifted_{Hor}	Output	Shifted horizontal gain pattern	n/a	181x1 Array (double)

3.2.3 Site coverage (Level 2)

Figure 3.4 is a Level 2 flow diagram describing the steps to compute the coverage of a site. The first step (block 5.1) is to enumerate through the sectors, threshold each of the grid points as covered or not covered (blocks 5.2 and 5.3).

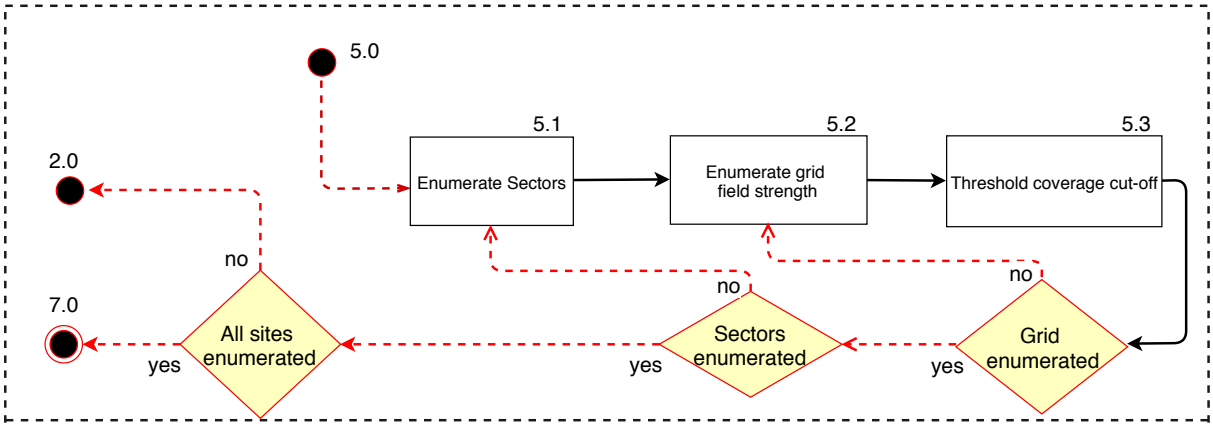

Figure 3.4: Level 2 flow diagram: Calculate site coverage

3.2.4 Pattern gain (Level 3)

The Level 3 flow diagram in Figure 3.5 defines the two steps (blocks 3.5.1 and 3.5.2), which is to first calculate the bearing angle (Receiver (RX) phi (block 3.5.1)) and to then obtain the power gain (block 3.5.2) of the propagation pattern at that specific bearing angle.

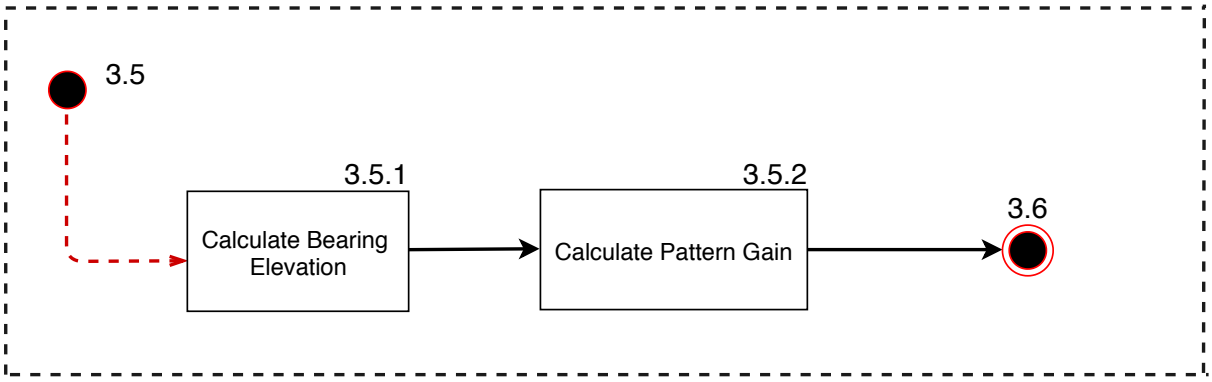

Figure 3.5: Level 3 flow diagram: Obtain parameters for pattern gain

3.2.5 Antenna adjustments (Level 3)

Figure 3.6 defines the steps to adjust the antenna parameters and transform the two-dimensional pattern files as necessary per antenna adjustment. Block 3.2.1 is the height

adjustment from 5 m to 15 m in 1 m increments; block 3.2.2 adjusts the tilt between -5° and 10° in 0.5° increments; block 3.2.3 transform the elevation pattern array as per tilt adjustment; 3.2.4 is the adjustment of the azimuth (shifting azimuth to the next sector); block 3.2.5 enumerates through the sectors and the azimuth pattern array is then transformed accordingly.

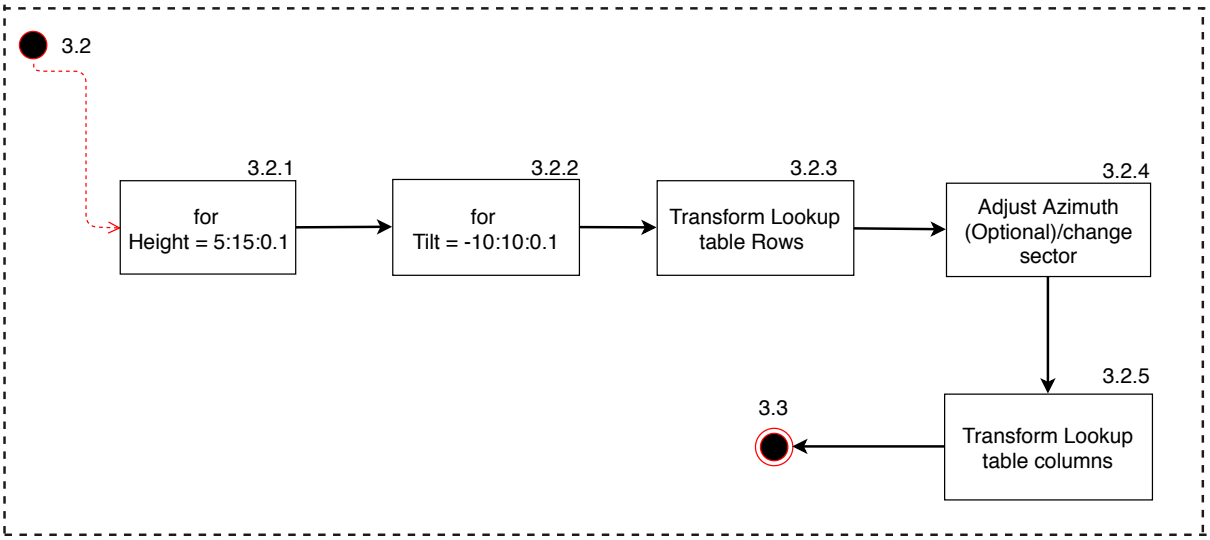

Figure 3.6: Level 3 flow diagram: Adjust simulation parameters

3.2.6 Terrain data (Level 2)

In Chapter 2, subsection, 2.7.1 two methods in obtaining the TRF was discussed. As mentioned, there is not enough information on the ITU method to be correctly implemented, therefore the Longley Rice ITM was used to calculate the TRF.

The effective height calculation is defined in Chapter 2, subsection 2.6.5. This effective height calculation was used as implemented in the ITU-R P.1546 model.

Figure 3.7 explains the steps to calculate the parameters defining the terrain around a site. The two terrain parameters (TRF and effective height) were calculated for every sector. The calculation was done on every degree of a sector and then averaged. Block 4.1 enumerates through every sector. Block 4.2 is the enumeration through every degree within the sector and block 4.3 is the calculation of the two terrain parameters.

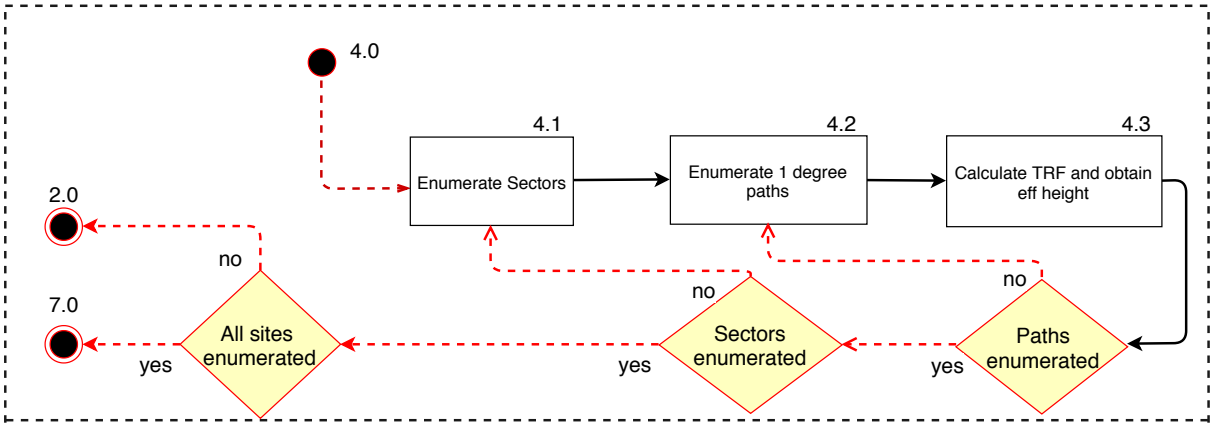

Figure 3.7: Level 2 flow diagram: Obtain terrain data

The next subsection is a breakdown of block 4.3, which describes the logic of obtaining the values of each parameter at each degree per sector. These values are stored to be analysed (more information on analysis in Chapter 5).

Terrain roughness factor and effective height

Figure 3.8 explains the steps to calculate the terrain roughness factor as per the ITM definition in Chapter 2. The first step is to remove the first and last 10% of data points from the path between the transmitter and the grid point (block 4.3.1). The effective height of the path is then obtained by the ITU-R P.1546 implementation (block 4.3.2). This value is also stored for analysis. The standard deviation is shown in block 3.7.3, after which the square root of the standard deviation is calculated (block 3.7.4), which defines the terrain roughness factor for that data point (refer to equation 2.22 in Chapter 2).

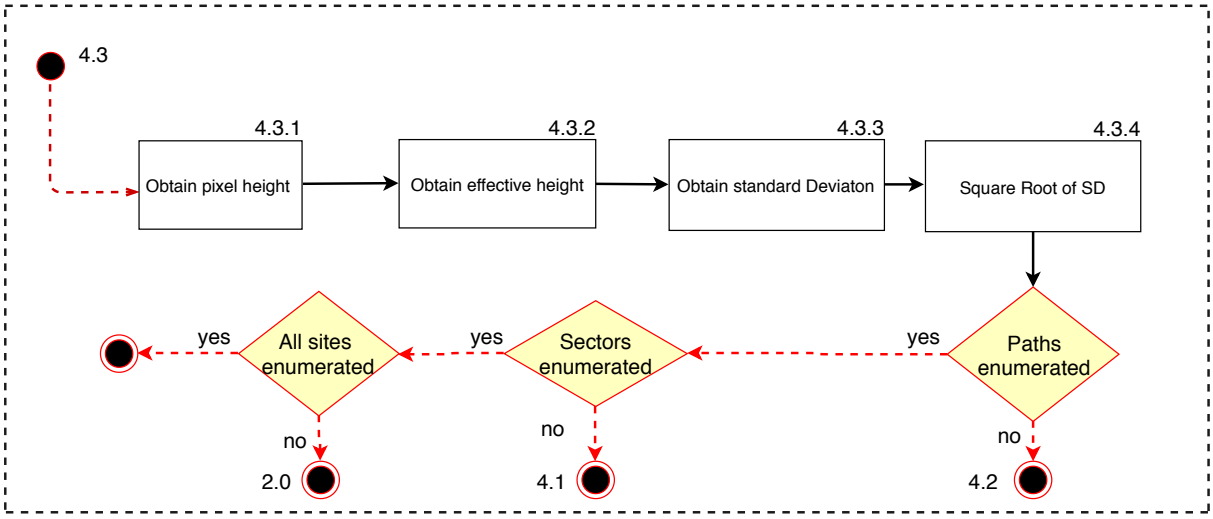

Figure 3.8: Level 3 flow diagram: Calculate terrain roughness for single grid space

3.2.7 Pattern gain (Level 4)

To obtain the three-dimensional pattern gain for a specific bearing, the level 4 flow diagram in Figure 3.9 was implemented. Block 3.5.2.1 interpolates the elevation and azimuth values in the separate two-dimensional pattern arrays. Block 3.5.2.2 converts the dBW values in the arrays to W. Block 3.5.2.3 is a summation of the elevation and azimuth gain values and block 3.5.2.4 converts the summed value to W (ERP).

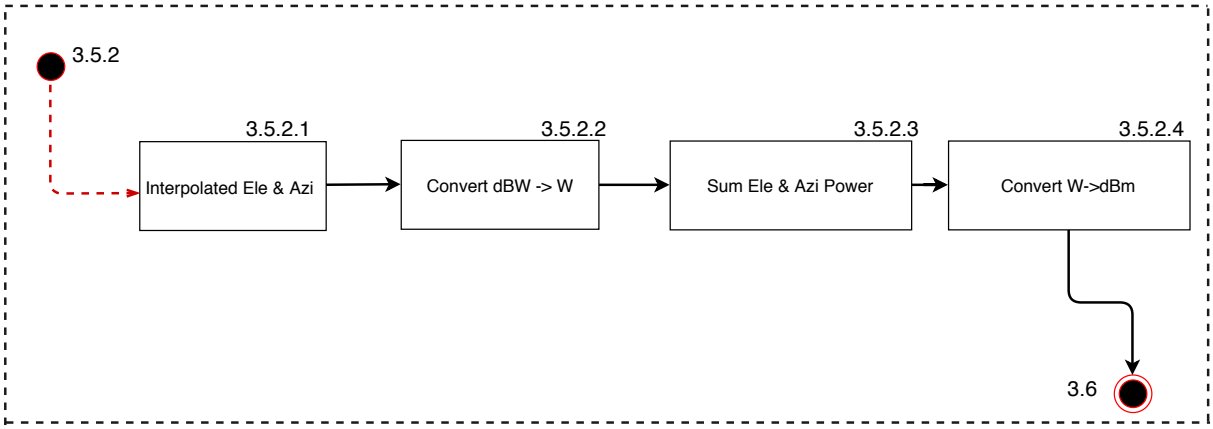

Figure 3.9: Level 4 flow diagram: Calculate pattern gain for single grid space

Table 3.5 defines the input and the output variables of the function that calculates the pattern gain for a specific receiver. The tilt and azimuth angles were the angles of the

beam pointing at the receiver in order to obtain the correct gain value. The "Ele " input variable was RX_{Phi} as described in Table 3.6.

Table 3.5: Input/Output variables to calculate pattern power gain

Input Variable	Variable type	Description	Unit	Type
Ele	Input	Receiver tilt angle	°	double
Azi	Input	Receiver azimuth beam angle	°	double
Shifted$_{Hor}$	Input	Shifted horizontal gain pattern	n/a	181x1 Array (double)
Shifted$_{Ver}$	Input	Shifted vertical gain pattern	n/a	181x1 Array (double)
Pattern Gain	Output	Pattern gain for specific receiver	dB	double

3.2.8 RX phi (Level 4)

The final level 4 flow diagram (Figure 3.10) defines the implementation of the function to calculate the bearing elevation angle (block 3.5.1). Block 3.5.1.1 calculates the summation of the transmitter and receiver height and height AMSL. Block 3.5.1.2 calculates the difference between the transmitter and the receiver total heights as calculated in block 3.5.1.1. The logic operator checks if the difference is greater or less than 0. Blocks 3.5.1.3 and 3.5.1.4 is defined by 3.8 bearing gain.

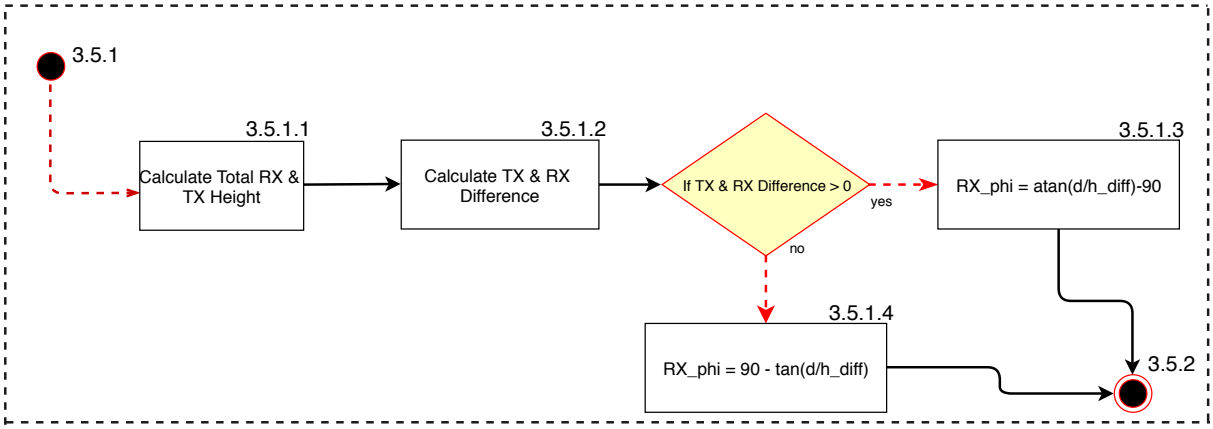

Figure 3.10: Level 4 flow diagram: Calculate receiver angle from transmitter

Table 3.6 defines the input and output variables of the function that determines the receiver angle from the transmitter. The calculation of RX_{Phi} is described in more detail in section 3.8.

Table 3.6: Input/Output variables to calculate receiver angle (RX_{phi})

Variable	Variable type	Description	Unit	Type
d	Input	Distance between transmitter and receiver	m	double
h_{RX}	Input	Receiver height above ground	m	double
h_{TX}	Input	Transmitter height above ground	m	double
$HASL_{RX}$	Input	Receiver height above mean sea level	m	double
$HASL_{TX}$	Input	Transmitter height above mean sea level	m	double
RX_{phi}	Output	Positive or negative angle from transmitter to receiver	°	double

3.3 Calculating maximum transmitter power

It is important to calculate the maximum power that can be transmitted by the transmitter, because regulations limit the amount of power that may be dissipated.

As defined by the Electronic Communications Committee (ECC), the maximum power output at a transmitter site is 65 dBm effective isotropic radiated power (EIRP) per 10 MHz of bandwidth for LTE technology [6]. It can, therefore, be concluded that with 10 MHz bandwidth on the implemented site, a maximum of 65 dBm EIRP may be transmitted. Figure 3.11 depicts the amount of power that can be used per 5 MHz resource block on the DL, which means it is also 5 MHz on the UL at the same time. Therefore not more than 65 dBm can be used for 10 MHz of bandwidth (UL and DL). The power profile in Figure 3.11 is the same for both UL and DL. Δ is the falling or rising edge of the LTE UL and DL.

To calculate the amount of power (in Watt) the following calculation is done:

If the maximum power is 65 dBm and the antenna gain is 17.4 dBi (as per antenna specification), then the maximum power from the feeder is 47.6 dBm using equation (3.1).

$$P_{feed}(dBm) = EIRP_{MAX} - G_{ant} \tag{3.1}$$

Converting to dBW using equation (3.2) means that the maximum output power (P_{feed}

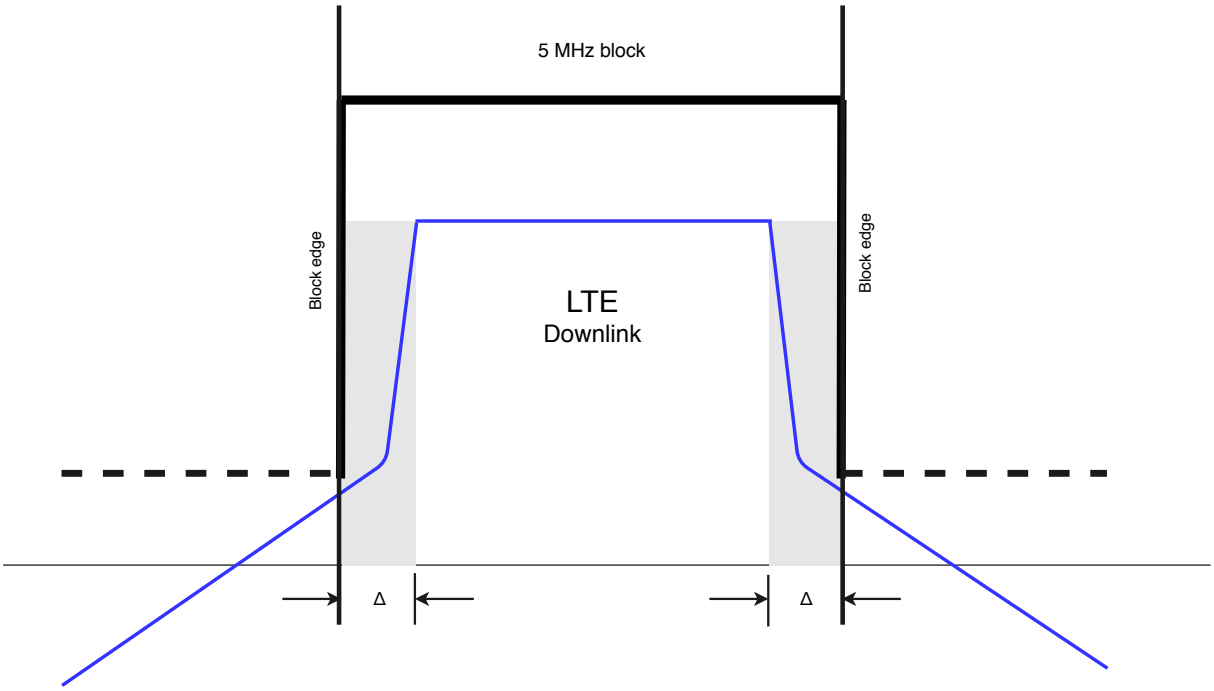

Figure 3.11: Maximum power over a 5 MHz resource block [6]

(dBW)) from the feeder can be 17.6 dBW.

$$P_{feed}(dBW) = P_{feed}(dBm) - 30 \tag{3.2}$$

The maximum output power($P_{feed}(W)$) can be calculated as 57.54 W using equation (3.3).

$$P_{feed}(W) = 10^{\left(\frac{P_{feed}(dBW)}{10}\right)} \tag{3.3}$$

3.4 Calculating maximum coverage distance

Two different propagation models were compared to determine the minimum distance to a receiver from the transmitter. The distance was used to determine the coverage of the site. This calculation is important, because it provides the area around the site

analysed in the simulation.

3.4.1 Free space loss

Using equation (3.4), the minimum coverage distance from the transmitter can be calculated.

$$FSPL = 20log_{10}(d) + 20log_{10}(f) + 20log_{10}(\frac{4\pi}{c}) - G_{TX} - G_{RX} \tag{3.4}$$

If the distance and frequency are measured in km and MHz, the constant k becomes 32,45 dB. This means the FSPL equation becomes:

$$FSPL = 20log_{10}(d) + 20log_{10}(f) + 32.45 - G_{TX} - G_{RX} \tag{3.5}$$

Substituting f = 1862.6 MHz (value discussed in subsection 3.5.1), making the transmitter and receiver gains zero (ignoring for extremities) with an FSPL of 150.11 dB, the maximum covered radius as per FSPL definition is 410 km. Heights and the effects of earth's curvature were also ignored.

It can be seen that the FSPL exceeds the maximum possible coverage of an LTE site. Using the Hata rural model, a more realistic maximum coverage distance can be calculated.

3.4.2 Okumura Hata model (rural)

Using equations (3.6), (3.7) and (3.8) [15], the minimum coverage distance from the transmitter can be estimated.

When substituting the frequency (f) with 1862.6 MHz; making h_B 20 m (minimum model requirements); making h_R 1.5 m with a path loss (L_O) of 150.11 dB, the maximum covered radius is approximately 30 km.

$$L_O = L_U - 4.78(log_{10}(f))^2 + 18.33log_{10}(f) + 40.98 \quad (3.6)$$

where

$$L_U = 69.55 + 26.16log_{10}(f) - 13.82log_{10}(h_B) - C_H + [44.9 - 6.55log_{10}h_B]log_{10}d \quad (3.7)$$

For a large rural area, C_H becomes:

$$C_H = 3.2(log11.75h_R)^2 - 4.97 \text{ for } f \geq 300 \text{ MHz} \quad (3.8)$$

The model was implemented for a flat surface and does not take DEM data into account.

3.5 Simulation parameters

To make the simulation as practical as possible, it was based on a practical reference site. Using a practical site ensures that the implemented parameters is within practical specifications and it also adheres to the fact that the results are based on a practical setup.

Two parameters are used in order to see if there is any correlation between the terrain around the site and the coverage. These two parameters describe the terrain in two different ways. The first parameter is the effective height and the second parameter is the TRF. These two parameters are described in Chapter 2 and the implementation of these parameters are described in Chapter 3, subsection 3.2.6. The two parameters are averaged over three separate parts of a sector on a site. These three parts of the sector represent the three parts of the pattern, which is the main beam of the pattern and the two side lobes. These three parts are:

- The sector as a whole.

- The part of the sector where only the main beam of the antenna gives coverage. This is the centre 65° of the sector.
- The part of the sector where only the side lobes of the antenna gives coverage. This is the other 35° in the sector.

Figure 3.12 shows how the sectors are divided in order to model the terrain as described above.

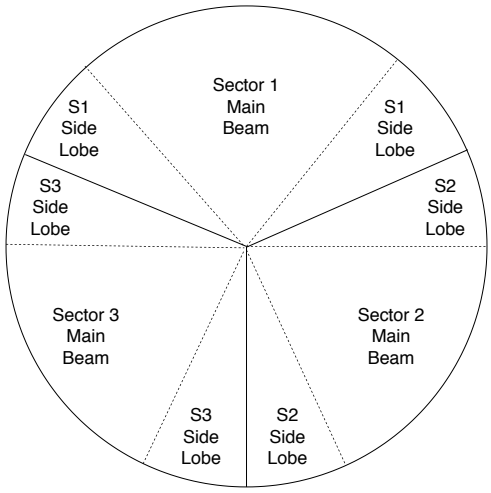

Figure 3.12: Sector divisions for terrain modelling

3.5.1 Reference transmitter site specifications

The reference site can be found in Noordrand, Roodepoort, South Africa. The coordinates of the site are Longitude: 27° 55" 16' East and Latitude: 26° 06" 39' South. The transmitting link that was used for the experiment was set up by Rain Service Provider. The site has three sectors at 10°, 160° and 250° each with down tilted antennas of 0°, 4° and 2° respectively. The frequencies of the three sectors were exactly the same, with a DL centre frequency of 1872.7 MHz and an UL centre frequency of 1777.7 MHz. The DL and UL frequency worked with a 5 MHz bandwidth each, which gave a total bandwidth of 10 MHz per sector. Table 3.7 gives a description of the theoretical specifications of the site. The site is 1595 m AMSL. All of the site information was provided by Vodacom through LS of SA radio communication services (pty) ltd.

Table 3.7: Reference site specifications

Parameter	**Value**
E-nodeB ID	900828
E-nodeB name	190110082NoordrandKerkVODSGS
Technology	LTE
Antenna	Kathrein 80010892 v.01
Antenna gain	17.4 $\pm$ 0.3 dBi
Antenna height	10.9 m
Sector count	3
Sectors azimuth	10°, 160°, 250°
Sectors downtilts	0°, 4°, 2°
DL frequency	1862.6 MHz
UL frequency	1767.6 MHz
Sector Bandwidth (BW)	10 MHz
Power per sector	19.18 W
Site coordinates	Long: 27° 55" 16’ East, Lat: 26° 06" 39’ South
Height AMSL	1595 m

Figure 3.13 describes how the transmitter feeder divides the power into the three different sectors. The feeder transmits a total of 57.54 W theoretically, dividing the power by three, which means the power fed to each sector is 19.18 W. The reason for dividing the power equally between the three sectors, is because each sector is seen as the transmission of a single antenna. A single sector is simulated as if it is a tower on its own and in order to compare the sectors (towers), the power transmitted through them must be equal. This also means that the carrier frequency used for every sector must be the same.

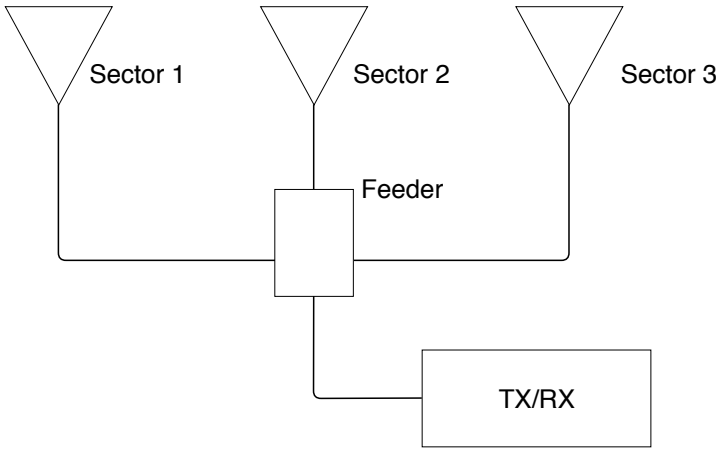

Figure 3.13: Feeder power division

Subsection 3.5.2 shows the variables that were implemented in the simulation. The following variables from the reference site were not used as constants, but were adjusted or changed to be able to test the impact of the installation parameters. The parameters that were adjusted for simulation are described in subsection 3.5.2.

3.5.2 Simulation parameters

The following section explains all of the parameters used to implement a single simulation. The simulation was done using self-written software. Table 3.8 includes the parameters.

Table 3.8: Single site simulation parameters

Parameter	**Value**
Tilt adjustment range	-5° to 10°
Tilt increment	0.5°
Height adjustment range	5 m to 15 m
Height increment	1 m
Receiver height	1.5 m
Coverage field strength cut-off	35 dBμV/m (-105 dBm)
Maximum covered radius from transmitter	30 km
Sector azimuths	0°, 120°, 240°
Transmitter feeder power	57.54 W
Digital elevation model	Shuttle Radar Topography Mission (SRTM) v4.1

The experiment is set-up to test two types of parameter adjustments. The first antenna adjustment is the mechanical tilt and the second adjustment is the height of the transmitter antenna. The mechanical tilt was adjusted -5° to 10° in 0.5° increments. The height was adjusted from 5 m to 15 m with 1 m increments. The sectors were adjusted to be the same size for every site simulated (120° per sector). The maximum covered radius was 30 km as calculated in sector 3.4. As calculated in equation (3.3), the maximum power that can be transmitted from the feeder was 57.54 W, which is less than the ITU permitted 60 W.

The DEM chosen for the simulations is the SRTM version 4.1. This is a 3-arc second resolution elevation model, which uses interpolation algorithms to fill void (non-existing) elevation data. Elevation data of 1 arc seconds is only available for Unites States [53].

3.5.3 ITU-R P.1546 path loss model parameters

The ITU-R P.1546 path loss model can be implemented with different parameter settings as well as different correction factors. Table 3.9 gives a description of how the model was implemented in our simulation software.

The time and location probability values were implemented, as explained in Chapter 2. The model gives the user a choice between the "effective clearance angle correction" and the "transmitter clearance angle correction" for negative height. The "effective clearance angle correction" was implemented because of the fact that the transmitter clearance angle is being calculated independently. The receiver angle correction was enabled in order to add a correction factor for a negative receiver angle for a maximum distance of 16 km from the receiver. The k-factor was set as the standard value of 1.33. Clutter correction was ignored because clutter information is not available. Tropospheric scattering was not taken into account. A standard value of -301.3 dN was used in order to take temperature variations of South Africa into account.

Table 3.9: ITU-R P.1546 input parameters of self-implemented software

Propagation Parameter	**Value**
Time probability	50%
Location probability	50%
Effective clearance angle correction for negative height	Yes
Transmitter clearance angle correction for negative height	No
Clearance angle receiver correction	Yes
Max distance from receiver	16km
k-factor	1.33
Clutter transmitter correction	No
Tropospheric scatter correction	No
Climatic region interference	-301.3 dN

3.5.4 Software constants and black box variables

This section describes the constants defined in the simulation software, as well as the variables obtained from the ITU-R P.1546 black box, which is a pre-written code, which

can be used to obtain the ITU-R P.1546 implemented path loss by sending it specific input data.

Table 3.10 gives the details of the simulation software global constants.

Table 3.10: Software constants of self implemented software

Constant	**Description**	**Unit**	**Type**
Hor_{Gain}	Horizontal gain pattern	n/a	360x2 Array (double)
Ver_{Gain}	Vertical gain pattern	n/a	181x2 Array (double)
Ver_{Inv}	Inverse Vertical gain pattern	n/a	181x1 Array (double)
TX_{Sites}	Transmitter site information (Table 3.1)	n/a	structure
Gridsize	Amount of receiver per tile	n/a	integer
RX_{h}	Receiver height above ground	m	double
Antenna_{Gain}	Maximum gain of antenna	dBi	double
TX_{Power}	Transmitter power	dBm	double

The ITU-R P.1546 implementation was used as a black box to obtain some terrain information and to determine every receiver point's field strength around each site. The ITU-R P.1546 Matlab implementation was obtained from [54]. Table 3.11 presents each of the variables obtained from the ITU-R P.1546 black box implementation.

Table 3.11: Black box output variables

Constant	**Description**	**Type**
GCD	Great Circle Distance (m)	double
TX_{AMSL}	Transmitter height above mean sea level (m)	double
RX_{AMSL}	Receiver height above mean sea level (m)	double
Path Loss	ITU-R P.1546 path loss (dB)	double
RX_{Path}	Path heights from transmitter to receiver	Variable Array (doubles)
RX_{Azi}	Receiver bearing azimuth angle (°)	double

The Great Circle Distance (GCD) is the distance on the surface of the earth from the transmitter to the receiver which is used to obtain the receiver bearing elevation angle together with the transmitter and receiver Height Above Mean Sea Level (HASL). The RX_{path} is an array of heights representing the profile of the path between the transmitter and the receiver.

3.6 LTE base station site selection

The simulation was done on multiple sites, which means that a number of practical sites were chosen to be used for statistical analysis. The following section describes the method in selecting the LTE base station sites for this study. The selection process was done by using filters to obtain probable and realistic LTE sites.

3.6.1 Site dataset description

A list of official site location was not available, but 'OpenCellID' [55] was available. OpenCellID has duplicate entries, inaccurate coordinates and irrelevant entries, that needs to be filtered to obtain a list of probable actual sites. Using a dataset obtained from a database called 'OpenCellID', the coordinates of chosen Vodacom sites using LTE technology can be selected using the parameters available for each site in the database as described below:

- Radio Technology ('radio') is the type of radio technology implemented on the transmitter site, for example, LTE, Global System for Mobile communication (GSM) and UMTS.
- Mobile Country Code (mcc) is the first field of the International Mobile Subscriber Identity (IMSI) which identifies a specific country. The code is three digits long, and it is possible that more than one mcc is assigned to a country. [3]
- Mobile Network Code (mnc) ('net') is the second field of the IMSI, which identifies the home network together with the mcc. [3]
- Location Area Code (LAC)/Tracking Area Code (TAC)/Network Identification (NID) ('area') is a code identifying the telephone service area in a country.
- Cell Identification (CID) ('cell') is the base station identification number.
- 'lon' is the longitude location of the site in decimal format.

- ' lat' is the latitude location of the site in decimal format.
- The 'range' is the radius offset in which the site can be located in (m).
- 'Samples' is the number of measurements that are processed to obtain the site coordinates.
- 'Changeable' is a boolean variable which is '0' if the location is obtained from the telecommunication firm and '1' means the site location has been determined from processed measurements.
- 'Created' is the variable defining the time when the specific cell was added to the database (UNIX time format).
- 'Update' is the variable defining when the site was last detected (UNIX time stamp).
- 'AverageSignal' is the average signal strength received from the site.

3.6.2 Site filtering

The filters support obtaining the number of sites necessary for statistical analysis and were implemented with the parameters in Table 3.12.

Table 3.12: LTE site filtering parameters

Parameter	**Value**	**Meaning**
Technology	LTE	
mcc	655	Sites in SA
mnc	1	Vodacom sites
Last Updated	2 years ago	
Minimum recorded samples	100	
Maximum error range	1500 m	

The first is to filter the radio type to LTE, the second is to filter the mcc to South Africa (655), and the third filter is the mnc, which is filtered to Vodacom (1).

The sites can then be filtered using histogram plots of the minimum site coordinate samples as well as the maximum error range of the site.

Figure 3.14 shows that the total number of sites which have more than 100 samples are 346. The summed amount of samples is 442525, which means if the sites are filtered above 100 samples, 0.078% Vodacom LTE sites will be left.

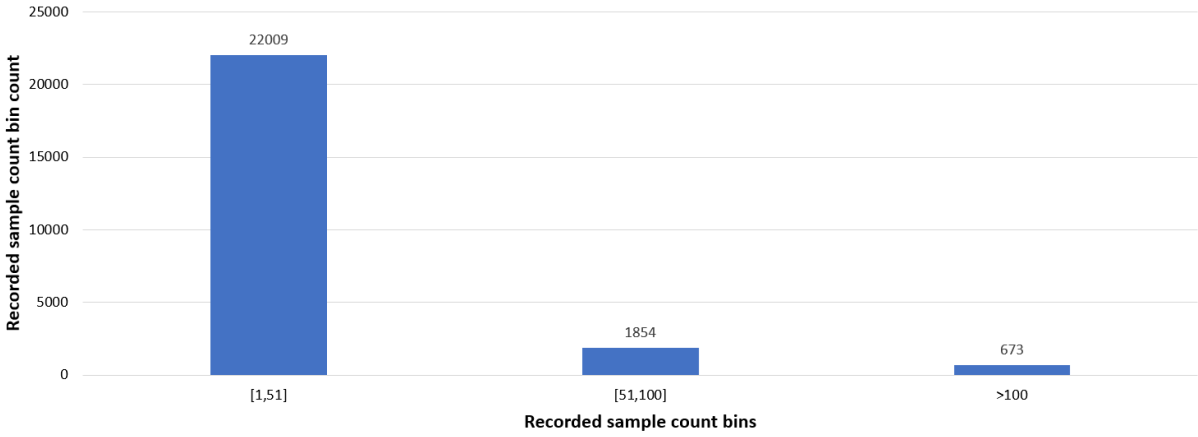

Figure 3.14: Histogram of LTE Vodacom sites coordinate samples

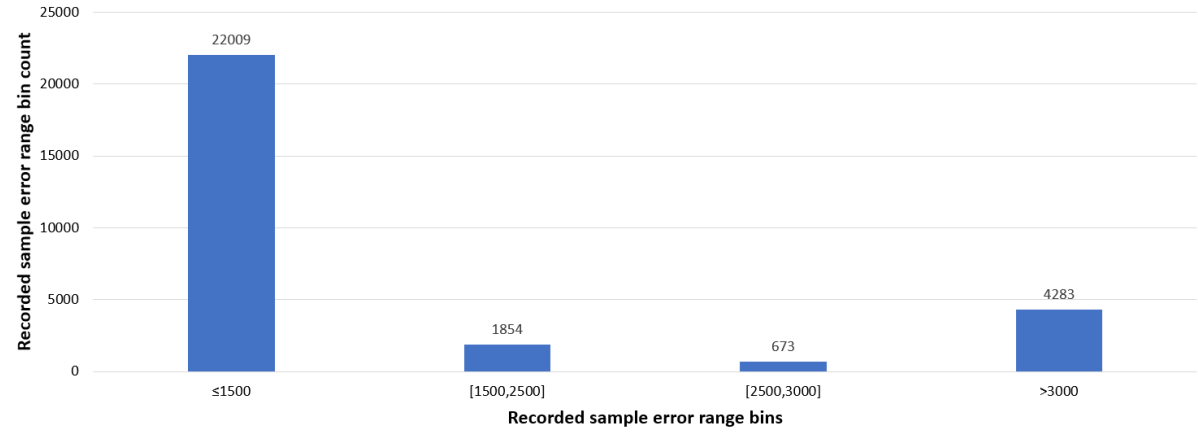

Figure 3.15: Histogram of LTE Vodacom sites coordinate error ranges

Figure 3.15 shows that the number of sites that have an error range below 1500 is 22009. The summed number of samples are 442525, which means if the sites are filtered below 1500 error range, 4.9% Vodacom LTE sites will be left.

If the technology, mcc, mnc, samples and error range filters as defined in Table 3.12 are

implemented, a number of 93 sites will be available.

By adding a circle with the error range of each site as radius, each site can be visually inspected to see whether the error radius of the sites collides. If the radii of the sites intersect, then the sites are filtered to keep the site with the highest probability of accurate location, because the sites which intersect have a high probability of being different sectors from the same tower. Figure 3.16 shows the intersection of 'range' errors.

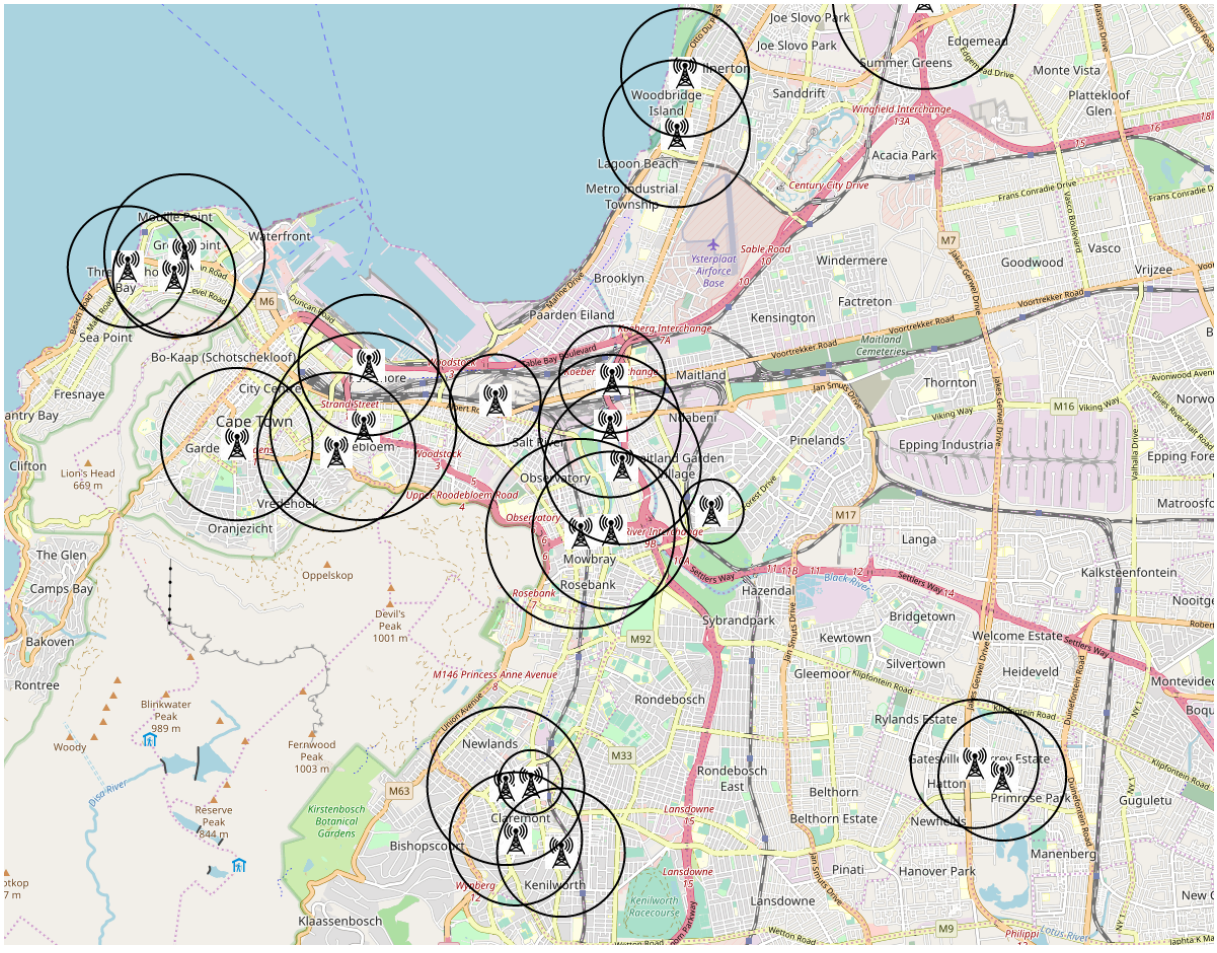

Figure 3.16: 'Range' error intersection of sites in Cape Town

The sites that intersect due to 'range' error were filtered to keep only one. They were firstly filtered with 'Last Updated' as priority and then filtered as sites with the most samples. By filtering the intersect sites in this manner, the site with the most accurate location could be obtained.

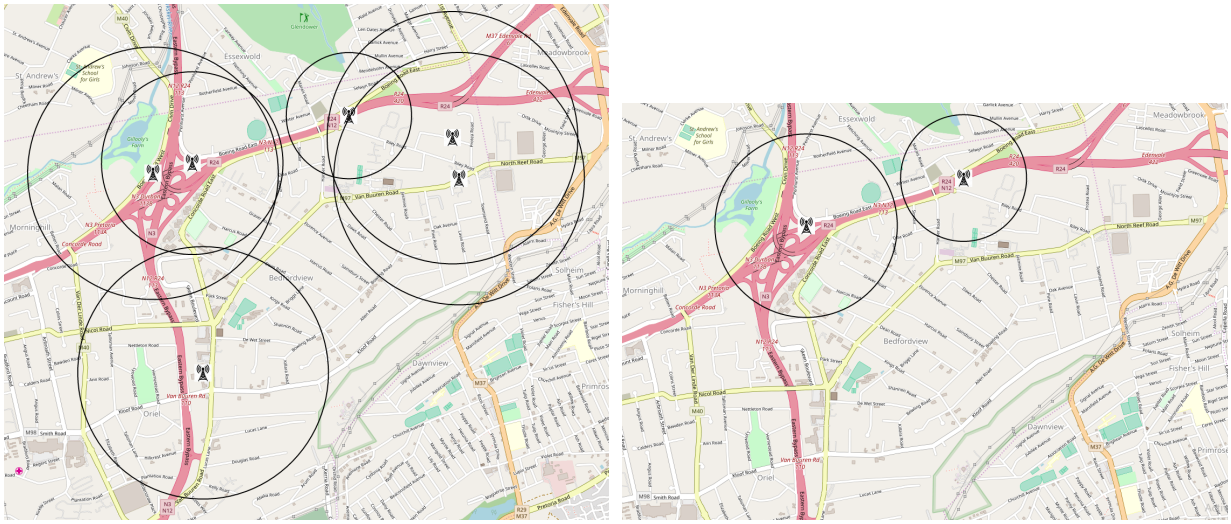

(a) Non filtered intersecting sites (b) Two smallest non-interseting error range

Figure 3.17: Comparison of filtered and unfiltered sites which collided

Figures 3.17(a) and 3.17(b) show the effect of filtering the colliding sites. The two sites left were the most accurate locations of an existing unique LTE site. Once the colliding sites had been filtered, 31 sites were left to be used. Each sector was used as a separate statistical analysis (thus giving 93 sets of data). This means 31 sites is a sufficient number of sites for a statistical analysis of the results. The 31 remaining sites are plotted on a geographical map for visual inspection (Figure 3.18).

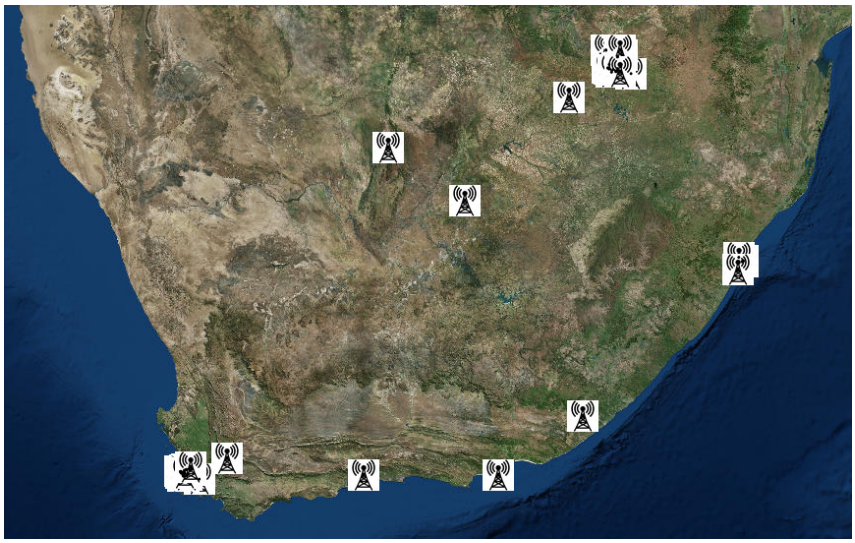

Figure 3.18: Filtered LTE sites on geographical map of South Africa [7]

3.7 Antenna tilt adjustment technique

When the antenna tilt is adjusted, the vertical pattern array must be transformed in order to simulate the adjustment accurately. The first step is to shift the original array upwards or downwards depending on the antenna tilt direction. Figure 3.19(a) displays the array before tilt. Figure 3.19(b) displays the array after a 10° upwards tilt.

After the array is transformed for an upwards tilt of 10°, the top 10 values are reflected to the bottom. They must now be replaced with the inverse (last values are first) of the original bottom ten values to transform the pattern symmetrically correct. The circled area in Figure 3.19(b) shows the effect of the top 10 shifted values in blue. The graph in Figure 3.19(b) shows the correct transformed array, where the graph in Figure 3.19(a) is the array pattern before transformation. For a zero tilt, the vertical pattern array will not be transformed.

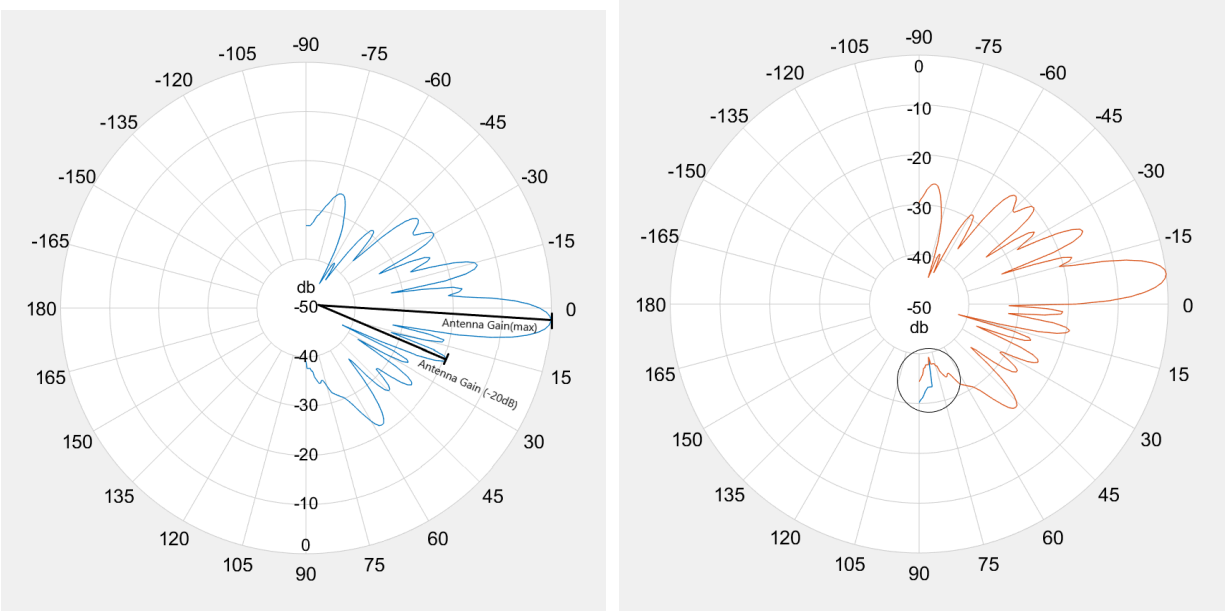

(a) Vertical gain pattern before tilting

(b) Vertical gain pattern after 10° upwards tilt

Figure 3.19: Visual description of vertical gain array transformation

In Figure 3.19(a), the maximum normalised pattern gain at 0dB (main lobe) as well as the normalised pattern at gain at -20dB (a side lobe) are indicated.

3.8 Obtain receiver bearing and bearing gain

3.8.1 Elevation bearing

For each receiver on the elevation map grid, a certain gain from the antenna pattern must be obtained. To obtain this gain value, the great circle distance (d), from transmitter to receiver, must be obtained. The other important parameters are the height of the transmitter antenna and the receiver antenna as well as their relative heights above sea level, which can be used to determine if the bearing angle is positive or negative.

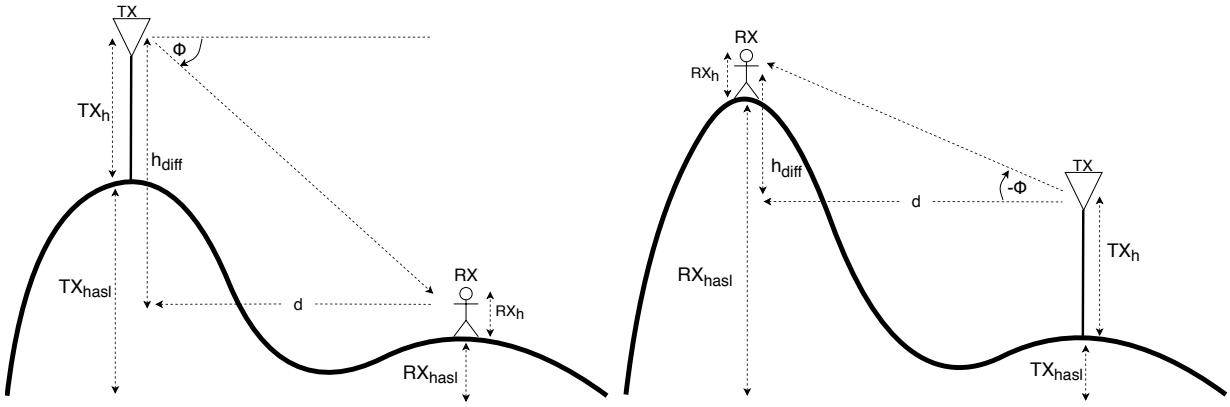

(a) Positive phi bearing

(b) Negative phi bearing

Figure 3.20: Phi angle calculation for negative and positive height difference

In Figures 3.20(a) and 3.20(b), it can be seen that if h_{diff} is positive, then the bearing angle phi is positive. When h_{diff} is negative, the bearing angle phi is negative. Equation (3.9) explains the calculation for h_{diff}.

$$h_diff = (TX_h + TX_{hasl}) - (RX_h + RX_{hasl}) \tag{3.9}$$

The azimuth bearing angle is obtained as a black box variable from the ITU-R P.1546 implementation. This is a very important parameter, because it enables, together with the azimuth, the acquisition of the ERP on that specific bearing

3.8.2 Antenna pattern gain calculation implementation

To obtain the antenna pattern gain per receiver bearing, the vertical and azimuth antenna gain values are interpolated separately to obtain the gain values of each bearing respectively. These two gain values are then summed as in equation 2.24 in Chapter 2 to give the normalised pattern gain.

3.9 Link budget

To obtain the receiver field strength P_{RX} value the following equation ((3.10)) was implemented:

$$P_{RX} = P_{TX} + G_{antpattern} - P_L \tag{3.10}$$

P_{TX} is the 'transmitter power'; $G_{antpattern}$ is the normalised pattern gain (will be 0 if the transmitter and receiver are on the same height), and P_L is the 'path loss' calculated by the ITU-R P.1546 model. The receiver gain is assumed to be zero. Figure 3.21 gives a visual representation of the link budget between transmitter and receiver.

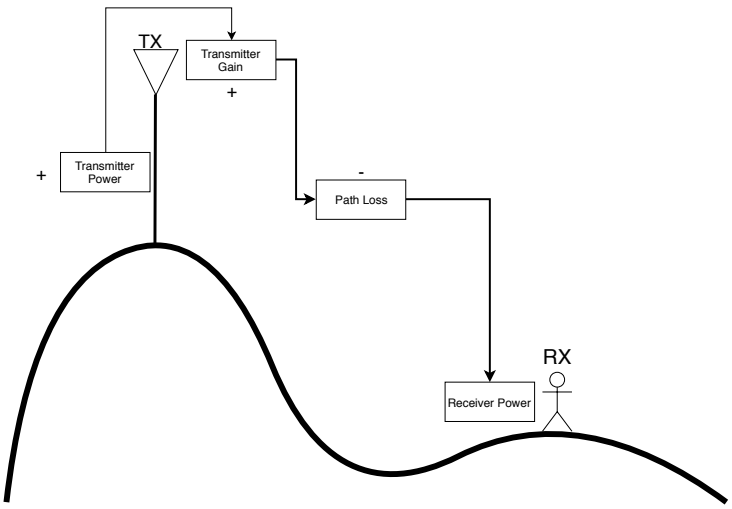

Figure 3.21: Link Budget

3.10 Map tile and grid layout

3.10.1 Map tiles

To improve the software processing, South Africa is divided into tiles of 1° x 1°. The reason for improving the software processing is to decrease the processing time, because of the large amount of data. The maximum coverage radius per site is 30 km, which is an offset of 0.2698° latitude and 0.2698° longitude from the site coordinate. If the site is on the edge of the tile, there is a possibility of four tiles that can be simultaneously covered by the site. The number of tiles that are simultaneously covered is calculated by the black box. The software accounted for nine tiles (a single set of tiles around the center tile).

Figure 3.22 together shows the layout (1-9) of the nine tiles that can be possibly covered by a site. In this example the four highlighted tiles are covered because of the position of the site relative to the middle of tile five. The tile in which the site is located will always be tile five.

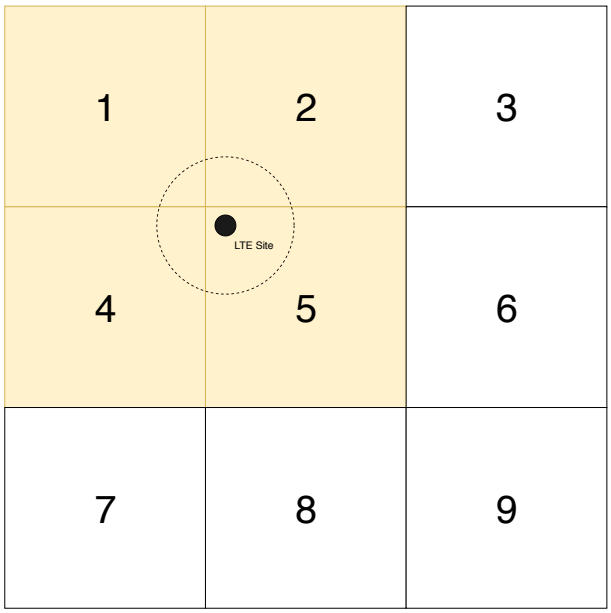

Figure 3.22: Indication of four tiles being covered by site

3.10.2 Tile grid layout

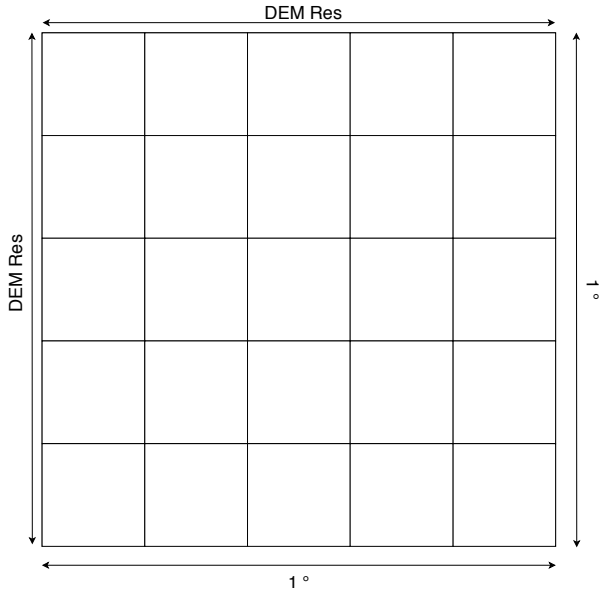

Figure 3.23: Grid spacing of a single 1° x 1° tile

Every tile consists of a grid, which size is a function of the DEM resolution. Figure 3.23 shows how the grids are divided into the 1° x 1° tiles. It can be seen that the grids are the same resolution as the DEM. The grid spacing is dependent on the number of receivers in a tile. The number of receivers is limited to the resolution of the DEM that is used to obtain the terrain height profiles, i.e. one receiver per grid.

Coverage is represented by the number of tiles. Due to the non-spherical shape of the earth's surface, it is more relevant to use 1° x 1° tiles as to scaling the coverage to m^2.

3.10.3 Grid space resolution comparison

To calculate the coverage, the resolution of the grid covering the simulated surface must be defined, because the resolution of the grid has a great impact on the processing time of the simulation. Thus an impact analysis is done to define the minimum grid resolution necessary to still obtain feasible results. The section analyses the impact of grid resolution on coverage calculation for a sector of a specific site. The three

resolutions that are tested are 120 x 120; 600 x 600 and 1200 x 1200 grids per tile. The impact of resolution will be tested on a single site for three sectors.

For the statistical analysis, the 1200 x 1200 grid spacing was used as the baseline and the other two were the predictors. Therefore two sets of statistics are given. Each set of statistics comprise of the mean error (ME), mean absolute error (MAE) and the Root Mean Square Error (RMSE). These parameters defined the error offset of the predictors from the baseline. An extra parameter called the Pearson's correlation coefficient defined how well the predictor data correlated with the baseline data. [1]

To calculate the ME, MAE and RMSE, equations (3.11), (3.12) and (3.13) were used:

$$ME = \frac{1}{n}\sum_{i=1}^{n}(x_{predicted_i} - x_{baseline_i}) \tag{3.11}$$

$$MAE = \frac{1}{n}\sum_{i=1}^{n}\left|x_{predicted_i} - x_{baseline_i}\right| \tag{3.12}$$

$$RMSE = \sqrt{\frac{1}{n}\sum_{i=1}^{n}(x_{predicted_i} - x_{baseline_i})^2} \tag{3.13}$$

Where n is the number of data points per sector per resolution setting.

To calculate the Pearson correlation coefficient, all three sector datasets were used. Equation (3.14) gives the formula to calculate the correlation between the different resolutions.

$$r = \frac{\sum_{i=1}^{n}(x_{predicted_i} - \bar{x}_{predicted})(x_{baseline_i} - \bar{x}_{baseline})}{\sqrt{\sum_{i=1}^{n}(x_{predicted_i} - \bar{x}_{predicted}))^2}\sqrt{\sum_{i=1}^{n}(x_{baseline_i} - \bar{x}_{baseline}))^2}} \tag{3.14}$$

Each set of data contains eight data points as input data, which are specifically chosen to cover the whole spectrum of antenna tilt adjustments with the minimum amount of data points. The tilt adjustments chosen are -5°, -0.5°, 0°, 0.5°, 1°, 1.5°, 2° and 10° at a

constant height of 10 m. Each data point represents the percentage tilt relative to the maximum covered area.

To obtain the statistical data, each sector coverage for the different tilt adjustments have been compared individually. Figures 3.24(a), 3.24(b) and 3.24(c) show the comparison between 1200 x 1200 and 120 x 120 grid spacing for each sector respectfully.

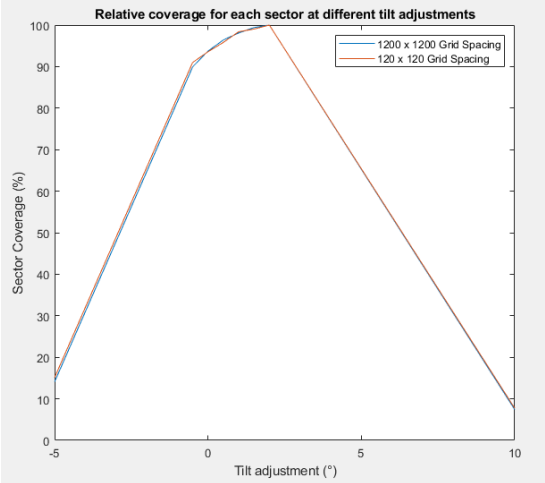

(a) Resolution comparison sector at 0°

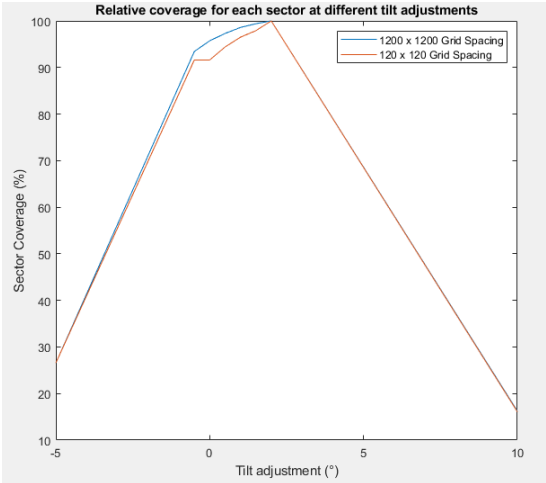

(b) Resolution comparison sector 120°

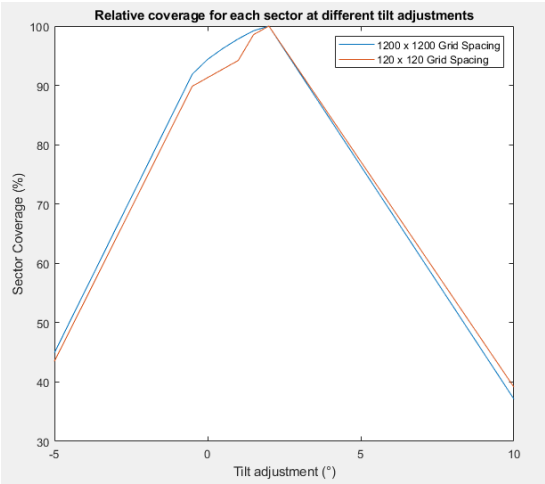

(c) Resolution comparison sector 240°

Figure 3.24: 1200 x 1200 vs. 120 x 120 receiver grid spacing

Table 3.13 show the statistical results for the 120 x 120 grid spacing as predictor data. When the 120 x 120 resolution data is correlated with the 1200 x 1200 resolution data,

a correlation coefficient of 0.999 is obtained. The small deviations between -1° and 2° on Figures 3.24(b) and 3.24(c), could be due to the sensitivity to the terrain of the larger grid spacing. This would not be a problem, because this is a relative study; therefore, the interest is in the correlation between the two graphs.

Table 3.13: Statistical data for 120 x 120 resolution as predictor and 1200 x 1200 resolution as baseline

Sector	**ME**	**MAE**	**RMSE**
0°	0.2001	0.4786	0.6009
120°	-1.5669	1.5761	2.1012
240°	-1.5421	2.0442	2.386

Figures 3.25(a), 3.25(b) and 3.25(c) show the comparison between 1200 x 1200 and 600 x 600 grid spacing.

Table 3.14 shows the statistical results for the 600 x 600 grid spacing as predictor data. The 600 x 600 resolution data correlates 100% with the 1200 x 1200 resolution data, because of a Pearsons correlation coefficient of 1.

Table 3.14: Statistical data for 600 x 600 resolution as predictor and 1200 x 1200 resolution as baseline

Sector	**ME**	**MAE**	**RMSE**
0°	-0.0017	0.0412	0.0542
120°	0.0017	0.0617	0.0927
240°	-0.2682	0.2682	0.3043

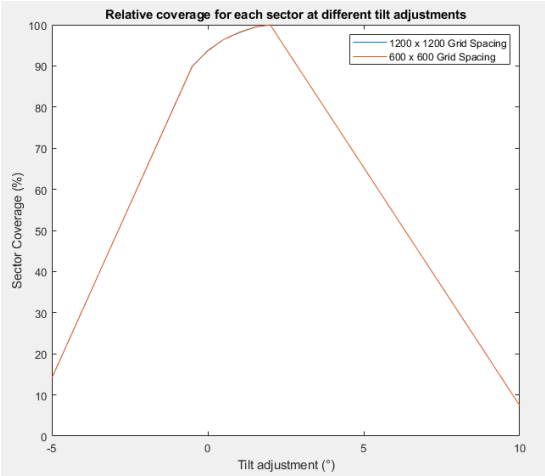

(a) Resolution comparison sector 0°

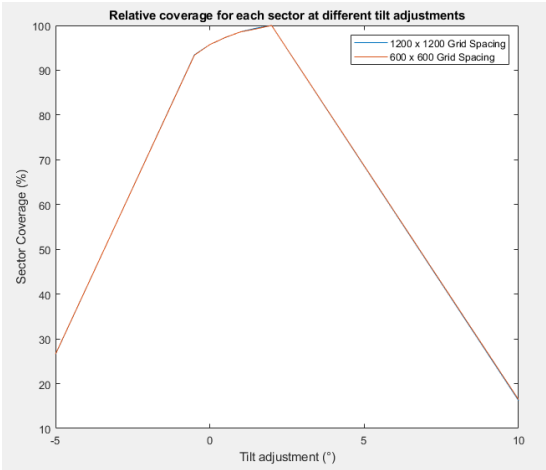

(b) Resolution comparison sector 120°

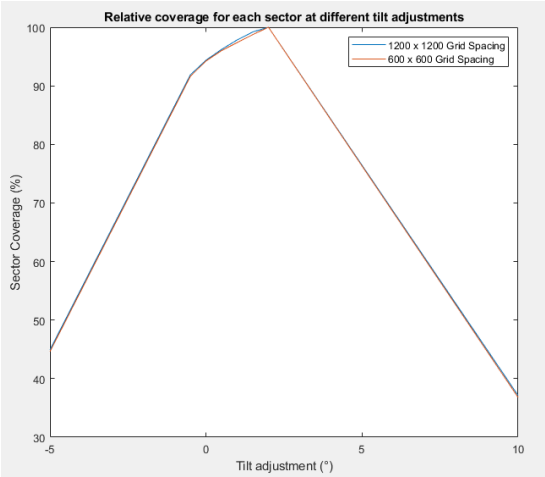

(c) Resolution comparison sector 240°

Figure 3.25: 1200 x 1200 vs. 600 x 600 receiver grid spacing

It can therefore be concluded that a 120 x 120 grid resolution can be used, because of the small errors and the significant correlation between the coverage graphs.

3.11 Effective path loss calculation

An analysis was done on the impact of the tilt and height parameters on the path loss calculations. This would provide insight into the chronological order in which

path loss is calculated. Knowing the dependencies of the path loss parameters, the simulation software can be optimised for processing time.

$$P_L = func(d, Terrain_{eff_h}, f, TX_{ca}, RX_{ca}) \tag{3.15}$$

(P_L) is a function of the transmitter height. The effective terrain height ($Terrain_{eff_h}$), transmitter clearance angle (TX_{ca}) and receiver clearance angle RX_{ca} from equation (3.15) are a function of the transmitter height and not a function of tilt. This indicates that the path loss (P_L) only has to be calculated for every height adjustment iteration and not in combination with the tilt adjustment iterations. This will improve the processing time for calculating the P_L.

3.12 Results structure

In order to store the results effectively to extract the data easily at a later stage, a data structure is designed to obtain every site's results separately. Table 3.15 at the end of the chapter, defines each of the data parameters within the transmitter results structure. Figure 3.26 at the end of the chapter, shows how the structure is designed to save the results for each of the sites. Level 1 saves the information details of each site. Level 2 is the structure containing the information for every height adjustment. Level 3 is a structure containing the information for every tilt adjustment. Level 4 contains the necessary result data to analyse each of the sites.

3.13 Conclusion

This chapter discussed the simulation model that was implemented. The first section addressed the simulation model for a single path, discussing every parameter from the transmitter through to the field strength obtained at the receiver. The simulation input

parameter limitations (height and tilt adjustments) were also introduced.

Flow diagrams and tables were included to ensure the understanding of the logical flow of the software. The simulation model was broken down into four different levels to explain the detail and flow of the simulation model. The flow diagrams covered every detail from importing the filtered LTE sites to analysing the site coverage and terrain data. As mentioned at the beginning of the chapter, a full layout of the simulation flow diagram can be seen in Appendix A, Figure A.1.

Important calculations such as the maximum transmitting power and the maximum coverage were done. The maximum transmitting power was calculated as 57.54 W and the maximum coverage distance 30 km, which was then used as the maximum radius from the transmitter under analysis.

Reference site information as provided by Vodacom through LS of SA radio communications services (Pty) Ltd. and the parameters that would be implemented in the simulation were given. A more detailed description of the ITU-R P.1546 path loss model parameters, software constants and ITU-R P.1546 black box variables were provided.

A selection process was implemented to obtain the LTE base station site locations for the study. Thirty-one [31] sites were identified with three sectors per site, which means that 93 datasets were available for statistical analysis.

We introduced a technique to simulate the adjustment of tilt analysis. Benefits of this technique are the ability to calculate the bearing of the receiver and the gain at a specific bearing. A link budget was introduced to obtain the field strength values for every transmitter-receiver pair. The link budget comprises elements such as transmitter gain, path loss and transmitter power.

South Africa was divided into tiles of 1° x 1° to improve software processing time. A detailed discussion of how the grid and tile system works was provided. A comparison was then done to evaluate at which resolution the grids must be spaced for simulation purposes. It was found that a grid resolution of 120 x 120 is sufficient.

A layout of the results structure was provided to ensure simplified access to data for analysis. With the system model confirmed, it is possible to implement the software that simulates the sites and produce the necessary results for analysis.

Table 3.15: Description of result structure parameters

Parameter	**Level**	**Description**
Name	1	Transmitter site name
Number	1	Transmitter site number
tile distance vector	1	Distance of each receiver from the transmitter
tile $RX_AMSLvector$	1	AMSL for each of the receiver
tile ref vector	1	A reference vector unique for each tile around the transmitter
$sector_count$	1	The number of sector the site consists of
tile count	1	The number of tiles that are covered by the site propagation
DEM AMSL	1	The site AMSL
ant h vector	1	Consists of the values for each height adjustment
ant elev vector	1	Consists of the values for each tilt adjustment
Site ID	1	Transmitter site identification number as in data source
Sec	1	Number of sectors on site (each sector consists of a structure (Level 2))
Height	2	Each height adjustment consists of a structure (Level 3)
Tilt	3	Each tilt adjustment consists of a structure (Level 4)
RX Phi	3	The angle of each receiver relative to the transmitter
Tile FS coverage count	4	Array consisting of the amount of receiver covered per tile
Tile FS coverage sum	4	The sum of the amount of receiver covered per tile

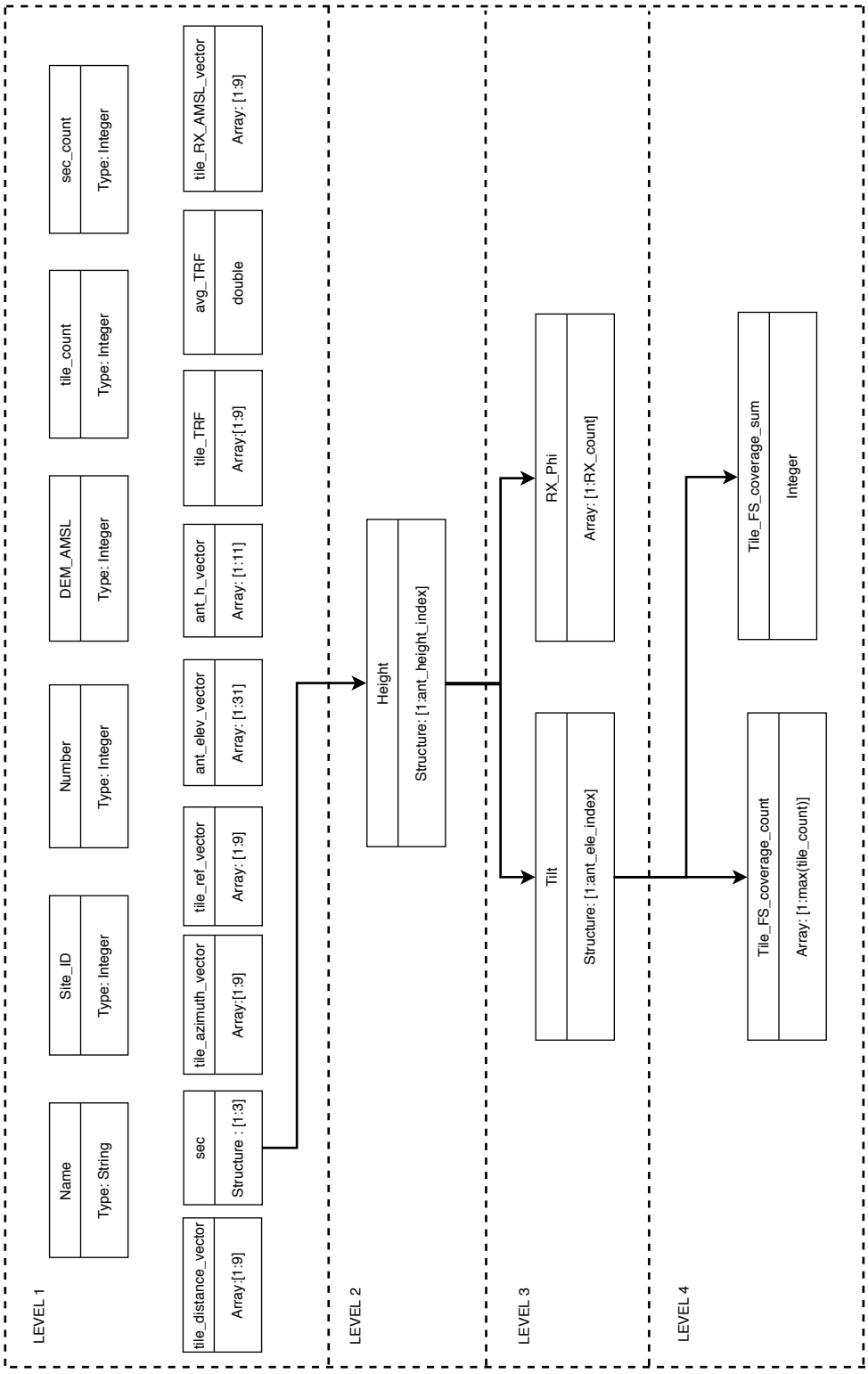

Figure 3.26: Transmitter results structure

Chapter 4

Verification and validation

Chapter 4 includes all information related to verification and validation. Verification and validation are divided into separate sections. The first section is the verification of all the critical equations implemented in the simulation software. Section 2 provides the validation of a single simulation using the self-implemented software against an industry-standard software "CHIRplus BC".

4.1 Introduction

A Matlab implementation was developed in order to address the shortcomings of current commercial software CHIRPlus BC. CHIRPlus BC is a software that was used for broadcast network planning, with the option of implementing various propagation models. With CHIRPlus BC it is not possible to automatically repeat the simulation for more than one site, within a reasonable amount of time, because certain steps were done manually. The Matlab implementation enables automatic repeat-ability of a single simulation. It also enables the storage of results in a self-developed data structure, which simplifies the analysis of the data.

In this chapter, CHIRPlus BC is used to validate and verify the results obtained from the Matlab-implementated software.

4.2 Verification

The general verification process followed, used sample data to test the implementation of specific functions. The first step was to use the sample input data to calculate the results by means of calculations by hand, validated online calculators or calculations by an industry-standard software package. These results were then compared to the results obtained by the individual function within the Matlab simulation software. Results that were within a verified margin, verify the function. Figure 4.1 illustrates the verification process.

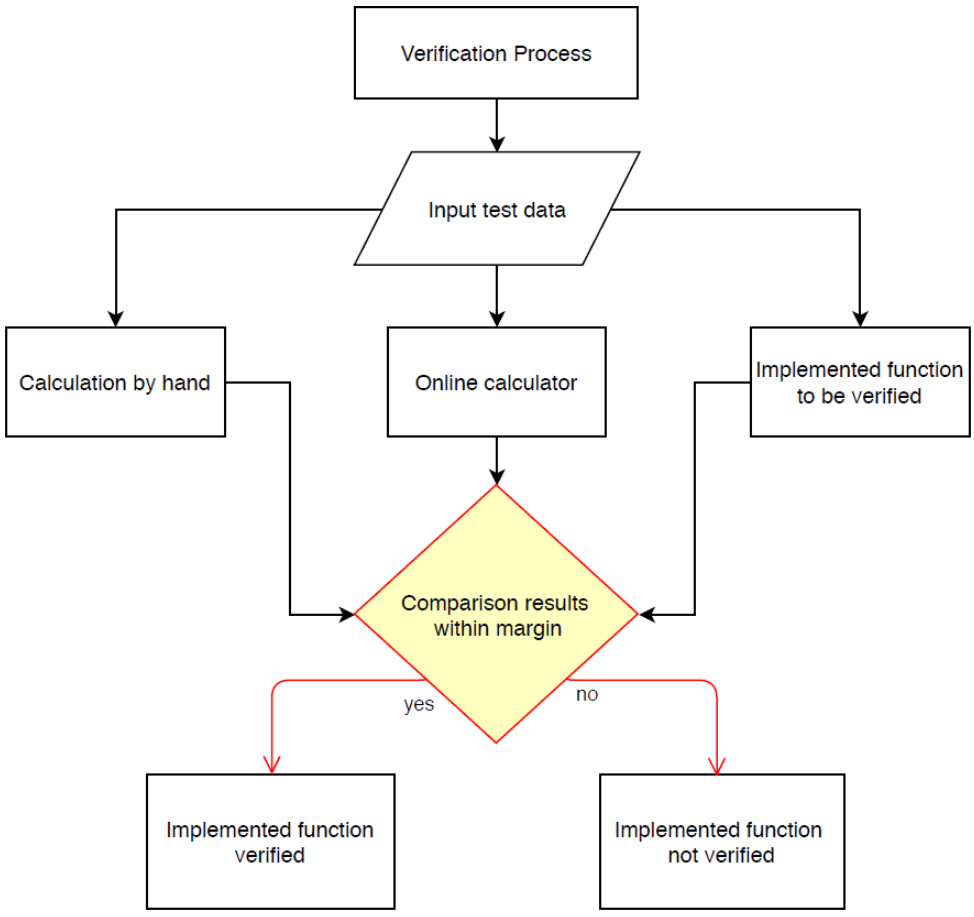

Figure 4.1: Flow diagram of the verification process

4.2.1 EARFCN to frequency band conversion

The reference site UL and DL frequencies are provided in EARFCN code format. An EARFCN calculator was used to convert the frequency bands from EARFCN code format to actual frequency values. To ensure the calculator is accurate, a verification was done by comparing the results with calculations by hand. Using six different EARFCN codes, a verification was done to see if the calculator results were within the 3GPP TS 36.101 specification for LTE bands. The frequencies in Table 4.1 were obtained using an online conversion calculator [56] as well as calculations by hand.

Table 4.1: EARFCN to frequency band conversion verification

EARFCN DL	**EARFCN UL**	**Calculator**		**Hand calculations**	
		DL frequency (MHz)	**UL frequency (MHz)**	**DL frequency (MHz)**	**UL frequency (MHz)**
1877	19877	1872.7	1777.7	1872.7	1777.7
1776	19776	1862.6	1767.6	1862.6	1767.6
37900	37900	2585	2585	2585	2585

Equations 2.1 and 2.2 in Chapter 2 where used to verify the EARFCN online calculator, which means it implements the 3GPP TS 36.101 specification conversion equation.

4.2.2 Antenna gain pattern

A Kathrein 80010892V01 antenna pattern was used in the Matlab simulation, as stated in subsection 4.3.3. In order to ensure the pattern used in the Matlab program is the same as the pattern used in the CHIRPlus BC software (ensuring the pattern is implemented correctly), the azimuth and elevation patterns must be verified. CHIRPlus BC contains an industry software tool to view antenna patterns and analyse antenna patterns. Using a plot function, the pattern as implemented in Matlab could be visually compared with the pattern that can be viewed in CHIRPlus BC.

Figures 4.2(a) and 4.2(b) show that the azimuth patterns used in both the CHIRPlus BC and the Matlab software are visually similar. Figures 4.3(a) and 4.3(b) show the

similarity between the elevation patterns.

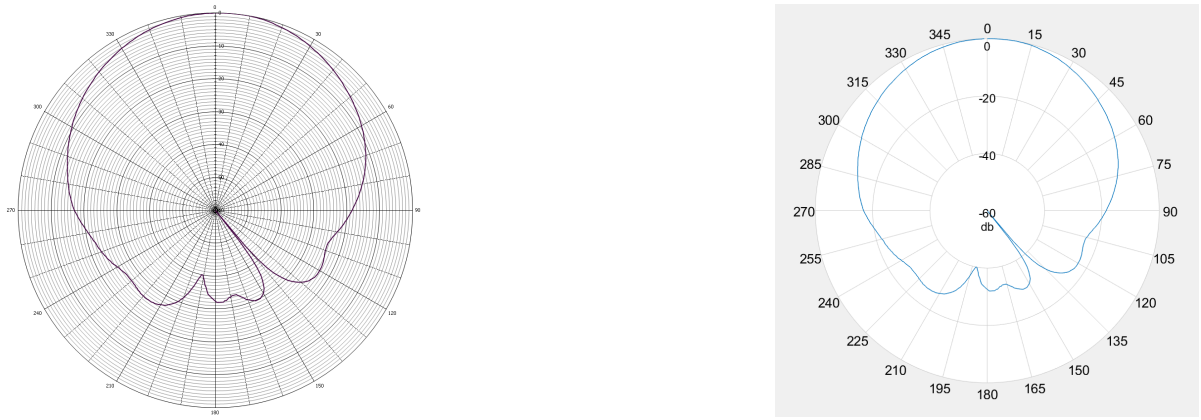

(a) CHIRPlus BC implementation (b) Matlab implementation

Figure 4.2: Kathrein azimuth antenna pattern visual representation

(a) CHIRPlus BC implementation (b) Matlab implementation

Figure 4.3: Kathrein elevation antenna pattern visual representation

Comparing every degree of the power value of the patterns generated by CHIRPlus BC with the power values of the patterns generated by Matlab, it was found that an average standard deviation of 0 dB was calculated. It can therefore be concluded that the azimuth and the elevation patterns was correctly implemented in the Matlab simulation software.

Figures 4.4(a) and 4.4(b) display the three dimensional patterns created in both CHIRPlus

BC and Matlab. The three dimensional antenna power radiation patterns where generated using the verified two dimensional pattern power values.

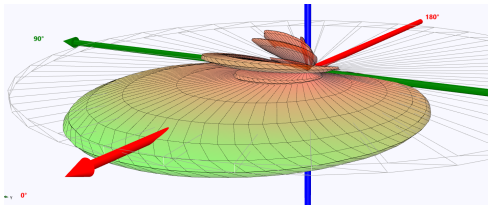

(a) Kathrein pattern as implemented in CHIRPlus BC software

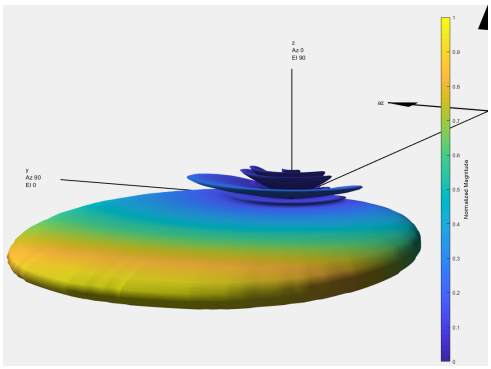

(b) Kathrein pattern as implemented in Matlab software

Figure 4.4: 3D Antenna pattern verification

4.2.3 Antenna adjustment verification

The simulations for the study include the adjustments of the antenna pattern. The pattern must be rotated in the azimuth and tilted in the elevation. To verify if the adjustment of the pattern in the Matlab software has been done correctly, a test was done between a set of randomly selected adjustments. The adjusted horizontal and vertical pattern array shifts due to the amount of azimuth shift or tilt adjustment. Five tilt adjustments and five azimuth adjustments where done.

Table 4.2 shows the power values obtained in CHIRPlus BC and Matlab, on a polar plot, when the tilt of the antenna has been adjusted:

Table 4.2: Verification adjusting tilt of the antenna

Tilt (°)	**Power Value (dB) CHIRPlus BC**	**Power Value (dB) Matlab**	**Error (dB)**
0	-2.4	-2.4	0
1	-4.5	-4.5	0
2	-7.5	-7.5	0
3	-11.8	-11.8	0
4	-17.7	-17.7	0
5	-20.9	-20.9	0

Table 4.3 shows the values obtained in CHIRPlus BC and Matlab, on a polar plot, when the azimuth of the antenna has been adjusted:

Table 4.3: Verification adjusting azimuth of the antenna

Tilt (°)	**Power Value (dB) CHIRPlus BC**	**Power Value (dB) Matlab**	**Error (dB)**
0	0	0	0
60	-9.6	-9.6	0
120	-25.5	-25.5	0
180	-32.4	-32.4	0
240	-23.4	-23.4	0
300	-8.7	-8.7	0

The comparison of Table 4.2 and Table 4.3 shows that the adjustments have been implemented correctly, because all of the power error values between CHIRPlus BC and Matlab are 0 dB.

4.2.4 Verification of antenna power

To obtain antenna power for a specific bearing, the azimuth and elevation power values are separately interpolated to obtain the specific bearing power value between the existing values. The original azimuth and elevation values are in 1° intervals . The antenna power values where verified in two steps. The first step was to verify the interpolation method (see section 2.10 in Chapter 2) applied in Matlab. The second step is to verify if the interpolated values are correct.

Interpolation verification

To verify the interpolation method as implemented in Matlab, the interpolation was applied to 10 randomly selected elevation values and to 10 randomly selected values of the azimuth. The calculated power values were then verified using a linear interpolation equation calculator site [57], which implements the standard interpolation equation. Table 4.4 shows the gain values at specific azimuth angles.

Table 4.4: Interpolation verification of azimuth power values as calculated in Matlab

Azimuth Angle (°)	**Power Value (dB) Matlab**	**Power Value (dB) Online Calculator**	**Power Value (dB) CHIRPlus BC**	**Error (dB)**
280.11	-14.57	-14.57	-14.57	0
139.92	-45.50	-45.50	-45.50	0
86.77	-17.21	-17.21	-17.21	0
145.00	-35.89	-35.89	-35.89	0
34.62	-3.23	-3.23	-3.23	0
47.38	-5.88	-5.88	-5.88	0
338.20	-1.78	-1.78	-1.78	0
343.25	-1.17	-1.17	-1.17	0
206.50	-27.95	-27.95	-27.95	0
21.46	-1.05	-1.05	-1.05	0

It was found that inserting the randomly selected elevation and azimuth values into the equation (in the online calculator) and obtaining the values from CHIRPlus BC, obtains a constant error of 0 dB, when compared to the values from the Matlab interpolation function. It can therefore be confirmed that the interpolation function, as implemented in Matlab, is verified using two sources.

Transmitter power at pattern bearing verification

The output power of the antenna should be interpolated to obtain the power at any bearing (decimal angle), when the antenna is at constant tilt and constant azimuth adjustment.

The following equation (eq. (4.1)) was used to obtain the linear interpolated transmitter power values, and Table 4.5 defines each variable in the equation :

$$y_2 = \frac{(x_2 - x_1)(y_3 - y_1)}{(x_3 - x_1) + Y_1} \tag{4.1}$$

Table 4.5: Interpolation equation variable definitions

Equation variable	Variable definition
x_1	Lowest absolute value
x_2	Interpolated value
x_3	Highest absolute value
y_1	Lowest absolute pair
y_2	Interpolation pair
y_3	Highest absolute pair

To verify the transmitter power at a specific bearing, the same values used and obtained in Table 4.4 were used to calculate the transmitter power values of the 10 randomly selected bearings. Table 4.6 shows the values as calculated in Matlab.

Table 4.6: Summation of elevation and azimuth power values

Power Value (Matlab) (dBm)	Power Value (Hand calculation) (dBm)	Error (dBm)
-30.78	-30.78	0
-45.59	-45.59	0
-39.23	-39.23	0
-39.90	-39.90	0
-35.53	-35.53	0
-23.07	-23.07	0
-26.42	-26.42	0
-24.82	-24.82	0
-30.96	-30.96	0
-11.50	-11.50	0

When the same formula, as implemented in Matlab, was used to calculate the transmitter power for each of the randomly selected bearings by use of calculation by hand, it was found that the answers were 100% the same, with a constant error of 0 dB.

4.2.5 Terrain Roughness Factor (TRF) verification

The following section provides the information to show that the Longley Rice IMT terrain roughness factor as, explained in Chapter 2 is correctly implemented. To calculate

the factor, different calculations have to be implemented. The first calculation taking place is to calculate the least mean square regression line (eq. 2.19).

Because of the variance in input data, the implementation of calculating the regression line was verified by testing it with data already verified with an online least mean square regression online calculator.

Table 4.7 shows the test data was used:

Table 4.7: Input data for calculating the least mean square regression line

x-axis Values	**y-axis Values**
1	23
2	41
3	56
4	47
5	64
6	59
7	77
8	92
9	80

Using the online calculator, the following least mean square regression line is obtained:

$$y = 7.25x + 23.64 \tag{4.2}$$

Using the implemented least mean square regression line function, the following is obtained:

$$y = 7.25x + 23.63889 \tag{4.3}$$

4.2.6 Verification conclusion

It can, therefore, be concluded that all of the critical functions used in the Matlab simulation have been verified for correctness. The next step is to validate the simulation results of the Matlab program with the CHIRPlus BC results.

4.3 Validation

Validation is divided into three sections. The first section shows that the terrain profiles used in the Matlab implementation are the same as implemented in CHIRPlus BC. The second section shows the calculations used to ensure that the ERP values that are inserted into CHIRPlus BC are the same as used in the Matlab implementation and a breakdown of the parameters used to determine field strength in CHIRPlus BC. The last section provides the validation of the results as obtained in CHIRPlus BC and the results as obtained in Matlab for a single site.

4.3.1 Path profile validation

The following section shows that the method calculating the terrain profile path from transmitting site to every individual receiver, has been implemented correctly. The validation was done by the visual representation of the terrain profile as calculated by CHIRPlus BC as well as the Matlab software.

Table 4.8 shows the comparison of the terrain profiles height values between CHIRPlus BC and Matlab.

Table 4.8: Comparison between terrain profiles

Distance from transmitter	Height CHIRPlus BC	Height Matlab	Absolute error
250 m	1662.3 m	1664	1.7 m
1300 m	1635 m	1641 m	6 m
2100 m	1600 m	1599 m	1 m
3200 m	1565.3 m	1559 m	6.3 m
4700 m	1540 m	1543 m	3 m
6600 m	1538.5 m	1537 m	1.5 m
8600 m	1499.2 m	1496 m	3.2 m
9800 m	1447 m	1446 m	1 m
11300 m	1423.3 m	1420 m	3.3 m
13400 m	1470.8 m	1469 m	1.8 m

Figure 4.5 represents the terrain profile as calculated by CHIRPlus BC and Figure 4.6 represents the terrain profile as calculated by Matlab.

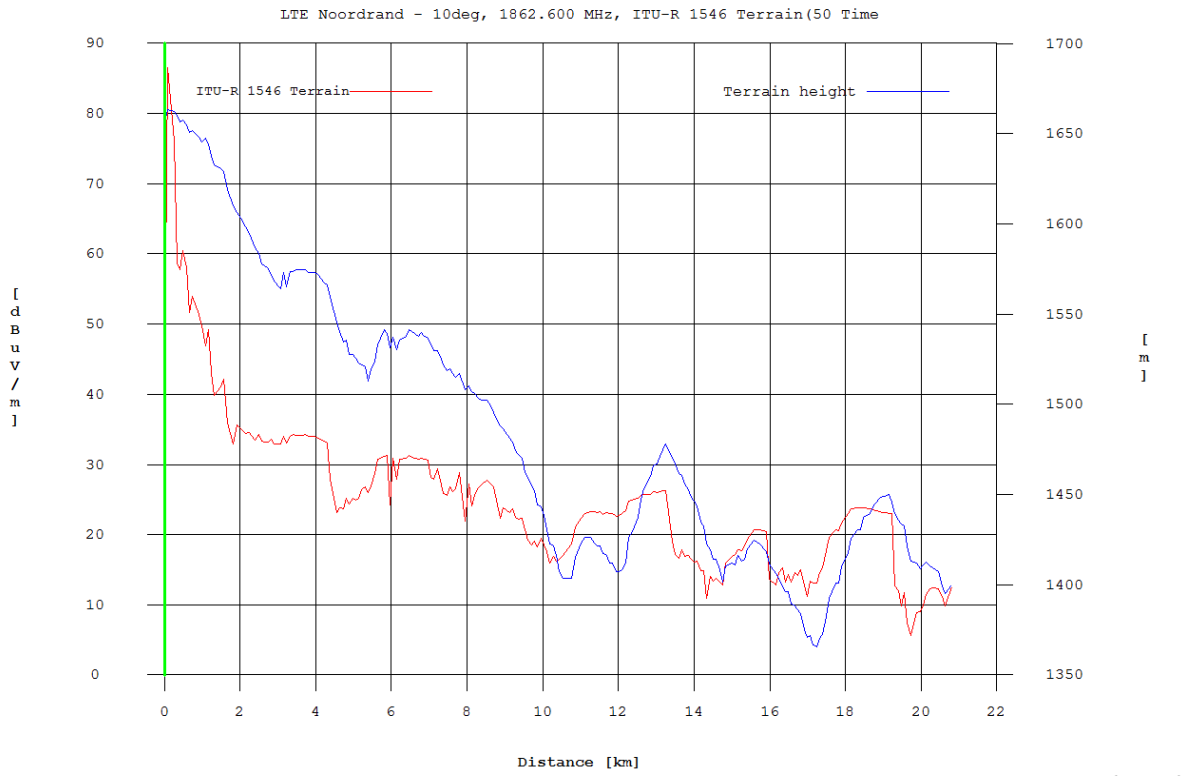

Figure 4.5: Terrain profile as calculated by CHIRPlus BC software in blue

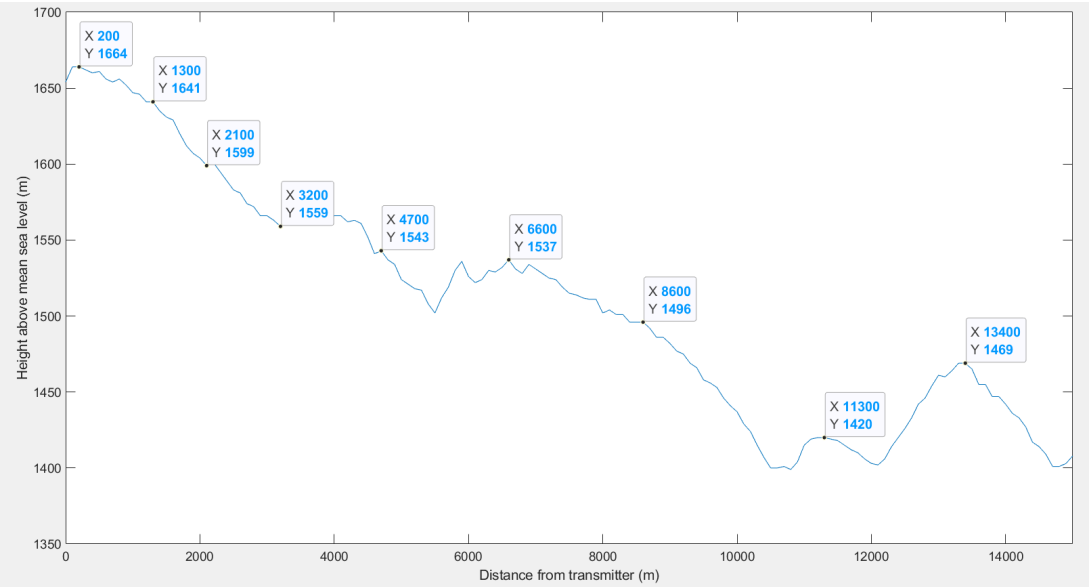

Figure 4.6: Terrain profile as calculated by Matlab software

In Figure 4.6, 10 data points have been marked that are used to validate how close the height values of the two graphs are to each other.

The average standard deviation of the values in Table 4.8 is 2.88 m. This represents an average error of 0.2%. Even though this is the case, if referred back to the effective height equation (2.11) in subsection 2.8.5 it is seen that the terrain height above mean sea level is eliminated from the equation when calculating the transmitter and receiver antenna heights. This difference between the two terrain profiles does not affect the implemented ITU-R P.1546 path loss model. The reason for the difference between the two terrain profiles can be explained due to the uncertainty of the interpolation method used to obtain the height values. All the height data is dependent on SRTM files, which contain terrain height data of 1 arc-second per file. Interpolation is then used to obtain the height values not provided by the file. The interpolation method implemented in Matlab is a bi-linear polarisation method.

4.3.2 ERP calculation CHIRPlus BC

The following section describes how the transmitter ERP values must be formatted to be correctly inserted into the CHIRPlus BC software. CHIRPlus BC accepts only ERP values in the horizontal (ERP H) and vertical (ERP V) plane respectively and converts to total ERP thereafter. The following calculations were used to achieve the above-mentioned:

Equation (4.4) uses the transmitter power (P_{TX}) and transmitter antenna gain ($G_{TX_{ant}}$) to calculate the ERP in dBW. P_{TX} = 13 dBW and G_{TX_ant} = 19.55 dBi.

$$ERP_{dBW} = P_{TX} + G_{TX_{ant}} \tag{4.4}$$

ERP_{dBW} = 32.55 dBW and by using equation (4.5), ERP_W can be calculated as 1798.87 W. Converting ERP_W to ERP_{dBm} using equation (4.6), a value of 62.55 dBm is obtained. This states that the ERP complies with the LTE ERP regulatory limit of 65

dBm.

$$ERP_W = 10^{\left(\frac{ERP_{dBW}}{10}\right)} \tag{4.5}$$

$$ERP_{dBm} = 10log_{10}(ERP_W) \tag{4.6}$$

Assuming the power is split equally between the two polarisations (horizontal and vertical) [58], we divide the ERP_W value by two so that the ERP H and ERP V can now be obtained. Both planes would then have a value of 899.44 W, respectively. These values are inserted into CHIRPlus BC, where the power is added and use the total ERP is used as 1798.87 W, as calculated earlier.

4.3.3 Validation setup and parameters

As mention in Chapter 3, subsection 3.5.1, an existing LTE reference site was used as a baseline for the simulation. It has been stated that some of the site parameters were used as constants, while other parameters were adjusted for research purposes. The following subsection provides more information on the simulation setup and parameters.

Antenna implemented on transmitter site

The LTE test site was equiped with Kathrein 80010892 v.01 antennas. These antennas are suitable for two frequency ranges (698 MHz to 960 MHz; 1710 MHz to 2690 MHz) with 10 connector ports. The antenna is dual-polarised with a horizontal pattern beamwidth of 65° and an adjustable electrical down tilt of 2.5° to 12°.

The Kathrein 80010892 antenna pattern files were the only pattern files obtainable, and differs from the implemented antenna on the reference transmitter site. This implies

that another valid LTE frequency band will then be used on the reference site for the rest of the study.

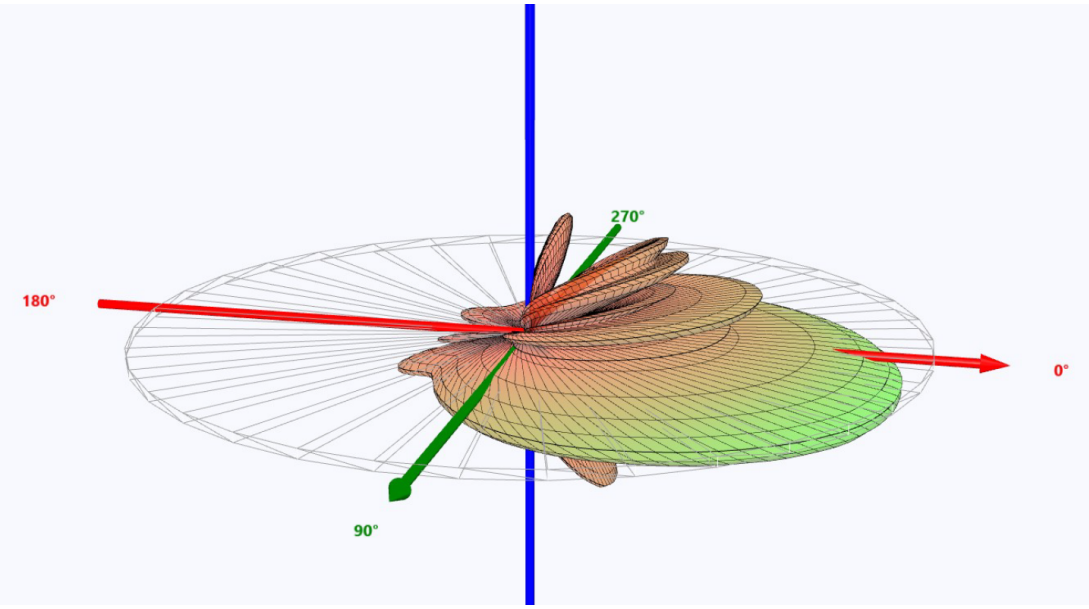

Figure 4.7: Kathrein 3D pattern

Figures 4.4(a) and 4.4(b) shows the azimuth as well as the elevation pattern of the Kathrein antenna. Figure 4.7 shows the 3D propagation pattern when the elevation and the azimuth patterns are combined.

Validation parameters

This section lists and explains the simulation parameters used in both CHIRPlus BC as well as Matlab. Table 4.9 summarises all the important parameters that influence the results directly or indirectly.

Table 4.9: Validation site simulation parameters

Parameter	**CHIRPlus BC Value**	**Matlab Value**
Location probability	50%	50%
Time probability	50%	50%
Elevation model	DEM 50 m SA	SRTM 4.1
Transmitter clearance angle	Yes	Yes
Receiver clearance angle	Yes	Yes
Tropospheric Scatter correction	No	No
Radio climate zone	-43.3 dN	-43.3 dN
Radio climate zone adjustment	No	No
Propagation path	No Sea, Land only	No Sea, Land only
Coverage prediction limit	Auto area - 35 dBμV/m	Manual 30 km
Negative height correction	Terrain clearance angle	Effective clearance angle

As discussed in Chapter 2, subsection 2.6.6, there are some differences between ITU-R P.1546 version 4 and version 5. Version 4 was implemented for simulation. This version was chosen due to the availability in the Matlab implementation. The differences between version 4 and version 5 would not affect the simulation in any manner.

Three of the parameters were not implemented the same for the following reasons:

- The Digital Elevation Model (DEM) with 50 m resolution used in CHIRPlus BC was not available in the format needed to be used in the Matlab software. Therefore, the highest resolution SRTM file was implemented in the Matlab software. SRTM version 4.1 has a data resolution of 100 m.
- The coverage prediction limit for CHIRPlus BC can be set to automatic, which means the minimum coverage area is predicted to a receive power of 35 dBμV/m. This could not be implemented in Matlab; therefore, a maximum distance of 30 km is predicted to ensure all the areas containing receiver power of 35 dBμV/m and better, are included.

Two different negative height correction methods were implemented to test the impact of these two methods on the coverage prediction. These two methods were implemented as described in the ITU-R P.1546-4 regulation.

4.3.4 Validation results

Validation was done on a single site, for a single transmitter-receiver pair. The path between transmitter and receiver is at an azimuth of 35.6° East from North in the first sector of the site. The validation is also done at 0° tilt and 10.9 m height adjustment. Figure 4.8 shows a plot of the coverage prediction obtained from both the Matlab and CHIRPlus BC simulation.

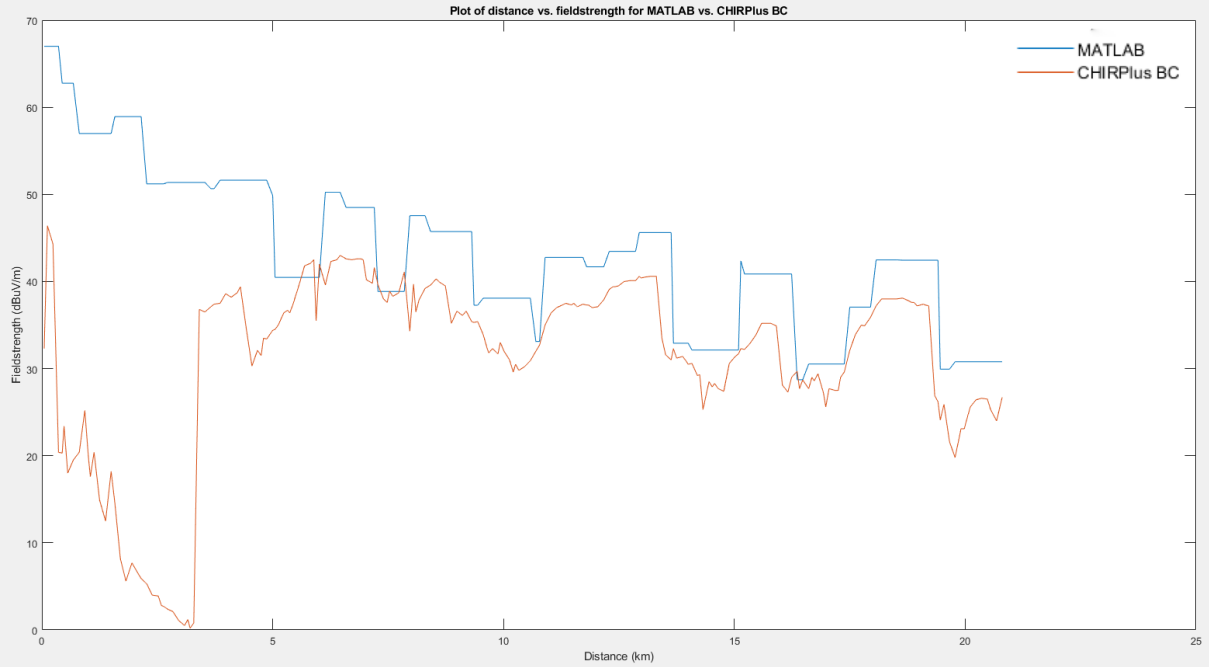

Figure 4.8: Coverage prediction of Matlab vs. CHIRPlus BC simulation software

There is a very good correlation from 6 km on, with the Matlab simulation generally giving higher field strength values. The difference in correlation from distance 0 to 3 km can be explained by the different corrections implemented, by the two software suites, for a negative height value. This site has negative height values. In the recommendation ITU-R P.1546-4, it is explained that the first method (terrain clearance angle method) calculates the clearance angle from 0 m up to 15 km for the specific path. The calculated clearance angle, which is positive, was used for the correction. It may cause discontinuity in field strength (at 3 km) as can be seen on the CHIRPlus BC results plot in Figure 4.8. The second method (effective clearance angle method) regards the

ground as approximating an irregular wedge over the range of 3 to 15 km from the transmitter, with its mean value at 9 km. This method takes fewer explicit account of terrain height changes, but ensures continuity in field strength around the transmitter. This is the reason why the effective clearance angle method was implemented in the Matlab simulation software; the continuity ensures no loss in coverage data in the first 3 km from the transmitter, as shown in the case for CHIRPlus BC.

The statistics in Table 4.10 were calculated using validation datasets (only from 3 km upwards) as seen in Figure 4.8, considering CHIRPlus BC as the baseline.

Table 4.10: Statistical data for validation test

ME	**MAE**	**RMSE**
6.04	6.16	6.93

The correlation coefficient for the two datasets was calculated to be 0.7296, which means there is a 73% correlation within a range from 3 to 15 km from the transmitter. The error margins are between 6 and 7 dBμV/m as obtained by three different statistical methods seen in Table 4.10, which is below 15% of the maximum coverage in a range from 3 to 15 km from the transmitter. The difference could be due to the fact that certain path loss constants have not been implemented in the Matlab simulation, because of possible missing information. This does not affect the results, because the offset is constant for all values above 3 km. The CHIRPlus BC validation tool could not be used to validate the Matlab simulation software over the first 3 km coverage calculation.

4.4 Conclusion

This chapter presented the verification and validation of specific models and functions implemented in the software. These functions include the EARFCN to frequency band conversion, antenna gain patterns and antenna power at a specific bearing. All of the verification exercises resulted in no error, which means that the sub-functions and

equations implemented in the simulation software were correctly implemented and all the outputs were tested.

The validation section gave proof of the validity of the simulation results based on correlation with a commercial validated software suite, CHIRPlus BC. Validation was done on a single site, for a single transmitter, receiver pair. The function for obtaining the path height profile was validated first and it was found that the standard deviation of the values between CHIRPlus BC and Matlab were 2.88 m. This means that an average error of 0.2% is obtained. It was found that there was a difference of 15% in the maximum coverage between CHIRPlus BC and Matlab. The two datasets also showed a correlation between the field strength results for a single path obtained by CHIRPlus BC and Matlab of 73%. The validation gives a good indication that the simulation software produces valid results.

The next section contains the results used to answer the research questions.

Chapter 5

Results and analysis

Chapter 5 gives a description of the experimental setup and the methodology describing how the results were obtained. It includes input and output data as well as the results obtained.

5.1 Results introduction

In this chapter, the method of how the experiments were executed is discussed. The different input and output parameters are explained, followed by a description of how the results were obtained. A statistical analysis was done to be able to draw valid conclusions based on the predicted coverage data. Each analysis is shown and explained in detail.

5.2 Experimental method

This section explains the experimental method used to obtain the results before statistical analysis. The methodology is explained visually by using the logical flow diagram

in Figure 5.1, followed by a discussion of the steps.

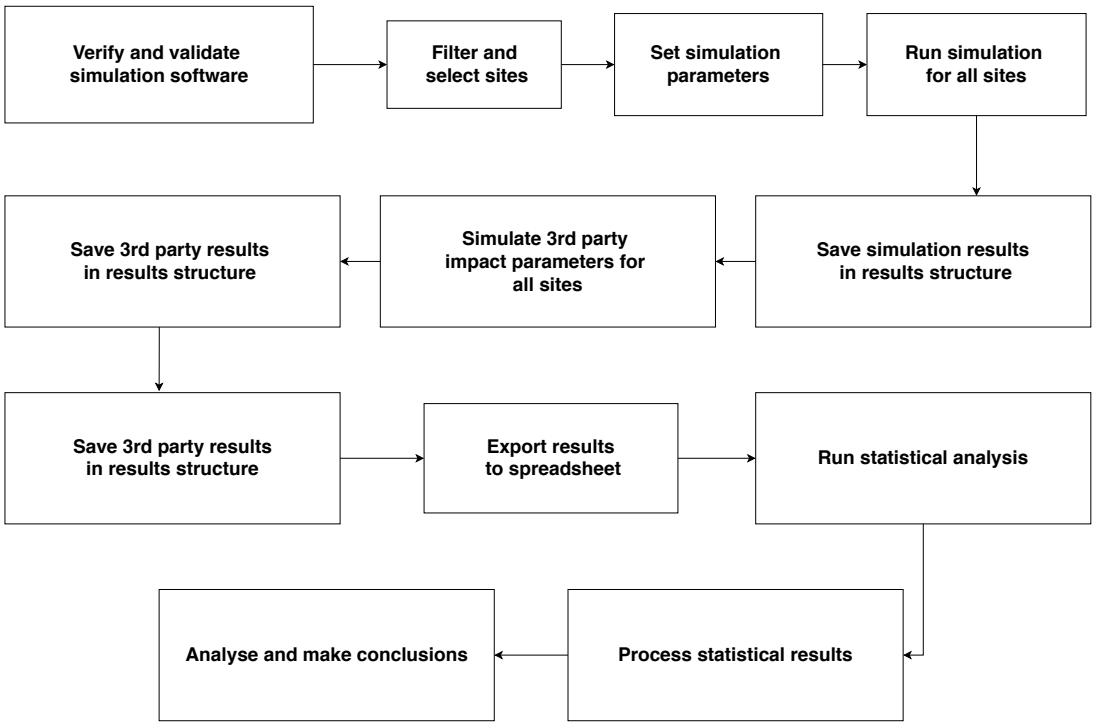

Figure 5.1: Data generation and analysis process

The experimental method begins with verifying and validating the simulation software. This ensures that the results used to answer the experimental questions are valid and that the functions and processes have been verified. The verification and validation can be viewed in Chapter 4. Chapter 3 includes the system model, which shows the layout of the simulation software. This chapter also includes the method to filter and select the sites that were used for the statistical analysis. The 31 most accurately positioned sites were filtered to be used as the statistical sites for analysis.

The next step is to set the simulation parameters. These parameters are inserted within the software code. Table 3.8 in subsection 3.5.2 defines the simulation parameters and describes how they were implemented in the simulation software.

The path loss model parameters must then be selected. The ITU-R P.1546-4 path loss model can be implemented with different parameter settings as well as different correction factors as in the ITU specification document. Table 3.9, subsection 3.5.3, explains how the path loss model parameters were implemented.

After the simulation parameters are set, the simulation is executed for all the sites and saved in the transmitter results structure as defined in Chapter 3, subsection 3.12.

After the effective height and TRF parameters have been simulated for each sector, they are also exported and saved to the results structure.

The transmitter results structure can now be used to export all the data to a spreadsheet, which were used to run the statistical analysis. The data was processed to provide results that were analysed and used for meaningful conclusions on the experimental question.

Table 5.1 gives a description of the spreadsheet layout and the parameters that were used for the statistical analysis:

Table 5.1: Parameters for statistical analysis

Variable Name	**Data type**	**Limitations**	**Variable type**
Site ID	Integer	Arbitrary	-
Sector	Integer	[0,120,240]	-
Height	Integer	5:1:15	Predictor
Tilt	Decimal	-5:0.5:10	Predictor
Coverage	Integer	MIN:10 / MAX: 595	Response
mean TRF	Decimal	MIN: 5.71/ MAX: 156.55	constant
mean Effective height	Decimal	MIN: -333.38/ MAX: 151.7	constant
mean TRF, main beam	Decimal	MIN: 5.11/ MAX: 200.33	constant
mean Effective height, main beam	Decimal	MIN: -462.55/ MAX: 166.73	constant
mean TRF, side lobes	Decimal	MIN: MIN: 6.28/ MAX: 105.73	constant
mean Effective height, side lobes	Decimal	MIN: -183.46/ MAX: 134.3	constant

The following is a description of the terms as seen in Table 5.1:

- Site ID: Is the ID of each site as referenced in the online source ("open-cell ID").
- Sector: The angle at which the main sector beam faces relative to true North.
- Height: Height of the antenna above ground.
- Tilt: Tilt angle from flat mounted antenna on mast.
- Coverage: Number of receivers above the coverage threshold.

- Mean TRF: Average TRF per sector.
- Mean effective height: Average normalised effective height per sector.
- Mean TRF, main lobe: Average TRF covering the main beam of the sector.
- Mean effective height, main lobe: Average normalised effective height covering the main beam of the sector.
- Mean TRF, side lobes: Average TRF covering the side lobes of the sector.
- Mean effective, side lobes: Average normalised effective height covering the side lobes of the sector.

5.3 Statistical analysis

To analyse the impact of the tilt and height adjustments on coverage, three types of statistical analyses were done. The first analysis was done on the impact of tilt adjustment at a constant height. The second analysis was done on the impact of height adjustment at a constant tilt and the third analysis analyses the combined impact of height and tilt. Each analysis included the following statistical information:

- Statistical significance.
- Co-variance parameters.
- Estimated marginal mean and pairwise comparison.

5.3.1 Statistical significance [1]

The first important parameter is called the p-value, which describes the statistical significance of the results. A set of results is said to be statistically significant if the p-value is smaller than 0.05. Statistical significance does not necessarily imply that the results

are important in practice, but if the results are statistically insignificant, the results will have no practical significance.

5.3.2 Co-variance parameters

The second set of parameters are called estimates of co-variance parameters. There are two values that are important. The first variable is called the residual, which can be seen as the mean square error (MSE) of the intra-site impact of the adjustment on coverage. The second variable is called the variance, which is a hierarchical or multi-level analysis. This analysis uses the MSE, which explains the inter-site variability of the cluster data, with the different sites as the outcome variable of interest. Intra-site can be explained as the impact of the adjustment within a single site. Inter-site can be explained as the impact of the adjustment with the position of the sites taken into account. [59]

5.3.3 Estimated marginal means and pairwise comparison

The estimated marginal means gives the average coverage for each adjustment over all the sites. For each set of adjustments, a graph is shown to visually show the impact of the adjustment.

The pairwise comparison is made to analyse the amount of effect each of the adjustments had on coverage. This was done by comparing each of the adjustment's impact individually against all the other adjustment's impact.

5.3.4 Effect size and practical significance [2]

In [2] effect size is described as a parameter that can be used to define the practical significance of the adjustments. Effect size, d, can be calculated by obtaining the standardized difference between the means of two populations. The following equation

explains how effect size was calculated:

$$d = \frac{|\bar{x}_i - \bar{x}_j|}{\sqrt{MSE}} \tag{5.1}$$

where x_i and x_j are the two mean values that are compared, and MSE is the mean square error of the co-variance analysis. The following table presents a qualitative assessment of the effect of d on practical significance:

Table 5.2: Effect size values

Value	Effect
0.2	Small effect
0.5	Medium effect
0.8	Large effect

The effects of each adjustment are shown in a table. This describes the practical significance of each adjustment on coverage.

5.3.5 Correlation analysis

A correlation study was done in order to see if a trend can be seen from correlating the TRF as well as the normalised effective height parameters with coverage. Two correlation studies have been done. The first correlation is a parametric correlation, assuming an underlying statistical distribution of the data. The second correlation was a non-parametric correlation, which does not rely on any distribution of the data.

5.4 Tilt analysis

The following section contains the information of statistically analyzing the impact of the antenna tilt adjustment on coverage. It includes the mean coverage analysis for all tilt adjustments, and it includes the co-variance curves. The pairwise comparison

includes a table showing the impact on a change in adjustment. The practicality of the impact was discussed using the effect size variable.

5.4.1 Mean coverage analysis

A mean coverage analysis was done on the tilt adjustment to analyse the impact of tilt on coverage. The analysis was used to reveal the impact of tilt on the mean coverage of the 31 sites. Figure 5.2 shows the statistical coverage results for the tilt analysis.

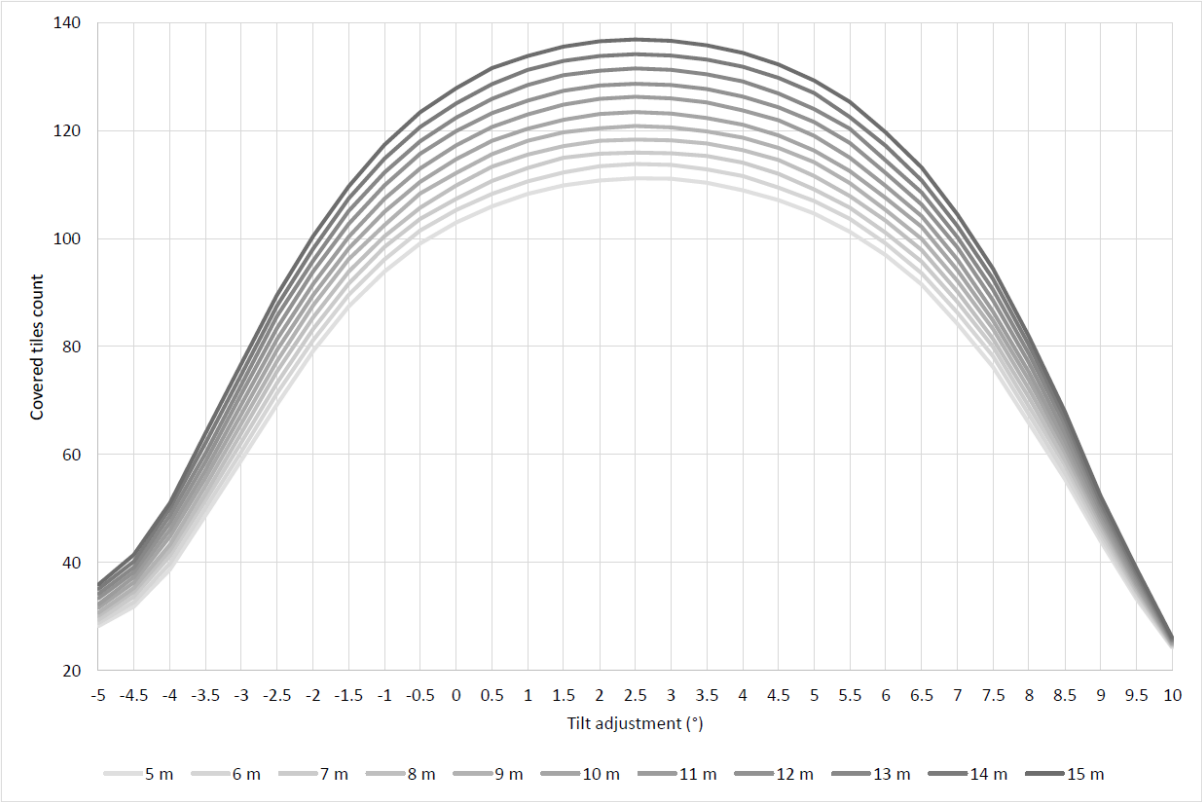

Figure 5.2: Mean coverage for tilt adjustments at every height

The curves in Figure 5.2, have a very flat response. At the maximum mean coverage curve (15 m height), the mean coverage decreases 25% of the maximum mean coverage with a down tilt adjustment of 5°. From here the gradient increases and the coverage decreases to 50% of the maximum mean coverage with another 5° down tilt. This shows that the impact of tilt on mean coverage increases exponentially when errors

are made in regions not around the optimal tilt adjustment. It can be seen from Figure 5.2 that the average impact of the tilt adjustment follows the same behaviour.

Looking at the height adjustment curves at -5°, the mean coverage increases with 17%, from the 5 m height curve up to the 15 m height curve. Looking at the optimal tilt adjustment (2.5°), the mean coverage increases with 19%, from the 5 m height curve up to the 15 m height curve. At a tilt adjustment of 10°, the coverage increases with 4% with an upwards height adjustment from 5 m to 15 m.

It is important to note that the optimal coverage is not around 0° tilt. This is due to the antenna pattern that is designed to have electrical down tilt.

5.4.2 Co-variance analysis

The co-variance analysis was done to reveal if tilt adjustment error(residual impact) would have a greater impact on coverage if the impact of terrain as a factor is also accounted for (variance impact) in the calculation of coverage. Figure 5.3 shows the residual and variance plot for tilt at each of the height adjustments.

From Figure 5.3, it can be seen that the graphs follow the same behavior. It is evident that the residual effect of tilt is almost half of the effect of the variance around the optimal tilt adjustment. This implies that the position of the site plays a significant role on the coverage amount when taking tilt adjustment into account. The position of the site defines how the terrain height varies, which states that the terrain plays an important role when the impact of tilt adjustment is analysed. It is important to note that the variance curve differs much more from the residual curve around the optimal tilt adjustment, which means around optimal tilt, the impact of terrain around the site is much more significant on coverage.

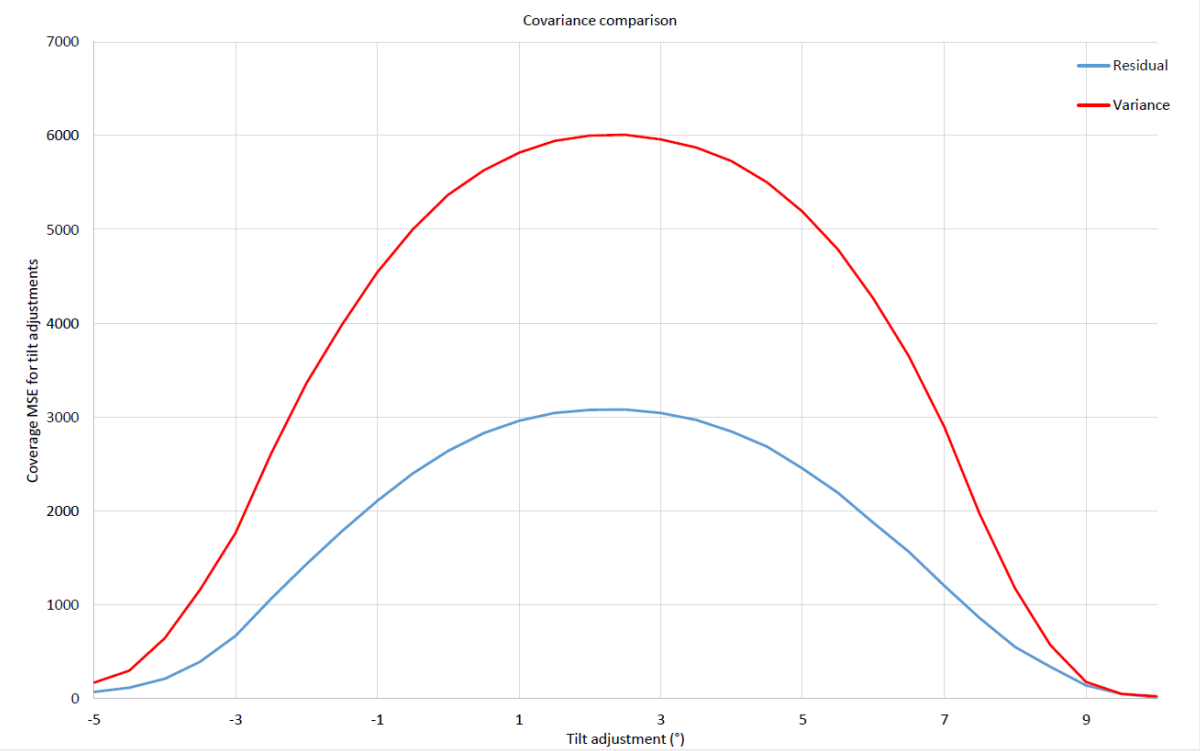

Figure 5.3: Co-variance comparison for tilt adjustments

5.4.3 Pairwise comparison

To test the significance of the impact of each tilt adjustment on coverage, a pairwise comparison is made. Each of the tilt adjustments is compared to one another to show the impact of the change in tilt. Table 5.3 shows the pairwise tilt comparison. Each comparison is marked with alphabetical symbols to show the mean amount of covered tiles for each tilt adjustment at different heights. For each height adjustment, the pairwise impact differs.

Table 5.3: Pairwise comparison of tilt adjustments

Tilt (°)	- 5	- 4.5	- 4	- 3.5	- 3	- 2.5	- 2	- 1.5	- 1	- 0.5	0	0.5	1	1.5	2	2.5	3	3.5	4	4.5	5	5.5	6	6.5	7	7.5	8	8.5	9	9.5	10
-5	x				c	d			g		h	h	h	h	h	h	h	h	h	h	h	g	g	f	d	d	c	b			
-4.5		x			b	c			f		g	h	h	h	h	h	h	h	h	h	h	g	f	f	d	d	c	a			
-4			x		a	b			g		f	g	h	g	g	g	g	g	g	g	g	g	g	f	d	d	b				a
-3.5	ab	a		x		a			g		f	g	h	g	g	f	f	f	g	g	f	f	d	d	d	c	b			a	b
-3	c	b	a		x				d		d	d	d	d	d	f	f	d	d	d	d	d	c	c	c	b				a	b	d
-2.5	d	c	b	a		x			d		d	c	d	c	c	c	c	c	c	c	c	b	b	b	a				a	b	d	e
-2	e	d	c	b	a		x		b		a	b	d	c	b	b	b	b	b	b	b	a	a						b	c	e	f
-1.5	f	e	d	c	b	a		x			a	a	e	f	a	a	a	a	a	a	a								c	d	f	g
-1	g	f	d	d	c	a			x		a	a	d	f	a	a	a	a	a	a	a			a	a	a	b	a	c	e	f	h
-0.5	g	g	f	d	c	b	a			x	b	b	d	f	a	a	a	a	a	a	a			a	a	a	c	b	d	f	g	h
0	h	g	f	d	d	b	a				c	c	d	f	a	a	a	a	a	a	a			b	b	b	c	d	d	f	g	h
0.5	h	h	g	d	d	c	b				x	c	d	f	a	a	a	a	a	a	a			b	b	b	c	d	d	f	g	h
1	h	h	g	d	d	c	b	a				x	d	f	a	a	a	a	a	a	a			b	b	b	c	d	d	f	g	h
1.5	h	h	g	d	d	c	b	a	x				d	f	a	a	a	a	a	a	a			b	b	b	c	d	d	f	g	h
2	h	h	g	d	d	c	b	a					d	f	x	a	a	a	a	a	a			b	b	b	c	d	d	f	g	h
2.5	h	h	g	d	d	c	b	a					d	f		x	a	a	a	a	a			b	b	b	c	d	d	f	g	h
3	h	h	g	d	d	c	b	a					d	f			x	a	a	a	a			b	b	b	c	d	d	f	g	h
3.5	h	h	g	d	d	c	b	a					d	f				x	a	a	a			b	b	b	c	d	d	f	g	h
4	h	h	g	d	d	c	b	a					d	f					x	a	a			b	b	b	c	d	d	f	g	h
4.5	h	h	g	d	d	c	b	a					d	f						x	a			b	b	b	c	d	d	f	g	h
5	h	g	f	d	d	b	a						d	f							x			b	b	b	c	d	d	f	g	h
5.5	g	g	f	d	c	b	a						d	f								x		b	b	b	c	d	d	f	g	h
6	g	f	d	d	c	b	a						d	f									x	b	b	b	c	d	d	f	g	h
6.5	f	f	d	d	c	b							d	f										x	b	b	c	d	d	f	g	h
7	d	d	d	c	b	a					a	a	b	f	a	a	a	a	a	a	a	a	a		x	b	b	d	d	f	g	h
7.5	d	d	c	b							a	b	b	f	a	a	a	a	a	a	a	a	a	x		a	b	d	d	f	g	h
8	c	c	b								b	c	c	f	a	a	a	a	a	a	a	a	a	b	a		a	d	d	f	g	h
8.5	b	b	a								c	c	c	f	a	a	a	a	a	a	a	a	a	b	b	a		x	d	f	g	h
9	a										c	c	c	f	a	a	a	a	a	a	a	a	a	b	b	a	x		a	f	g	h
9.5											c	c	c	f	a	a	a	a	a	a	a	a	a	b	b	a	x	a		f	g	h
10											c	c	c	f	a	a	a	a	a	a	a	a	a	b	b	a	x	b	a		g	h

Table 5.4 defines the keys for Table 5.3. Each number represent the mean covered amount of grid points for all the sites.

Table 5.4: Pairwise tilt symbol values

Symbol	**Value**
a	20-29
b	30-39
c	40-49
d	50-59
e	60-69
f	70-79
g	80-89
h	>90

It is clear from Table 5.3 that for every 0.5° tilt the covered tile count increases with an average of 10 tiles. This means that for a maximum coverage at tilt 2.5° and a height adjustment of 10 m, the impact of a 0.5° tilt error is 7% of the coverage at the mentioned adjustment settings.

In Chapter 2, subsection 2.11.1 [11], it was mentioned that an antenna tilt error of 3° can have an increased impact on the coverage up to 100%, implementing a UMTS network. This shows the significant impact that a tilt error can have on coverage. It can be seen that tilt does not have such a large impact on LTE as on a UMTS network.

If the tilt values on the horizontal axis are shifted so that the -5° and 10° are placed in the middle of the table, the values would produce an oval like pattern. The open cells in the table represent the adjustments pairs that would give zero coverage.

5.4.4 Tilt effect size

As discussed in subsection 5.3.4, the tilt effect size is a parameter that can be used to define the practical impact of the antenna adjustment on coverage. Table 5.5 is a summary of the tilt effect size calculated at each of the height adjustments, from 5 to 15 meters. The keys for Table 5.5 are defined in Table 5.2.

It can be seen from Table 5.5 that there is a high practical effect (symbol *c*) at a pairwise adjustment comparison of -0.5° and -2°, which means that a tilt error of 1.5° could have a high practical effect on coverage at that specific adjustment. This special case could be due to the error around the optimal tilt adjustment. An average tilt error between 1° and 2° can have a small practical effect on coverage. An average tilt error between 2° and 3° has a medium practical effect on coverage; and an average tilt error above 3 degrees has a significant practical effect on coverage. The open cells in the table represent the adjustments that would have zero impact on coverage.

Table 5.5: Effect size of tilt adjustments

Tilt (°)	- 5	- 4.5	- 4	- 3.5	- 3	- 2.5	- 2	- 1.5	- 1	- 0.5	0	0.5	1	1.5	2	2.5	3	3.5	4	4.5	5	5.5	6	6.5	7	7.5	8	8.5	9	9.5	10
-5	x			a	b							c	c	c	c	c	c	c	c	c	c	c	c	c	c	c	b	a	a		
-4.5		x		a	b							c	c	c	c	c	c	c	c	c	c	c	c	c	c	c	b	a			a
-4	a		x	a	a							c	c	c	c	c	c	c	c	c	c	c	c	c	c	b	a	a			a
-3.5	a	a	a	x								c	c	c	c	c	c	c	c	c	c	c	b	b	b	a	a		a	b	b
-3	b	b	a		x							c	c	c	c	c	c	c	c	c	c	b	b	a	a			a	b	b	c
-2.5	c	b	b	a		x						b	b	b	b	b	b	b	b	b	b	b	a	a			a	b	b	c	c
-2	c	c	b	b	a		x					a	b	b	b	b	b	b	b	b	a	a	a			a	a	b	c	c	c
-1.5	c	c	c	b	b	a		x				a	a	a	a	a	a	a	a	a	a	a				a	b	b	c	c	c
-1	c	c	c	c	b	a	a		a			a	a	a	a	a	a	a	a	a	a					a	b	b	c	c	c
-0.5	c	c	c	c	b	b	a	a		x					a	a	a	a	a	a						a	b	c	c	c	c
0	c	c	c	c	c	b	b	a	a		x															a	b	c	c	c	c
0.5	c	c	c	c	c	b	a	a	a	a		x														a	b	c	c	c	c
1	c	c	c	c	c	b	b	a	a	a	a		x													a	b	c	c	c	c
1.5	c	c	c	c	c	b	b	a	a	a	a	a		x												a	b	c	c	c	c
2	c	c	c	c	c	b	b	a	a	a	a	a	a		x											a	b	c	c	c	c
2.5	c	c	c	c	c	b	b	a	a	a	a	a	a	a		x										a	b	c	c	c	c
3	c	c	c	c	c	b	b	a	a	a	a	a	a	a	a		x									a	b	c	c	c	c
3.5	c	c	c	c	c	b	b	a	a	a	a	a	a	a	a	a		x								a	b	c	c	c	c
4	c	c	c	c	c	b	b	a	a	a	a	a	a	a	a	a	a		x							a	b	c	c	c	c
4.5	c	c	c	c	c	b	a	a	a	a	a	a	a	a	a	a	a	a		x						a	b	c	c	c	c
5	c	c	c	c	c	b	b	a	a	a	a	a	a	a	a	a	a	a	a		x					a	b	c	c	c	c
5.5	c	c	c	c	c	b	b	a	a	a	a	a	a	a	a	a	a	a	a	a		x				a	b	c	c	c	c
6	c	c	c	c	c	b	a	a	a	a	a	a	a	a	a	a	a	a	a	a	a		x			a	b	c	c	c	c
6.5	c	c	c	c	b	a	a	a	a	a	a	a	a	a	a	a	a	a	a	a	a	a		x		a	b	c	c	c	c
7	c	c	c	b	a	a	a	a	a	a	a	a	a	a	a	a	a	a	a	a	a	a	a		x		a	b	c	c	c
7.5	c	c	b	a	a	a	a	a	a	a	a	a	a	a	a	a	a	a	a	a	a	a	a	a		x		a	b	c	c
8	b	b	a	a	a			a	a	a	a	a	a	a	a	a	a	a	a	a	a	a	a	a	a		x	a	a	b	c
8.5	a	a	a			a	b	b	b	c	c	c	c	c	c	c	c	c	c	c	c	c	c	b	b	a	a	x	a	a	b
9	a				a	b	b	b	b	c	c	c	c	c	c	c	c	c	c	c	c	c	c	c	b	a	a	a	x	a	a	
9.5				a	b	b	c	c	c	c	c	c	c	c	c	c	c	c	c	c	c	c	c	c	c	b	a	a	a	x		
10			a	b	b	c	c	c	c	c	c	c	c	c	c	c	c	c	c	c	c	c	c	c	c	c	b	a	a		x	

5.5 Height analysis

The following section contains the information of statistically analysing the impact of the antenna height adjustment on coverage. It includes the mean coverage analysis for all height adjustments, and it includes the co-variance curves. The pairwise comparison includes a table showing the impact on a change in adjustment. The practicality of the impact is also discussed using the effect size variable.

5.5.1 Mean coverage analysis

Figures 5.4 and 5.5 show the mean covered tiles of the height adjustment curves for every tilt adjustment. Figure 5.4 shows the curves for the tilt adjustments from -5° to 2.5° tilt and Figure 5.5 shows the curves for the tilt adjustments from 3° to 10°. The curves are put on two different plots for better visual analysis. The data labels are added to the curves in order to see the actual values of each curve; the values labelled in bold are the values of the covered tiles at maximum tilt.

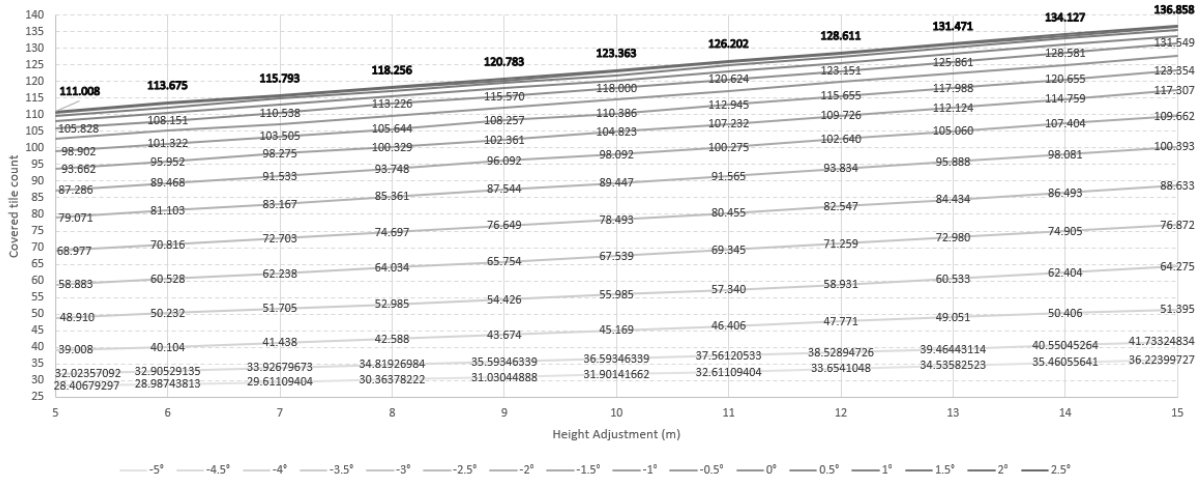

Figure 5.4: Mean coverage for height adjustments at every tilt

The increase in coverage from 5 to 10 m (5 m height adjustment) at -5° tilt is 22%; and at 2.5° (optimal tilt) there is a coverage increase of 18%; at 3° there is a coverage increase of 17%, and at 10° the increase is 7% of the coverage. It can be seen that all the curves

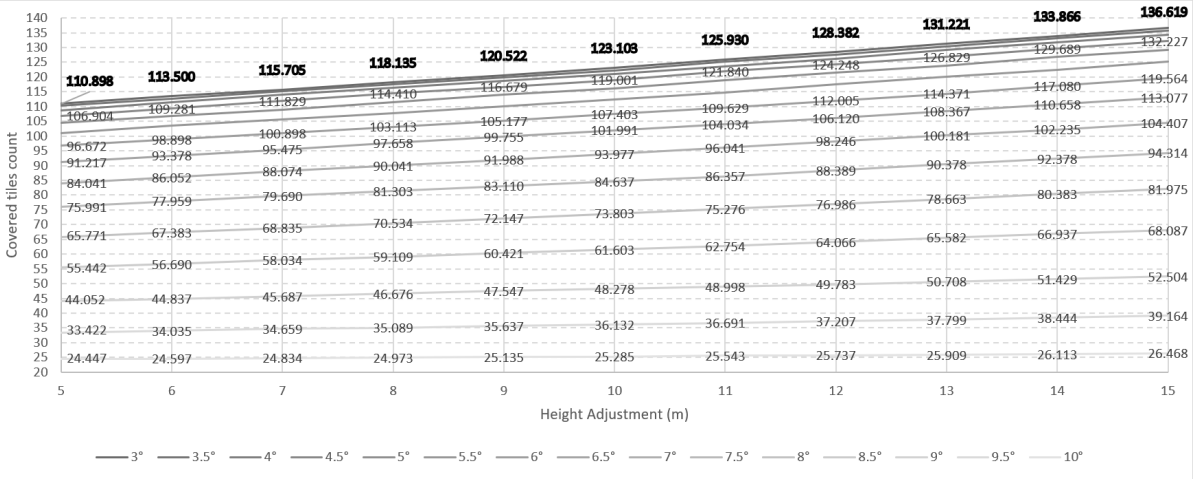

Figure 5.5: Mean coverage for height adjustments at every tilt

are linear, which implies that the impact of height on coverage is linear at each of the tilt settings.

It is evident from the two figures that as the tilt comes closer to the optimum coverage, the slope of the curves increases. This verifies that at optimal tilt adjustment (2.5°), the height has a much more significant impact on coverage than at the other tilt adjustments. As described in subsection 5.4.1, a tilt error has less of an impact on coverage around the optimal tilt adjustment, but the inverse is true for a height error.

5.5.2 Co-variance analysis

Figure 5.6 shows the residual and variance plot for tilt at each of the heights. The same co-variance analysis that has been done for tilt has been repeated for the height adjustments.

From Figure 5.3, it is clear that the residual and the variance effect is close to each other. This implies that the position of the site does not have any significant effect on coverage when taking height adjustment into account. When height is adjusted, it can be seen as a constant offset from the height terrain around the site.

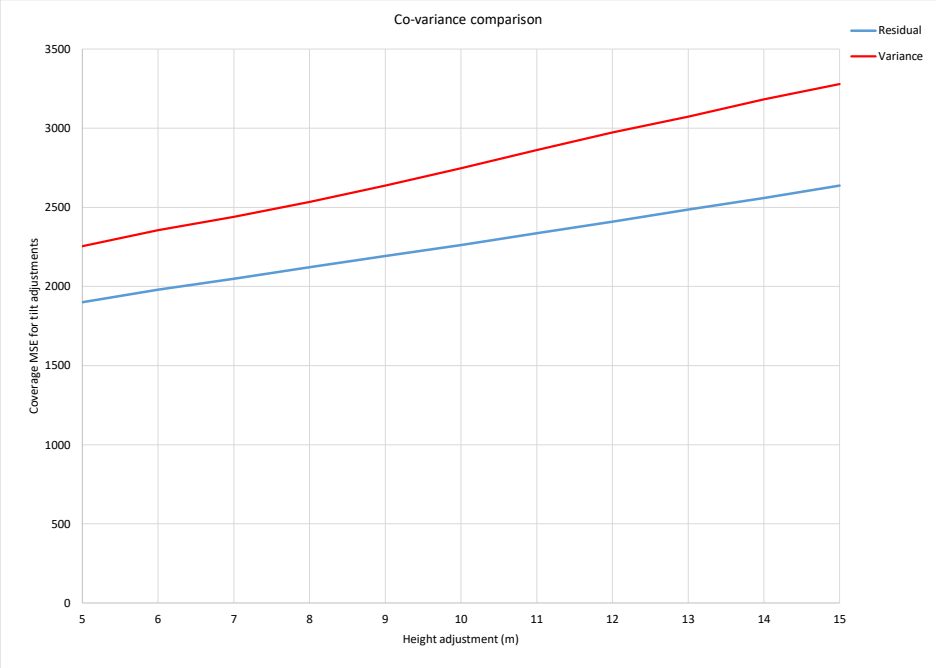

Figure 5.6: Co-variance comparison for height adjustments

5.5.3 Pairwise comparison

A pairwise comparison is also made to test the significance of the impact of each height adjustment on coverage. The coverage at each of the height adjustments is compared to one another to show the impact of the change in height on coverage. Table 5.6 shows the pairwise height comparison. Each comparison is marked with alphabetical symbols to show the significance of the impact of the height adjustment over the range of tilt adjustments.

Table 5.7 describes the symbols as used in Table 5.6. Analysing the information in Table 5.7, with an average height error of 2 m, the impact on coverage count is 5 to 9. This means that an average error of ± 2 m in height at the optimal tilt setting reduces or increases coverage by 6%.

As mentioned in Chapter 2, subsection 2.11.2 [49], the impact of an increase in height

Table 5.6: Pairwise comparison of height adjustments

Height (m)	**5**	**6**	**7**	**8**	**9**	**10**	**11**	**12**	**13**	**14**	**15**
5	x		a	a	a	b	c	c	d	d	e
6		x		a	a	a	b	c	c	d	d
7	a		x		a	a	b	b	c	c	d
8	a	a		x			a	b	b	c	c
9	a	a	a		x		a	a	b	b	c
10	b	a	a			x		a	a	b	b
11	c	b	b	a	a		x		a	a	b
12	c	c	b	b	a	a		x		a	a
13	d	c	c	b	b	a	a		x		a
14	d	d	c	c	b	b	a	a		x	
15	e	d	d	c	c	b	b	a	a		x

Table 5.7: Pairwise height symbol values

Symbol	**Value**
a	5-9
b	10-14
c	15-19
d	20-24
e	>25

can increase cell-edge interference. It is therefore important to note the impact of height if coverage can be increased by 6%: if there is a height error of 2 m, it can increase interference between sites using a cell re-use system. The open cells in the table represent the adjustments that would have zero impact on coverage.

5.5.4 Height effect size

Table 5.8 is a summary of the height effect size calculated at each of the tilt adjustments from -5° to 10°. The keys for Table 5.8 are defined in Table 5.2.

Table 5.8: Effect size of height adjustments

Height (m)	**5**	**6**	**7**	**8**	**9**	**10**	**11**	**12**	**13**	**14**	**15**
5	x		a	a	b	b	c	c	c	c	c
6		x		a	a	b	c	c	c	c	c
7	a		x		a	a	b	c	c	c	c
8	a	a		x		a	b	b	c	c	c
9	b	a	a		x		a	b	b	c	c
10	b	b	a	a		x		a	b	b	c
11	c	c	b	b	a		x		a	b	b
12	c	c	c	b	b	a		x		a	b
13	c	c	c	c	b	b	a		x		a
14	c	c	c	c	c	b	b	a		x	
15	c	c	c	c	c	c	b	b	a		x

It is clear from Table 5.8 that an average height error of 2 to 3 m has a small practical effect on coverage. An average height error of 4 to 5 m has a medium practical effect on coverage and an average height error above 6 m can have a high practical effect on network coverage. The open cells in the table represent the adjustments that would have zero impact on coverage.

5.6 Combined analysis

An analysis was done on the combined impact of the adjustments on coverage. It was found that the combined impact of the two adjustment is not statistical significant. This means that the impact of the combined adjustment does not reveal any unique optimisation compared to the optimised state of the two adjustments individually. The impact of the combined adjustment can be effectively analysed considering the two adjustments separately.

5.7 Terrain correlation

Tables 5.9 and 5.10 shows the correlation of each statistical terrain variable against coverage. It can be seen that there is a very weak correlation between coverage and the TRF, but the correlation of coverage against effective height is significant. The parametric and non-parametric parameters are explained earlier in subsection 5.3.5.

Table 5.9: Parametric terrain impact correlation

Terrain Parameter	**Correlation value**
mean TRF	0.083%
Mean effective height	0.484%
Mean TRF, main lobe	0.076%
Mean effective height, main lobe	0.432%
Mean TRF, side lobes	0.084%
Mean effective, side lobes	0.41%

Table 5.10: Non-parametric terrain impact correlation

Terrain Parameter	**Correlation value**
mean TRF	0.192%
Mean effective height	0.481%
Mean TRF, main lobe	0.226%
Mean effective height, main lobe	0.452%
Mean TRF, side lobes	0.147%
Mean effective, side lobes	0.493%

It can therefore be concluded that the TRF cannot be used as a predictor for coverage, because it does not correlate with coverage. Effective height has a good correlation, which means is can be used to predict the impact of the terrain on coverage around a site. It was mentioned that tilt adjustments are dependent on the effect of terrain when coverage is predicted. It can therefore be concluded that the effect of the tilt adjustment together with the effective height must be used as a predictor of the site coverage. The height adjustment is independent of terrain effect to predict coverage.

5.8 Conclusion

In this chapter, each of the adjustment parameters, tilt and height, were individually analysed to determine the impact of these two parameters on network coverage. It was possible to obtain the statistical as well as the practical impact (effect size) on coverage.

The tilt analysis revealed that a 0.5° tilt error can have an impact of 7% on coverage. From the co-variance analysis, it can be seen that the position of the site plays a big role in the impact of tilt adjustment. In a more practical sense, the effect size parameter implies that tilt adjustment error already has a significant practical effect from 3° upwards.

The height analysis revealed that a height error has a much higher impact on coverage at optimal tilt adjustment. At optimal tilt the maximum height error of 10 m can have a coverage impact of 22%. The co-variance analysis revealed that the position of the site has no influence on the impact of height adjustment error on coverage and according to the effect size parameter, height adjustment error only has a high practical effect on coverage from 6 m and up.

The second analysis included a combination analysis. There was no change in coverage impact, when the adjustments are made in combination. It is therefore statistically insignificant to do a combination analysis on a single performance metric, which in this case is coverage.

The third analysis was a correlation study that determined the impact of different terrain parameters on the coverage result. The mean effective height had a very high correlation with coverage in comparison with the mean terrain roughness factor.

Chapter 6

Conclusion and Recommendations

Chapter 6 reflects on the research that has been done. It includes remarks and a conclusion on the results obtained through statistical analysis. It also includes recommendations for future work. This chapter answers the research questions and describes how the results address the research problem.

6.1 Work summary

The title of this dissertation is "Modelling the impact of antenna installation error on network performance", where the installation parameters are antenna height and mechanical tilt and the parameter under test is LTE network performance. The focus of the research is to determine what the impact of certain antenna installation parameters is on coverage and what the installation parameter tolerances should be. As mentioned in Chapter 1, network performance can be defined as the coverage of an LTE site, when assessing the impact of the antenna installation parameters.

The research problem has been addressed by answering the following three research

questions:

- What is the practical impact of a tilt adjustment error on coverage?
- What is the practical impact of a height adjustment error on coverage?
- What influence does the terrain have on coverage, taking the tilt and height into account?

In Chapter 2, a literature study was done to understand and investigate the important concepts of the study and present prior work. Chapter 3 describes the system model, which includes the calculations as well as the models developed to simulate a practical LTE site.

The verification and validation of the software and software functions are presented in Chapter 4. This ensures that the methods used to obtain the results are valid and proven to be implemented correctly.

The results and statistical analysis is shown in Chapter 5. This chapter also includes the analysis methods as well as the interpretation of all the results obtained. Chapter 5 obtains the information in order to answer the research questions as thoroughly as possible.

6.2 Remarks on results

As mentioned in Chapter 1, it is of great concern for cellular network operators that the implemented network performs as designed. It is therefore important to understand the effect of inaccurate installations. The impact of an error on antenna installation is evident, as reflected in the results of Chapter 5. These results support answering the three research questions as follows:

6.2.1 What is the practical impact of a tilt adjustment error on coverage?

Based on the tilt adjustment analysis that was done, it was found that the tilt has a statistically significant impact on coverage. The co-variance analysis shows that the inter-site or residual impact of tilt on coverage is much smaller than the variant impact of tilt on coverage. This means that the placement of the LTE site has a significant impact on the coverage when tilt is taken into account. Taking the tilt pairwise comparison into account gives some insight on the sensitivity of the tilt adjustment.

Statistically a minimum tilt adjustment error of 0.5° can have a maximum average impact of 7% on coverage. In [11], it was stated that the impact of 3° tilt adjustment error can decrease the coverage up to 100% for a UMTS system. If a minimal tilt adjustment error of 0.5° has a maximum average impact of 7%, it means for an LTE system, a 3° tilt adjustment error can have a coverage impact of 42%. It can be concluded that a UMTS system is more sensitive to tilt adjustment than an LTE system. In [50], literature stated that tilt can be used to manage interference between LTE cells. The effect size parameter is used to give a more practical perspective of coverage performance and states if there is a tilt error of 3 degrees or larger, the impact on coverage can be significant.

6.2.2 What is the practical impact of a height adjustment error on coverage?

In considering the height analysis, it was found that the antenna height also has a statistically significant impact on coverage. The co-variance analysis proves that the residual impact and variant impact is very similar, which indicates that the impact of antenna height should be constant, independent of the position of the LTE site.

From the pairwise comparison it can be confirmed that at a minimum height adjustment error of 2 meters, an average coverage impact of the error can be up to 6%. The effect size states that there can be a significant impact on the coverage if there is a height

installation error of 6 meters or more, but can already have a small practical impact at a height error of 2 meters. The importance of accurate height installation is confirmed by the conclusion in [50], where it has been stated that cell-edge interference can occur if the antenna is installed higher than the design criteria.

6.2.3 What influence does the terrain have on coverage, having taken the tilt and height into account?

The third research question focused on the analysis of the impact of the terrain around a site. It can be concluded that the average effective height around a site is a good possible predictor for coverage. The reason for effective height being a better predictor than TRF can be because the effective height definition takes negative height into account, whereas TRF does not. Effective height can also be used as a predictor to determine if it is necessary to do adjustment (height and tilt) optimisation for the specific site. This is especially valid for tilt adjustment, given the variance in coverage because of the location of the site when tilt is taken into account.

6.2.4 Concluding remarks

In answering the research problem that relates to what the impact of certain antenna installation parameters are on coverage and what the installation tolerances should be, the following conclusion can be drawn:

When site planning commences, the height and tilt adjustments are optimised using a network planning tool. The impact of height is not as sensitive to correct installation than tilt. A tilt error of as small as 0.5° can already have a practical impact on coverage. It is therefore important to make sure that the method to install the antenna should be accurate for at least up to 0.5°. If an antenna is not correctly installed, the covered area would not meet design specification, which could result in high cost as described in Chapter 1. Coverage is not so sensitive to the height adjustments, because an error on

height installation of 2 m can start to have a practical effect. Therefore current height installation methods should be sufficient in order to obtain predicted coverage.

6.3 Future work

This study is based on a specific LTE frequency and a specific LTE antenna pattern was used. This study can also be repeated for other frequencies and patterns. The model and software are written in such a way, that it would be possible to reproduce the results.

In order to account for processing time, a short study was done to choose which resolution of the grid spacing can be used to make the study feasible. It is possible to test the impact of the parameters using a higher resolution grid spacing, but more processing time and resources would be required.

The propagation model used in this study is the ITU-R P.1546-4 model. For future work, other models can be considered to test the impact of the propagation model on the coverage.

It may be considered that even though the tilt adjustment produces a significant error in coverage when compared to the error of height adjustment, extra cost to add extra height to a tower is substantially higher than the cost of adjusting the tilt.

The performance metric used in this study is coverage, for future reference it can be considered instead of using a single metric, to combine different metrics into a single metric to allow the comparison of more results.

6.4 Closure

The impact of two antenna installation parameters on coverage (defined as coverage of an LTE site) were modelled using software simulation and statistically analysing the results. As mentioned, the impact of tilt on coverage is much more sensitive than the impact of height adjustment. It can also be concluded that the impact of tilt is subjected to the terrain deviations surrounding the LTE tower.

Using a higher resolution grid spacing would provide more detail on the impact of tilt adjustment, but it can be concluded from the research that tilt is an important factor when it comes to coverage and installation must be done as accurately as possible in order to meet the design specification. The simulation and results supported the answer to the research questions, and valid conclusions could be drawn. The statistical analysis was an important factor to understand the extent of the influence of practice on the adjustments.

Bibliography

[1] J. Devore and N. Farnum, *Applied statistics for engineers and scientists*, 2nd ed. Thomson Brooks/Cole, 2005.

[2] H. Ellis, S.M. Steyn, "Practical significance (effect sizes) versus or in combination with statistical significance (p-values)," *Management Dynamics*, 2003.

[3] (2016) Recommendation ITU-T E.212: The international identification plan for public networks and subscriptions. Telecommunication standarization sector of ITU.

[4] L. E. Frenzel, *Principles of Electronic communication systems*, 4th ed. McGraw-Hill, 2008.

[5] C. A. Balanis, *Antenna Theory: Analysis and Design*, 4th ed. Hoboken, New Jersey: John Wiley & Sons, Inc, 2016.

[6] (2018) NB-IoT and the ECC framework for MFCN frequency bands. CEPT-ECC. [Online]. Available: http://www.erodocdb.dk/docs/doc98/official/pdf/ECCDEC0205.pdf

[7] World map view of South Africa (MATLAB implementation), U.S. Geological Survey, 2019. [Online]. Available: http://viewer.nationalmap.gov/services

[8] "ITU-R M.1036-5: Frequency arrangements for implementation of the terrestrial component of International Mobile Telecommunications (IMT) in the bands identified for IMT in the Radio Regulations (RR)," Radio Communication sector of ITU, 2015.

[9] A. Z. Yonis, M. F. L. Abdullah, and M. F. Ghanim, "LTE-FDD and LTE-TDD for Cellular Communications," *Progress In Electromagnetics Research Symposium Proceedings*, pp. 1467–1471, 2012.

[10] *Are you sure, your antennas are installed correctly?*, Spectrum: LS Telcom Customer News Magazine, 2016, Special Edition 1 Broadcast. [Online]. Available: https://www.lstelcom.com/en/company/downloads/customer-magazine/

[11] E. Dinan and A. Kurochkin, "The effects of antenna orientation errors on UMTS network performance," *IEEE International Symposium on Personal, Indoor and Mobile Radio Communications, PIMRC*, pp. 0–4, 2006.

[12] J. Schreiber, "Antenna pattem reconstitution using unmanned aerial vehicles (UAVs)," *Antenna Measurements Applications (CAMA), 2016 IEEE Conference*, pp. 6–8, 2016.

[13] A. Ghasemi, A. Abedi, and F. Ghasemi, *Propogation Engineering in Wireless Communications*, 1st ed. New York: Springer Science + Business Media, 2012.

[14] (2018) Government Gazette Staatskoerant. Department of Basic Education. [Online]. Available: http://www.greengazette.co.za/pages/national-gazette-37230-of-17-january-2014-vol-583_20140117-GGN-37230-003

[15] T. Rappaport, *Wireless Communications: Principles and Practice*, 2nd ed. Pearson India, 2009.

[16] A. Jajszczyk, *Wireless Engineering Body of Knowledge*, 2nd ed. New Jersey: John Wiley and Sons, Ltd., 2012.

[17] D. Witkowski. (2017) Technical White Paper RF Antenna Misalignment Effects on 4G/LTE Data Throughput Considerations for Maximizing Return on your Spectrum Investments. [Online]. Available: https://www.sunsight.com

[18] K. Akpado, O. Oguejiofor, C. Ezeagwu, and A. Okolibe, "Investigating the impacts of base station antenna height, tilt and transmitter power on network coverage," *International Journal of Engineering Science Invention*, 2013.

[19] *TETRA measurements at BOS sites via remotely piloted aircraft*, Spectrum: LS Telcom Customer News Magazine, 2016, Edition 1. [Online]. Available: https://www.lstelcom.com/en/company/downloads/customer-magazine/

[20] M. Sierra, F. Saccardi, and L. Foged, "Gain antenna measurement using single cut near field measurements," in *AMTA 2016 Proceedings*, Autin, TX, USA, 2016, pp. 1–4.

[21] *Namibia: LS telcom carries out countrywide broadcast site audits via remotely piloted aircraft (RPA)*, Spectrum: LS Telcom Customer News Magazine, 2015, Edition 1. [Online]. Available: https://www.lstelcom.com/en/company/downloads/customer-magazine/

[22] *Major European broadcast operators confirm high-value of airborne measurements via remotely piloted aircraft system*, Spectrum: LS Telcom Customer News Magazine, 2015, Edition 1. [Online]. Available: https://www.lstelcom.com/en/company/downloads/customer-magazine/

[23] M. Nohrborg. (2019) Lte. 3rd Generation Partnership Project. [Online]. Available: https://www.3gpp.org/technologies/keywords-acronyms/98-lte

[24] "UTRA-UTRAN Long Term Evolution (LTE) and 3GPP System Architecture Evolution (SAE) Long Term Evolution of the 3GPP radio technology," pp. 2–3, March 2006.

[25] M. R. Bhalla and A. V. Bhalla, "Generations of mobile wireless technology: a survey," *International Journal of Computer Applications*, vol. 5, no. 4, p. 7, 2010.

[26] A. Chakraborty and P. Medinipur, "A Study on Third Generation Mobile Technology (3G) and Comparison among All Generations of Mobile Communication," 2013.

[27] "LTE; Evolved Universal Terrestrial Radio Access (E-UTRA); User Equipment (UE) radio transmission and reception (3GPP TS 36.101 version 15.3.0 Release 15)," ETSI, 2018.

[28] "IEEE Standard for Definitions of Terms for Antennas (IEEE Std 145)," IEEE standards association, 2013.

[29] I. Szini, G. F. Pedersen, A. Scannavini, and L. J. Foged, "MIMO 2x2 reference antennas concept," *European Conference on Antennas and Propagation (EUCAP)*, 2012.

[30] S. Kozono, T. Tsuruhara, and M. Sakamoto, "Base station polarization diversity reception for mobile radio," *IEEE Transactions on Vehicular Technology*, vol. 33, no. 4, pp. 301–306, 1984.

[31] T. Penttinen, *The LTE-Advanced Deployment Handbook: The Planning Guidelines for the Fourth Generation Networks*, 1st ed., T. Penttinen, Ed. Wiley, John and sons Ltd, 2016.

[32] T. K. Sarkar, Z. Ji, K. Kim, A. Medouri, and M. Salazar-Palma, "A Survey of Various Propagation Models for Mobile Communication," *IEEE Antennas and Propagation Magazine*, vol. 45, no. 3, pp. 51–82, 2003.

[33] J. D. Parsons and R. C. V. MacArio, *The Mobile Radio Propagation Channel*. John Wiley and Sons ltd, 2000, vol. 38, no. 6.

[34] A. Longley and P. Rice. (2018) ESSA Technical Report ERL 79-ITS 67 - Prediction of Tropospheric Radio Transmission Loss Over Irregular Terrain. [Online]. Available: http://www.its.bldrdoc.gov/pub/essa/essa_erl_79-its_67/

[35] V. Abhayawardhana, I. Wassell, D. Crosby, M. Sellars, and M. Brown, "Comparison of Empirical Propagation Path Loss Models for Fixed Wireless Access Systems," *2005 IEEE 61st Vehicular Technology Conference*, vol. 1, no. c, pp. 73–77, 2005.

[36] M. Shahajahan and A. Q. M. Abdulla Hes-Shafi, "Analysis of propagation models for wimax at 3.5 ghz," Master's thesis, Blekinge Institute of Technology, Sep 2009.

[37] "ITU-R P.1546-5: Method for point-to-area predictions for terrestrial services in the frequency range 30 MHz to 3000 MHz," Radiocommunication sector of ITU, 2013.

[38] "ITU-R P.1546-4: Method for point-to-area predictions for terrestrial services in the frequency range 30 MHz to 3000 MHz," Radiocommunication sector of ITU, pp. 1–57, 2009.

[39] (2019) RSRQ and RSRP measurement in LTE. Arimas. [Online]. Available: https://arimas.com/78-rsrp-and-rsrq-measurement-in-lte

[40] E. C. Commitee, "ECC Report 256: LTE coverage measurements," October 2016.

[41] "3rd Generation Partnership Project; Technical Specification Group Radio Access Network; Evolved Universal Terrestrial Radio Access (E-UTRA); User Equipment (UE) procedures in idle mode," 2016.

[42] "Quality measurement in major events," ITU-T, Recommendation E.811, 2017.

[43] "ITU-R P.452-11: Prediction procedure for the evaluation of microwave interference between stations on the surface of the Earth Annex 1," Radiocommunication sector of ITU, 2003.

[44] S. Shumate, Givens, and Bell, "Longley-Rice's Terrain Irregularity Parameter, Delta-H," *IEEE Broadcast Technology Society Newsletter*, vol. 16, no. 4, pp. 23–25, 2008.

[45] L. Thiele, T. Wirth, K. Borner, M. Olbrich, and V. Jungnickel, "Modeling of 3d field patterns of downtilted antennas and their impact on cellular systems," *International ITG Workshop on Smart Antennas (WSA)*, 2009.

[46] T. Petrita and A. Ignea, "A new method for interpolation of 3D antenna pattern from 2D plane patterns," *2012 10th International Symposium on Electronics and Telecommunications, ISETC 2012 - Conference Proceedings*, vol. 2, pp. 393–396, 2012.

[47] N. Herscovici, C. Christodoulou, F. Gil, A. R. Claro, J. M. Ferreira, C. Pardelinha, and L. M. Correia, "A 3D interpolation method for base-station-antenna radiation patterns," *IEEE Antennas and Propagation Magazine*, vol. 43, no. 2, pp. 132–137, 2001.

[48] Parikh and Jolly, "Impact of base station antenna height and antenna tilt on performance of LTE systems," *IOSR Journal of Electrical and Electronics Engineering (IOSR-JEEE)*, vol. 9, no. 4, pp. 06–11, 2014.

[49] "Technical specification group radio access network; evolved universal terrestrial radio access (e-utra); radio frequency (rf) system scenarios (release 11," 3rd Generation Partnership Projec, 2012.

[50] J. Niemela and J. Lempiainen, "Impact of the base station antenna beamwidth on capacity in WCDMA cellular networks," *The 57th IEEE Semiannual Vehicular Technology Conference, 2003. VTC 2003-Spring.*, vol. 1, pp. 80–84, 2003.

[51] H. A. Hakim, H. Eckhardt, and S. Valentin, "Decoupling antenna height and tilt adaptation in large cellular networks," *Proceedings of the International Symposium on Wireless Communication Systems*, pp. 11–15, 2011.

[52] D. Lee and Ce Xu, "Mechanical antenna downtilt and its impact on system design," *1997 IEEE 47th Vehicular Technology Conference. Technology in Motion*, vol. 2, no. 1, pp. 447–451.

[53] (2016) USGS EROS Archive - Digital Elevation - Shuttle Radar Topography Mission (SRTM) 1 Arc-Second Global. USGS. [Online]. Available: https://www.usgs.gov/centers/eros/science/usgs-eros-archive-digital-elevation-shuttle-radar-topography-mission-srtm-1-arc?qt-science_center_objects=0#qt-science_center_objects

[54] M. Ferreira, "Spectral opportunity analysis of the terrestrial television frequency bands in South Africa," Ph.D. dissertation, North-West University, Potchefstroom Campus, 2013. [Online]. Available: http://hdl.handle.net/10394/9656

[55] (2019) Unwired labs OpenCellid. Unwired Labs. [Online]. Available: https://opencellid.org/#zoom=16&lat=37.77889&lon=-122.41942

[56] (2019) LTE frequency band. Niviuk. Paris. [Online]. Available: http://niviuk.free.fr/lte_band.php

[57] (2018) Linear interpolation equation calculator. [Online]. Available: https://www.ajdesigner.com/phpinterpolation/linear_interpolation_equation.php#ajscroll

[58] Y. L. He Huang and S. Gong, "A Novel Dual-Broadband and Dual-Polarized Antenna for 2G/3G/LTE Base Stations," *EEE Transactions on antennas and propagation*, vol. 64, no. 9, September 2016.

[59] G. Hancock, R. Mueller, and L. Stapleton, *The reviewers guide to quantitative methods in the social sciences*. New York: Routledge, 2005.

Appendix A

Combined simulation flow diagram

Figure A.1 shows the flow diagram of the full system model as implemented in the Matlab software. Each sub-diagram is shown by means of a frame and the sub-diagrams are labelled on the top right corner of the frame.

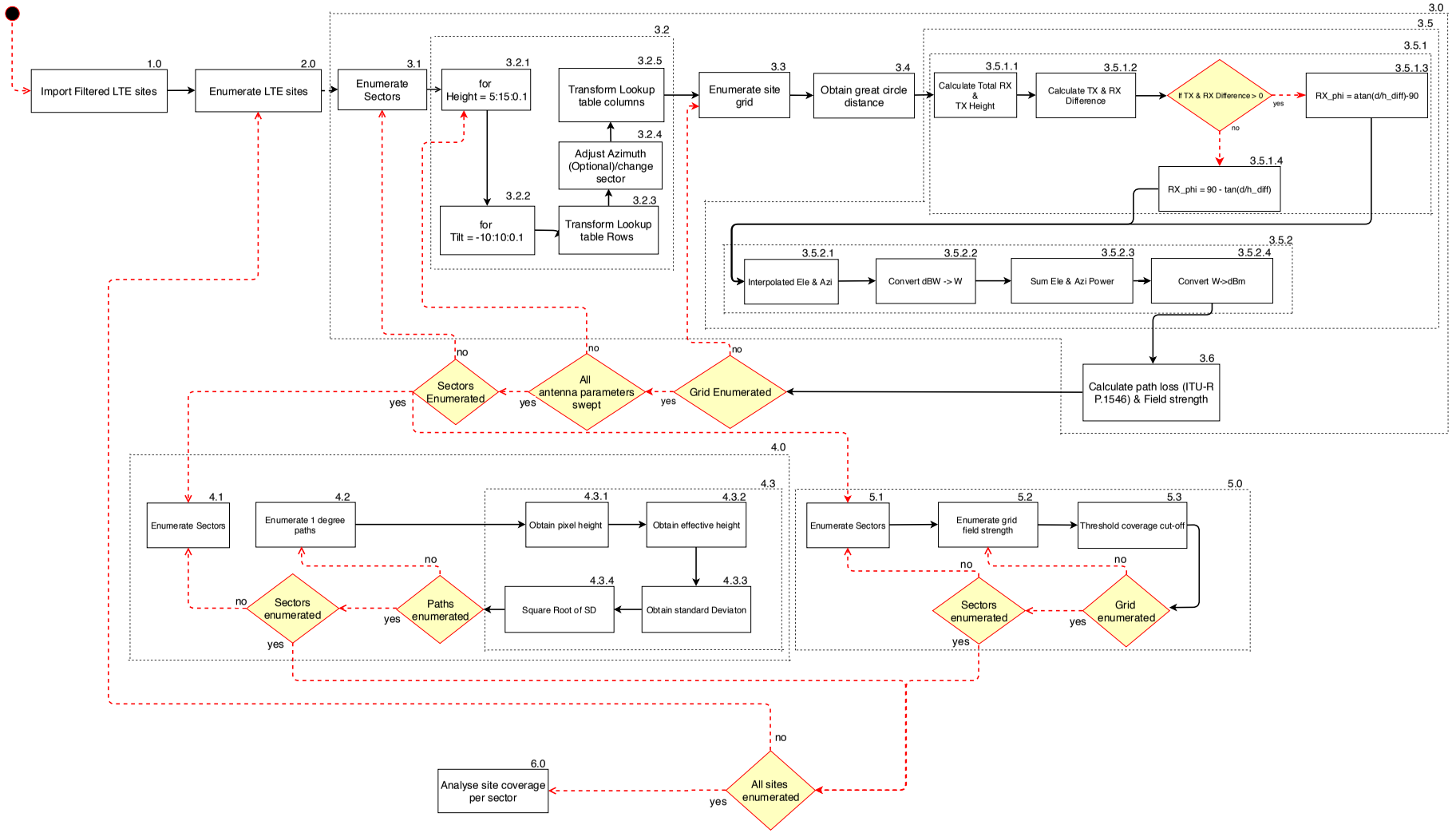

Figure A.1: Combined flow diagram of the implemented system model

Appendix B

Matlab code to execute simulation for multiple sites

The code inserted below is the Matlab code to execute the simulation of multiple sites. The important variables such as grid spacing, height adjustment and tilt adjustment variables are set.

The "Buildcoveragestruct2 " function was used to build the structure files for the transmitter results structure.

The function is also written to simulate multiple sites using separate processor cores. This decreases the processing time by the amount of cores available.

The "Analyse towers louwrens func " function contains all of the calculations and calls all the helper function necessary to obtain the results and store them in the transmitter results structure.

B.1 Matlab code

```
1 clear all ;
```

```
2
3 %Grid_spacing of the 1x1 degree tile
4 grid_spacing = 120;
5 % Spec number of cores (will generate list to enumrate for each
      core in output window)
6 cores = 4;
7
8 % Run-time parameters
9 ant_h_vector = 5:1:15; %Define range of antenna heights (meters
    ) & step size to enumerate on tower
10 ant_elev_vector = -5:0.5:10; %Define range of elevation angles
    (degrees) & step size to enumerate on tower
11
12 %%%%Import Sites%%%
13 load('TX_Sites_31.mat');
14
15 % Build coverage struct based on required tiles
16 TX_Sites = Buildcoveragestruct2(grid_spacing,TX_Sites,
    ant_h_vector,ant_elev_vector);
17
18 load('TX_Sites_Final_31.mat');
19
20 % Now assign the tile numbers that this instance needs to run
21 number = length(TX_Sites);
22
23 sites_per_core = floor(number / cores);
24 remainder = rem(number,cores);
25 count = 1;
26 fprintf('cores=%d\n',cores);
27 fprintf('grid=%d\n',grid_spacing);
```

```
28 fprintf('ant_h_vector=%d\n',ant_h_vector) ;
29 fprintf('ant_elev_vector=%d\n',ant_elev_vector) ;
30 fprintf('declare -a x=(') ;
31 for i = 1:cores
32     if remainder == 0
33      temp = count + sites_per_core - 1 ;
34      fprintf('%d:%d ',count,temp) ;
35      count = temp + 1 ;
36     else
37      temp = count + sites_per_core ;
38      fprintf('%d:%d ',count,temp) ;
39      count = temp + 1 ;
40      % Decrement remainder;
41      remainder = remainder - 1 ;
42     end
43 end
44 fprintf(')\n') ;
45 % This function calls the running script
46 Analyse_towers_louwrens_func(grid_spacing,1:15,TX_Sites,
    ant_h_vector,ant_elev_vector) ;
```

Appendix C

Conference contributions from dissertation

A subsection of the work in this dissertation was presented at, and appeared in the proceedings of the following conference:

B.L. Prinsloo, M. Ferreira and A. Helberg, "Modelling the impact of effective antenna height and antenna tilt on LTE cell coverage ", in Southern African Telecommunications and Networks Access Conference (SATNAC), Arabella, Hermanus, Sep. 2018.